ISAS - INTERNATIONAL SCHOOL FOR ADVANCED STUDIES

A Novel Technique for the Simulation of Interacting Fermion Systems

Thesis submitted for the degree of

"Doctor Philosophiæ"

CANDIDATE

Sandro Sorella

SUPERVISORS

Prof. Michele Parrinello

Prof. Stefano Baroni

Prof. Roberto Car

Prof. Erio Tosatti

December 1989

TRIESTE

SISSA - SCUOLA INTERNAZIONALE SUPERIORE DI STUDI AVANZATI

TRIESTE

Strada Costiera 11

Scuola Internazionale Superiore di Studi Avanzati

International School for Advanced Studies

A Novel Technique for the Simulation of Interacting Fermion Systems

Thesis submitted for the degree of

"Doctor Philosophiæ"

CANDIDATE

Sandro Sorella

SUPERVISORS

Prof. Michele Parrinello

Prof. Roberto Car

Prof. Stefano Baroni

Prof. Erio Tosatti

December 1989

Contents

Chapters

ACKNOWLEDGEMENTS

I am gratefully in debt with Professors S. Baroni, R. Car, M. Parrinello and, E. Tosatti for their constant help and useful suggestions throughout this work. I am very grateful also to Dr. A. Parola, for his fruitful collaboration in the last part of this work. Although I do not write down their names, I express my gratitude to many researchers who discussed with me and made useful comments on this work.

This work has been in part supported by the SISSA–CINECA collaborative project under the sponsorship of the Italian Ministry for Public Education.

to Luisa

INTRODUCTION

The many–body problem of interacting quantum particles has been a subject of interest for many years. Unfortunately very few models which take the correlation into consideration are analytically solvable and they all concern low dimensionality and a very simplified form of the interaction.

The enormous growth of computer power in the last few decades has opened a new possibility to solve the many body problem by numerical calculation. The various techniques used can be classified in three main groups: exact, approximate and statistical techniques.

The task of "exact diagonalization techniques" (full CI, Lanczos, conjugate gradients) is the evaluation of the exact ground state ψ_0 of a given hamiltonian $\hat{H}$. These calculations however face a very important difficulty because the number of degrees of freedom of a many body wavefunction grows at least exponentially with the size of the system and the number of electrons. Although recently it has been very successful to handle up to 16 electrons[1−4] the possibility to extend these methods to larger systems is clearly hopeless.

A great development in these exact calculation techniques is provided in principle by the density functional theory (DFT)[5]. In such scheme the problem of calculating the ground state energy and ground state correlation functions is mapped onto a minimization problem of a well defined functional which now depends only on the electronic density at each spatial coordinate. It is clear therefore that the number of variables used in this formulation is very much

decreased. However the main difficulty of this approach is that the functional that describes the theory is not known and it cannot be easily evaluated. In fact only approximate expression of this functional have been used so far.

Another group of techniques are the approximate ones. Among these methods it is worth mentioning the variational techniques like Hartree, Hartree Fork, Gutzwiller, Jastrow[6,7], the methods using many body perturbation theory like RPA[8-10], and finally the Local Density Approximation (LDA)[11,12], which is a very convenient approximation of DFT. The limitation of all these methods is that the approximations used are difficult to control systematically. As an example in DFT any attempt to go beyond the LDA has not led to systematic and substantial improvement. On the other hand the variational techniques are too much dependent on the choice of the form of the variational wavefunction. When the problem is particularly hard and simple minded approximations of the ground state does not work, as for example in the Hubbard model[13], these variational methods are largely prejudiced by the assumed variational wavefunction.

The last group of techniques in the simulation of quantum systems deals with the calculation of exact ground state properties using classical statistical method. One of these is the so called Quantum Monte Carlo method QMC[14-16]. As in many other techniques the ground state ψ_0 of the Hamiltonian H is obtained by filtering out from an initial trial wavefunction ψ_T its ground state component by applying to ψ_T the imaginary time propagator e^{-Ht} for large enough time t. $\psi_t = e^{-Ht}|\psi_T>$ can be obtained as a solution of the imaginary time Schrodinger equation. In order to decrease the prohibitive amount of variables contained in ψ_t, the many body wavefunction is sampled using a statistical method. The weight chosen for the statistical sampling has a direct relation with the many

body wavefunction ψ_t (usually the weight is the absolute value of ψ_t). It is clear that the method works very well for bosons because ψ_t is always positive. However there are still severe difficulties for fermions because the antisymmetry of the fermion wavefunction determines regions of ψ_t with positive and negative sign. This is the well known "fermion sign problem" that in this case has a very clear physical meaning. In fact each part with definite sign ψ_t^+ and ψ_t^- of the propagated wavefunction $\psi_t = \psi_t^+ - \psi_t^-$ has a non vanishing component on the more stable boson ground state. The calculation in this case becomes unstable because, through the imaginary time propagation, each part of the wavefunction ψ_t^+ and ψ_t^- is attracted by the bosonic ground state, until the fermionic component becomes numerically undetectable.

A similar instability occurs in the so called "world line approach"[17-20], although in this case the underlying more stable state is not exactly the boson ground state. Instead of sampling a wavefunction a convenient basis is chosen to write the matrix elements of the hamiltonian H. Then a finite temperature partition function is statistically evaluated to achieve asymptotically the $0\,K$ limit. Even in this case "the fermion sign problem" appears when it is not possible to choose a basis such that the off diagonal matrix elements of the hamiltonian have a definite sign. This is indeed the case for fermion systems in 2D or 3D and non trivial interactions.

New possibilities of approaching the many body electronic problem are discussed in the present thesis using a well known method: the Hubbard-Stratonovich Transformation (HST). This transformation has been known for long time in many branches of physics but only very recently it has been systematically applied to numerical calculations[21-30].

The imaginary time evolution $e^{-\hat{H}t}$ is convenient for numerical treatment when the Hamiltonian contains only one body operators and no interaction term. The HST is basically a method that allows to transform a many-body operator into a coherent superposition of one-body operators, depending on a fluctuating time dependent bosonic field σ. In this way the HST transforms the many body problem in a functional integral over the variables σ. This functional integration is performed by evaluating the propagation of a trial function $|\psi_T>$ in a time dependent one body hamiltonian containing the integration variables σ. As far as the functional integral is concerned, it is calculated using a statistical method which is well established in literature: the Langevin dynamic (LD).

Our method is similar to QMC, as far the imaginary time evolution of a trial wave function is concerned, but at variance with QMC it has the considerable advantage to preserve the antisymmetric property of the fermion wave-function at any time of such evolution. In the present thesis we also show how to preserve such property in a very efficient numerical way (see ch. 4).

Until now the most successful application of the HST was done by Hirsch and Scalapino[23,27,30], using a discretized version of the HST in which the functional integration is replaced with a trace over Ising variables (σ assumes the values $+1$ or -1). The goal of their calculation is to evaluate the finite-temperature partition function of a short range interacting system of electrons. However the discretized version of the HST is convenient only for short range interaction and has therefore a limited applicability. Moreover until very recently this method was unstable for low temperatures and only very recently[24,25] it was possible to generalize the special orthogonalization technique to stabilize the algorithm in the low temperature regime. This technique was firstly used by Koonin[21,22]

using a different and less efficient algorithm, then we firstly pointed out[31] that the orthogonalization technique has to be used just for stabilizing the computer simulation of Fermions at low temperatures.

In fact after our work a lot of progress has been achieved in the performances of existing algorithms.

The most important difficulty in the application of this method is that the statistical weight obtained by a straightforward application of the HST may be not positive definite —the fermion sign problem reappears— and there may be an instability of the method for large imaginary time similar to the one that occurs for QMC and the world line approach.

In the first part of our thesis we analyze, as rigorously as possible, this "sign problem" in the HST formulation. We show in fact that in many non trivial cases the method is stable for arbitrary large imaginary time. Although this property has not been proved to hold in general, the HST has opened new possibilities[24,26,32] for the simulation of interacting fermions.

In the second part we describe an algorithm that enables to use the LD for the statistical sampling of weights with negative sign.

In the last part we show some of the results obtained with this new method. We consider a simple, but very interesting model, the Hubbard model in 1 and 2D. In 1D we found, quite surprisingly a very sharp jump, at the Fermi momentum k_F, in the momentum distribution function. This is especially evident at low density. Then with a careful size scaling analysis we show that this jump is only a finite size effect, and it is instead replaced, for the infinite system, by a power low singularity close to k_F, in agreement with previous argument based on Renormalization Group Methods. This behaviour suggest that the 1D Hubbard

model is a marginal conductor away from half filling because the quasi particle are not Fermi–liquid like.

In 2D at half filling we studied the properties of the ground state in order to understand if a possible Mott transition takes place by increasing the on–site interaction U. We found that our numerical results for cluster up to 242 sites strongly suggest the existence of long range antiferromagnetic AF order even for relatively weak interaction. We performed also a size scaling analysis of the momentum distribution and we found no evidence of a Fermi surface at half filing. Then our numerical simulation suggests that the ground state of the half filled Hubbard model is an antiferromagnetic insulator even in the small coupling regime.

Away from half filling in 2D the main difficulty is that the statistical weight obtained with the HST is non positive definite and its average sign can reach extremely small values for low temperatures. In this case we performed calculations by using a different but related statistical weight which gives the same ground state properties of the exact non positive weight provided the average sign of the weight does not vanishes exponentially as the temperature is decreased.

It is not possible, at the moment, to verify numerically such a convergence condition for such large size, because the statistical evaluation of the average sign is prohibitive whenever this average sign is an extremely small number. In the present numerical calculation, as in the calculation performed by other people, it is not possible to distinguish whether the average sign is vanishing or converging to some small constant. Tests on small size clusters, which can be exactly diagonalized, show that the calculation performed in this way, i.e. neglecting the sign, can be considered at least as a good approximation. Within this approximation we found that away from half filling the 2D antiferromagnetic order is initially destroyed

albeit without any clear Fermi liquid behaviour. Then it is possible that the 2D Hubbard model away from half filling has a special kind of ground state which may provide the basis for the understanding of High-T_c superconductivity.

We are at the moment systematically improving our calculation away from half–filling and for larger coupling constant.

Chapter I

A functional integral formulation for interacting fermions

1.1 The Hubbard–Stratonovich transformation and the projected trial wavefunction technique

In the following we describe a formalism to calculate ground state properties of a many body system by using a classical statistical method. The scheme can be applied to a large class of many body hamiltonians defined in finite lattice containing N_a sites:

$$\hat{H} = \hat{K} + \hat{V} \tag{1.1.1}$$

where $\hat{K}$ is a one body operator which we call the kinetic term and $\hat{V}$ is a two body interaction term.

For reason of simplicity we restrict our analysis to the well known Hubbard model but all the following results are completely general and do not depend on the particular choice of the Hamiltonian (1.1.1). In the Hubbard model one pictures the electrons in a narrow energy band hopping between the localized states of neighboring lattice sites with a repulsive interaction energy between two electrons of opposite spins occupying the same lattice site. Consider a crystal (one, two, or three-dimensional) of N_a lattice sites with a total of $N \leq 2N_a$ electrons. It is supposed that the electrons can hop between the Wannier states of neighboring lattice sites, and that each site is capable of accommodating two electrons of opposite spins, with an interaction energy $U > 0$. The hamiltonian to consider is then $\hat{H} = \hat{K} + \hat{V}$ with:

$$\hat{V} = U \sum_{i=1}^{N_a} n_{i\uparrow} n_{i\downarrow} \tag{1.1.2}$$

and

$$\hat{K} = t \sum_{<i,j>\alpha} c_{i\alpha}^{+} c_{j\alpha} \tag{1.1.3}$$

where $n_{i\uparrow}$ ($n_{i\downarrow}$) is the fermion spin–up (spin–down) density operator at the site i, and U is the on–site interaction. Moreover the number of spin-up $N_\uparrow$ and spin-down $N_\downarrow$ particles as well as the total $N = N_\uparrow + N_\downarrow$ is fixed, $<i,j>$ stands for next neighbour sums and $c_{i\alpha}$, $c_{i\alpha}^{+}$ are the usual creation and annihilation operators of a particle at site i with spin α.

Following Koonin et al.[21,22] instead of considering the thermodynamic partition function $Z = \text{tr } e^{-\beta H}$, where β indicates the inverse temperature $\frac{1}{T}$, we introduce a "pseudo" partition function

$$Q = <\psi_T \mid e^{-\beta \hat{H}} \mid \psi_T > \tag{1.1.4}$$

where ψ_T is a trial wavefunction and β can be thought of as an imaginary time. If the ground state of $\hat{H}$ ψ_0, has non vanishing overlap with the trial wavefunction ψ_T, the imaginary time propagator $e^{-\beta H}$ for $\beta \rightarrow \infty$ projects from ψ_T its component along ψ_0, and Q behaves asymptotically as the true partition function Z:

$$Q \rightarrow <\psi_0 \mid \psi_T>^2 \ e^{-\beta E_0} \tag{1.1.5}$$

Moreover if the trial wavefunction is orthogonal to the lower $n-1$ eigenstates of $\hat{H}$ one has

$$Q \rightarrow <\psi_n \mid \psi_T>^2 \ e^{-\beta E_n} \tag{1.1.6}$$

where ψ_n is the n^{th} excited eigenstate of $\hat{H}$ non orthogonal to ψ_T and E_n the corresponding energy. Unless otherwise specified we will restrict ourselves to consideration of states belonging to a finite Hilbert space of dimension D and such that $<\psi_0|\psi_T> \neq 0$. In terms of Q the ground state energy is given by:

$$E_0 = \lim_{\beta \rightarrow \infty} -\frac{1}{\beta} \ln Q \tag{1.1.7}$$

More general expression for other ground state expectation values are obtained by differentiating eq. 1.1.7 with respect to appropriate external fields coupled to the quantity of interest. In fact the Hellmann–Feynmann theorem allows to

calculate the ground state expectation values of a general operator $<\psi_0\,\hat{O}\,\psi_0>$ by differentiating with respect to λ the ground state energy of the corresponding perturbed Hamiltonian $H\,+\,\lambda\,\hat{O}$:

$$<\psi_0\,O\,\psi_0>=\,\frac{d}{d\lambda}\,|_{\lambda=0}E_0(\lambda)\,=\,\lim_{\beta\to\infty}\,-\frac{1}{\beta}\,\frac{\partial}{\partial\lambda}\,|_{\lambda=0}\,\ln Q \qquad (1.1.8)$$

Hence in this scheme the "pseudo" partition function Q can be considered as the generator of all the ground state correlation functions.

In order to evaluate $<\,\psi_T\,e^{-H\beta}\,\psi_T\,>$ we split the total imaginary time propagator into a product of P short time propagators and apply the Trotter approximation to each of them:

$$\begin{aligned}\exp\,-H\beta\,&=\,(\exp\,-\Delta\tau H)^P\\&\simeq\,(\exp\,-\frac{\Delta\tau}{2}\,\hat{K}\,\exp\,-\Delta\tau\,\hat{V}\,\exp\,-\frac{\Delta\tau}{2}\,\hat{K})^P\,+\,o(\Delta\tau^3)\end{aligned} \qquad (1.1.9)$$

with $\Delta\tau\,=\,\frac{\beta}{P}$. The short time propagator $\exp\,-\frac{\Delta\tau}{2}\,\hat{K}\,\exp\,-\Delta\tau\,V\,\exp\,-\frac{\Delta\tau}{2}\,\hat{K}$ is clearly hermitian and positive definite. Then we can rewrite the approximated short time propagator of the Hamiltonian H as an exact short time propagator of an equivalent Hamiltonian $\tilde{H}$:

$$\exp\,-\tilde{H}\,\Delta\tau\,=\,\exp\,-\frac{\Delta\tau}{2}\,\hat{K}\,\exp\,-\Delta\tau\,\hat{V}\,\exp\,-\frac{\Delta\tau}{2}\hat{K} \qquad (1.1.10)$$

and $\tilde{H}$ differs by $o(\Delta\tau^2)$ from the exact Hamiltonian $\hat{H}$. All the calculations obtained by using the Trotter approximation give exact ground state properties of the effective Hamiltonian $\tilde{H}$ which differ at most by $o(\Delta\tau^2)$ from the desired ground state properties of the Hamiltonian $\hat{H}$.

The evaluation of the propagator (1.1.10) is numerically tractable when the Hamiltonian $\hat{H}$ contains only one body operators. In order to overcome the latter difficulty it is worth mentioning that a very simple relation allows to write a many–body operator

$$e^{\alpha^2 \hat{O}^2} \tag{1.1.11}$$

by means of an integral containing only one-body hermitian operators $\hat{O}$:

$$e^{\alpha^2 \hat{O}^2} = \frac{\int_{-\infty}^{+\infty} d\sigma \, e^{-\alpha\sigma \hat{O} - \frac{1}{2}\sigma^2}}{\int_{-\infty}^{+\infty} d\sigma \, e^{-\frac{1}{2}\sigma^2}}. \tag{1.1.12}$$

The last relation can be very easily verified by expanding the R.H.S. of the previous equation in powers of $\hat{O}$ and using the value of the gaussian averages

$$<\sigma^{2k}> = \frac{(2k)!}{2^k k!} \tag{1.1.13}$$

Equation (1.1.5) is very instructive and represents the fundamental step in the Hubbard–Stratonovich transformation (HST) because it allows to write a many body operator as a coherent superposition of single particle operators. This step, as we shall see in the following, allows to write the propagator (1.1.1) in a numerical feasible form. As it is also clear the previous transformation (1.1.5) can be applied only for negative definite two-body operators contained in the hamiltonian $\hat{H}$ unless considering imaginary α. While this property is certainly not true in general, it can always be guaranteed to be so, as shown in app.1, for quite general two-body fermionic operators.

We present here a generalization of the HST defined in (1.1.12), which is convenient for the Hubbard model and may be extended to other models. In the

present scheme only one classical-spin variable $\sigma_r(i)$ for each site r and Trotter slice i is used. These variables are independently distributed according to a probability density $\rho(\sigma_i)$ and are coupled to the local magnetic operator along the z axis at the site i $m_i = n_{i\uparrow} - n_{i\downarrow}$. Then, analogously to (1.1.5) we can write the many body propagator as an integral containing only one body propagators:

$$\exp -\hat{V}\Delta\tau = \exp -\frac{U\Delta\tau}{2}(N_\uparrow + N_\downarrow) \prod_{r=1}^{N_a} \int_{-\Lambda}^{\Lambda} d\sigma\, \rho(\sigma_r) \exp \sigma_r m_r \qquad (1.1.14)$$

In fact from the basic relation $n_{i\alpha}^2 = n_{i\alpha}$, coming from the usual fermionic commutation rules, the exponential term in the previous expression can be simplified as:

$$\begin{aligned} \exp \sigma_r m_r &= \exp \sigma_r n_{r\uparrow} \exp -\sigma_r n_{r\downarrow} \\ &= (1 + (\exp \sigma_r - 1)\, n_{r\uparrow})\,(1 + (\exp -\sigma_r - 1)\, n_{r\downarrow}) \end{aligned} \qquad (1.1.15)$$

Then the identity (1.1.14) is easily verified if the probability density $\rho(\sigma)$ satisfies the following relations:

$$\int_{-\Lambda}^{\Lambda} \rho(\sigma)\, d\sigma = 1\,, \qquad \rho(\sigma) = \rho(-\sigma) \qquad (1.1.16a)$$

and:

$$\int_{-\Lambda}^{\Lambda} \rho(\sigma) \cosh \sigma\, d\sigma = \exp \frac{U\Delta\tau}{2} \qquad (1.1.16b)$$

where the value of Λ is implicitly defined by eqs.(1.1.16). We note in passing that for $U < 0$ similar relations hold if magnetization m_r is substituted with the density n_r.

Note that for $U < 0$ it is enough to substitute in (1.1.14) the local magnetic operator with the density operator at the site r and take the same definition of Λ and $\rho(\sigma)$.

In this formalism the usual HST is obtained with infinite Λ by taking $\rho(\sigma)$ as a gaussian weight.

$$\rho(\sigma) = \frac{1}{\sqrt{2\pi U\Delta\tau}} \exp -\frac{\sigma^2 U\Delta\tau}{2} \tag{1.1.17}$$

Another convenient distribution has been introduced by Hirsch[28]:

$$\rho(\sigma) = \frac{1}{2}\{\delta(\sigma-\Lambda) + \delta(\sigma+\Lambda)\} \tag{1.1.18}$$

where from (1.1.13) Λ becomes finite: $\Lambda = \cosh^{-1} \exp \frac{U\Delta\tau}{2}$. The basic advantage of the previous distribution is that the variable σ is bounded $|\sigma| < \Lambda$ and the operator $\exp \sigma m_r$ is always close to the identity for sufficiently small Trotter time interval $\Delta\tau$ (since $\Lambda \to 0$ for $\Delta\tau \to 0$). However in order to get a finite Λ it is not necessary to use a discrete distribution. An alternative choice intermediate between eq. (1.1.17) and (1.1.18) is to take:

$$\rho(\sigma) = \frac{1}{\pi\sqrt{\Lambda^2-\sigma^2}} \quad for \quad |\sigma| < \Lambda \tag{1.1.19}$$

For $\Lambda = \sqrt{2U\Delta\tau}\,[1 + \frac{U\Delta\tau}{16})]$ one can satisfy eq.(1.1.13) up to $o(\Delta\tau^3)$. This distribution is particularly indicated for methods of sampling[32-35] based on forces. In fact with a simple change of variable $\sigma = \Lambda\cos\theta$, one get a uniform and smooth probability density for the new variable θ ($\rho(\sigma)d\sigma = \frac{d\theta}{2\pi}$). This will be our choice in the most recent sets of calculation.

Using the identity (1.1.14–16) in equation (1.1.9) to express the full many body propagator we can finally write the "pseudo" partition function Q in (1.1.2)

as a multi–dimensional integral over variables $\sigma_{r,l}$ where l indicates each Trotter time slice:

$$Q = \int <\psi_T U_\sigma \psi_T > \; d\mu_\sigma \tag{1.1.20}$$

$$d\mu_\sigma = \prod_{l=1}^{P} \prod_{r=1}^{N_a} \rho(\sigma_{r,l})\, d\sigma_{i,l} \tag{1.1.21}$$

and U_σ is the product of many positive definite one body propagators $\exp -\Delta\tau \hat{h}_l$ defined at each l^{th} time slice

$$U_\sigma = \prod_{l=1}^{P} \exp\, -\Delta\tau \hat{h}_l \tag{1.1.22}$$

where

$$\exp -\Delta\tau \hat{h}_l = \exp\, -\frac{\Delta\tau}{2}\hat{K} \exp \sum_r \sigma_{r,l}(n_{r\uparrow} - n_{r\downarrow}) \exp -\frac{\Delta\tau}{2}\hat{K}\; \exp -\frac{U\Delta\tau N}{2} \tag{1.1.23}$$

Note that U_σ acts independently on each spin component and can be written as the product of two propagators $U_\sigma = U_\sigma^{\uparrow} U_\sigma^{\downarrow}$, each acting on separate spin subspaces. It is also important to point out that, in case Λ is finite in (1.1.20), the fields $\sigma_{r,l}$ are always constrained to be smaller than Λ and any short time propagator $e^{-\hat{h}_i \Delta\tau}$ has always bounded eigenvalues. Hereafter we formally indicate with $E_{\min}$ and $E_{\max}$ the minimum and the maximum eigenvalue of $\hat{h}_i$ for any possible bounded configuration of the fields.

From (1.1.20) an estimate of $E_{\min}$ and $E_{\max}$ is roughly

$$E_{\max} \leq N_a \left(1 + \frac{\Lambda}{\Delta\tau}\right)$$
$$E_{\min} \geq -N_a \left(1 + \frac{\Lambda}{\Delta\tau}\right) \tag{1.1.24}$$

1.2 Mapping of the Quantum problem onto that of sampling classical partition functions

In the previous section we introduced classical auxiliary fields $\sigma_r(i)$ by means of the HST. Then a multi dimensional integral Q over these variables can be used for the study of the ground state properties of the electronic system. Of course this quantum problem would be solved if an exact numerical evaluation of this multi–dimensional integral were possible. Unfortunately this is not the case because the functional Q contains a prohibitively large number of variables. A very important advantage can be obtained using a statistical mechanic approach interpreting the functional Q as a classical partition function of the variables σ. In this case in fact one can use a statistical method for the evaluation of Q and related physical quantities.

In fact if the integrand in (1.1.20) is always positive definite Q can be thought of as a classical partition function of the variables $\sigma_{r,l}$ that interact through a potential

$$V(\sigma) = -\ln <\psi_T \,|\, \hat{U_\sigma} \,|\, \psi_T> . \tag{1.2.1}$$

Then using eq.(1.1.8) a well defined classical average corresponds to the ground state average of a given operator $\hat{O}$

$$<E_{\hat{o}}(\sigma)>_Q = Q^{-1} \int d\mu_\sigma E_0(\sigma) \exp -V_\sigma \tag{1.2.2}$$

$$E_{\hat{O}}(\sigma) = -\frac{1}{\beta}\frac{d}{d\lambda} \,|_{\lambda=0} \ln <\psi_T \, U_\sigma^\lambda \, \psi_T> \tag{1.2.3}$$

where U_σ^λ is obtained by adding to the kinetic term a perturbation $\lambda\hat{O}$.

So far we have assumed that the integrand in expression (1.1.20) $<\psi_T\, U_\sigma\, \psi_T>$ is always positive definite. This is in general not true because the propagated many body wavefunction $U_\sigma\psi_T$ can have a negative overlap with the initial trial wavefunction. However it is always possible to define a new classical partition function:

$$Q_M^\beta(\psi_T) = \int [d\mu_\sigma]\ |<\psi_T\, U_\sigma(\beta,0)\,\psi_T>| \tag{1.2.4}$$

and the corresponding asymptotic energy:

$$E_M = \lim_{\beta\to\infty} -\frac{1}{\beta}\ln Q_M^\beta(\psi_T) \tag{1.2.5}$$

In section 4 it will be analyzed in detail the existence of the limit (1.2.5) and its dependence on the trial wavefunction.

Whenever the quantity $<\psi_T|U_\sigma|\psi_T>$ is not positive definite the standard procedure would be to relate averages in the Q_M ensemble denoted by $<...>_M$ to the needed averages in the Q ensemble[27] by:

$$<\hat{O}> = \frac{<E_{\hat{O}}(\sigma)\ \times\ S>_M}{<S>_M} \tag{1.2.6}$$

where $S = \text{sgn}\ <\psi_T\, U_\sigma\, \psi_T>$. For finite β $<S>_M = \frac{Q}{Q_M}$ satisfies the inequalities: $0 <<S>_M \leq 1$ since $e^{-\beta H}$ is positive definite and $Q_M \geq Q$. However difficulties arise if the latter quantity $< S >_M$ becomes an arbitrary small number when $\beta \to \infty$.

As we will show in the next section $< S >_M$ is either bounded from below by $|<\psi_0\,|\,\psi_T>|^2$ or it vanishes exponentially with β for $\beta \to \infty$. In the latter case the mapping of the quantum many body system onto a classical system

described by the σ–variables is not well defined because expression (1.2.6), due to the vanishing denominator, becomes singular in this limit. On the other hand if $< S >_M \geq < \psi_0 \mid \psi_T >^2$ from the asymptotic behaviour of Q it follows that Q_M can replace Q in the calculation of ground state properties because:

$$E_M = \lim_{\beta \to \infty} \left[-\frac{1}{\beta} \ln Q + \frac{1}{\beta} \ln < S >_M \right] = E_0 \tag{1.2.7}$$

This means that the actual value of the average sign does not affect the previous limit and it does not appear in the physical quantity obtained by differentiating E_0 with respect to some external field as in (1.1.8), if $< S >_M \geq < \psi_0 \mid \psi_T >^2$ holds independently from the external perturbation $\lambda \hat{O}$. In fact by differentiating $E_M(\lambda)$ with respect to λ, instead of expression (1.2.6) we get a simplified and convenient form which does not depend on the average sign $< S >_M$:

$$\frac{\partial E_M(\lambda)}{\partial \lambda} = < E_0(\sigma) >_M \tag{1.2.8}$$

This gives the same expectation values of the exact (1.2.6) if the average sign does not vanishes even in presence of perturbations because $E_0(\lambda)$ is in this case identically equal to $E_M(\lambda)$. In section 5 it will be shown that this further requirement is not necessary in some cases. Therefore if $< S_M >_\beta \geq < \psi_0 \mid \psi_T >^2$ the way to relate averages in the Q ensemble with those in the Q_M ensemble as in (1.2.6) is an unnecessary complicated procedure.

Use of Q_M as a classical partition function presents some technical difficulties because the corresponding classical potential

$$V_\sigma^M = -\ln | < \psi_T \mid U_\sigma \mid \psi_T > | \tag{1.2.9}$$

is singular along the nodal surface $< \psi_T \, U_\sigma \, \psi_T > = 0$. A more convenient "pseudo" partition function[31] is obtained by replacing in the integrand of the original

"pseudo" partition function Q the norm of the propagated wavefunction:

$$Q_N^\beta(\psi_T) = \int d\mu_\sigma \left\| \hat{U}_\sigma \,|\, \psi_T > \right\| \tag{1.2.10}$$

Analogously the corresponding classical potential and the asymptotic energy are defined as:

$$\begin{aligned} E_N &= \lim_{\beta\to\infty} -\frac{1}{\beta} \ln Q_N^\beta \\ V_N(\sigma) &= -\ln \left\| \hat{U}_\sigma \,|\, \psi_T > \right\| \end{aligned} \tag{1.2.11}$$

The weight in (1.2.10) never vanishes because the norm of the wavefunction $\psi_t = U_\sigma(t,0)|\psi_T >$ propagated at any given finite imaginary time t is always positive. In fact after the application of $e^{-\hat{h}_i \Delta\tau}$ (1.1.23) to ψ_t the norm of the propagated wavefunction $\psi_{t+\Delta\tau}$ at the time $t+\Delta\tau$ cannot decrease faster than $e^{-E_{\max}\Delta\tau}$ (see 1.1.24) since $\hat{h}_i$ has a maximum eigenvalue ($\|\psi_{t+\Delta\tau}\|^2 =< \psi_t|e^{-\hat{h}_i\Delta\tau}|\psi_t > \geq e^{-2E_{\max}\Delta\tau}$). Then for any finite β the integrand of Q_N^β has to verify the bound:

$$\| U_\sigma|\psi_T > \| \geq e^{-E_{\max}\beta} \tag{1.2.12}$$

Analogously since $\hat{h}_i$ has a minimum eigenvalue (1.1.21):

$$\| U_\sigma|\psi_T > \| \leq e^{-E_{\min}\beta} \tag{1.2.13}$$

Hence the classical potential $V_N(\sigma)$ is always finite and smooth because from (1.2.12) and (1.2.13) satisfies:

$$\beta E_{\min} \leq V_N(\sigma) \leq \beta E_{\max} \tag{1.2.14}$$

It will be shown in section 3 that in any case $E_N = E_M$. Hence Q_N, as well as Q_M, can be used to calculate ground state properties if the condition $<S>_\beta \geq <\psi_0|\psi_T>^2$ is verified.

Chapter II

Positiveness of the statistical weight

In this chapter we study, as rigorously as possible, the asymptotic properties of the functionals $Q(\beta)$, $Q_M(\beta)$ and $Q_N(\beta)$ defined in the previous chapter, in the low temperature limit. The weight $Q(\beta)$ which was obtained by a straightforward application of the HST is not always positive definite and there is a difficulty of principle in interpreting it as a classical partition function. On the other hand the functionals Q_M and Q_N obtained by a small modification of the previous functional have always positive weight and do not present any difficulty in this sense. The basic question we would like to answer in this chapter is: under which conditions the asymptotic $\beta \to \infty$ ground state properties can be calculated by using these modified "classical partition functions" $Q_N(\beta)$ and $Q_M(\beta)$.

We found that there are many non trivial cases where these positive "classical partition functions" can be used instead of Q even when the weight appearing Q is not always positive definite.

However it remains an open question whether this property is valid in general as it will be discussed later, even though numerical cases have been found[24] in which this property does not seem to be satisfied.

2.1 An exact statement about the average sign of the weight in the asymptotic $T = 0$ limit

The asymptotic properties of the average sign of the functional Q introduced in section 1 can be related to the behaviour of Q and Q_M in this limit.

First of all we simply consider that $Q = <\psi_T e^{-H\beta}\psi_T>$ expressed in terms of the basis of the eigenstates ψ_i of H is

$$Q = \sum e^{-E_i\beta} <\psi_T|\psi_i>^2 \tag{2.1.1}$$

Since in the previous expression all the terms are positive Q can be bounded only by the ground state term of the previous sum:

$$Q \geq <\psi_0|\psi_T>^2 \; e^{-E_0\beta} \tag{2.1.2}$$

Now let us consider the properties of Q_M^β (1.2.4). Using the result (A2.4) of app.2 for $\psi_i = \psi_j = |\psi_T>$ one has that

$$(Q_M^\beta)^2 \leq Q_M^{2\beta} \tag{2.1.3}$$

The previous relation is typically satisfied by usual classical partition function and simply means that the Q_M^β behaves in an exponential way for $\beta \to \infty$. More rigorously we consider the sequence of "finite temperature free energies":

$$E_M(k) = -\frac{1}{\beta_k} \ln Q_M^{\beta_k} \tag{2.1.4}$$

for $\beta_k = 2^k \beta_0$, then from (2.1.3) it follows that

$$E_M(k+1) \leq E_M(k) \tag{2.1.5}$$

that is $E_M(k)$ is a monotonically decreasing sequence. On the other hand from the definition (1.2.4) the integrand in $Q_M(\beta)$ has always a maximum value for any field configuration (see 1.1.24):

$$| < \psi_T U_\sigma \psi_T > | \leq \|U_\sigma |\psi_T >\| \leq \exp -E_{\min}\beta. \tag{2.1.6}$$

By integrating both the positive sides of the previous inequality in $[d\mu_\sigma]$ and, using that $\int [d\mu_\sigma] = 1$ (see 1.1.21), we find that $Q_M^\beta \leq e^{-E_{\min}\beta}$ and therefore the monotonic sequence $E(k)$ is always greater than $E_{\min}$. Hence, for the elementary convergence property of a bounded monotonic sequence, $E(k)$ converges to a finite limit say E_M and it is possible to define this quantity as:

$$E_M = \lim_{k\to\infty} -\frac{1}{\beta_k} \ln Q_M(\beta_k) \tag{2.1.7}$$

Then we can express for convenience $Q_M^{\beta_k}$ as a product of a function $h_M(\beta_k)$ times its asymptotic exponential factor:

$$Q_M^{\beta_k} = h_M(\beta_k) e^{-E_M \beta_k} \tag{2.1.8}$$

We now show that

$$h_M(\beta_k) \leq 1 \quad \forall k \tag{2.1.9}$$

In fact substituting expression (2.1.8) in the inequality (2.1.3) the exponential factors cancel and:

$$h_M(\beta_{k+1}) \geq (h_M(\beta_k))^2 \tag{2.1.10}$$

Suppose now that (2.1.9) is not true and, for some k_0, $h_M(\beta_{k_0}) = e^{\delta}$ with $\delta > 0$. We will show that this is not possible. In fact by iterating L times inequality (2.1.10) from k_0 to $k_0 + L$:

$$h_M(\beta_{k_0+L}) \geq e^{2^L \delta} \tag{2.1.11}$$

As shown previously, the limit (2.1.7) converges to E_M, however from (2.1.11) and the definition (2.1.8):

$$E_M = \lim_{k\to\infty} -\frac{1}{\beta_k} \ln Q_M^{\beta_k} = \lim_{L\to\infty} \left[-\frac{\ln h_M(\beta_{k_0+L})}{\beta_{k_0+L}} + E_M \right] \leq E_M - \frac{\delta}{\beta_{k_0}} \tag{2.1.12}$$

This is clearly not possible and (2.1.9) is proven.

It is now possible to characterize the asymptotic $\beta \to \infty$ limit of the average sign. In fact from definition of $< S >_M = \frac{Q}{Q_M}$ only two cases are possible.

a)

If $E_M \neq E_0$ the average sign exponentially vanishes with a well defined energy scale

$$\Delta = \lim_{k\to\infty} -\frac{1}{\beta_k} \ln S_M(\beta_k) = E_0 - E_M \tag{2.1.13}$$

b)

If $E_M = E_0$ from the bounds (2.1.2) and (2.1.9)

$$S_M(\beta_k) \geq \frac{<\psi_0|\psi_T>^2}{h_M(\beta_k)} e^{(-E_0+E_M)\beta_k} \geq <\psi_0|\psi_T>^2 \qquad \forall\beta_k \tag{2.1.14}$$

This also means that if for some finite β $S_M(\beta) < <\psi_0|\psi_T>^2$ the average sign is exponentially vanishing with β. On the other hand if case *(b)* applies $Q_M(\beta)$ can replace Q for the calculation of ground state properties (1.2.7).

In general both in case (a) and (b) from the definitions (1.1.7) and (1.2.5) $Q_M^\beta(\psi_T)$ is always greater than the "pseudo" partition function $Q^\beta(\psi_T)$. This means that

$$E_M \leq E_0 \tag{2.1.15}$$

and $\Delta \geq 0$.

2.2 Asymptotic property of a different but related partition function

For practical and theoretical purpose it is useful to consider the "pseudo"

partition function Q_N (1.2.10) which, as shown later, has the same asymptotic behaviour of Q_M. In fact given an arbitrary orthonormal basis of vectors $\{\Phi_i\}$ with $\Phi_0 = \psi_T$, using the completeness of any basis, the following relation simply holds:

$$\|U_\sigma \,|\, \psi_T >\|^2 = \sum |<\psi_T \, U_\sigma \, \Phi_i>|^2 < \left(\sum |<\psi_T \,|\, U_\sigma \,|\, \Phi_i>|\right)^2 \qquad (2.2.1)$$

and Q_N (1.2.10) can be bounded by:

$$Q_N^\beta(\psi_T) \leq \sum_j \int |<\psi_T \,|\, U_\sigma \,|\, \Phi_j>| \, d\mu_\sigma \qquad (2.2.2)$$

Using the inequality (A2.4) of app.2 for $\psi_i = \psi_T$ and $\psi_j = \Phi_j$ for each term in (2.2.2), we find that:

$$Q_N\,(\psi_T) \leq D\left(\int d\mu_\sigma \, |<\psi_T \,|\, U_\sigma(2\beta,0)\,|\,\psi_T>|\right)^{1/2} = D\left(Q_M^{2\beta}(\psi_T)\right)^{\frac{1}{2}}. \quad (2.2.3)$$

On the other hand $\|U_\sigma \,|\, \psi_T >\| \geq |<\psi_T \,|\, U_\sigma \,|\, \psi_T>|$. Then by integrating both sides of the previous inequality and using (2.2.3) one easily obtains a two–sided inequality satisfied by Q_N:

$$Q_M(\beta) \leq Q_N(\beta) \leq D\, Q_M^{1/2}\,(2\beta) \qquad (2.2.4)$$

It is therefore clear that:

$$\lim_{\beta\to\infty} -\frac{1}{\beta} \ln Q_M(\beta) = \lim_{\beta\to\infty} -\frac{1}{\beta} \ln Q_N(\beta) \qquad (2.2.5)$$

that is $E_M = E_N$ as was already mentioned.

This is also an instructive example showing that the "pseudo" partition function Q_M^β is essentially dominated by a well defined energy scale. This energy

scale is not affected at all even though the norm of the propagated wavefunction in Q_N^β replaces the absolute value of its overlap with the initial trial wavefunction as in Q_M^β. If this energy scale also dominates the asymptotic behavior of the original Q^β "pseudo" partition function we are in Case (b) in (2.1.14) and it is possible to define different but related "pseudo" partition functions such as Q_M and Q_N which are positive definite and give the same ground state properties of the many body quantum system.

2.3 Existence of the $T = 0$ limit and its dependence on the trial wavefunction

The existence of the limit

$$E_M = \lim_{\beta\to\infty} -\frac{1}{\beta} \ln Q_M^\beta(\psi_T) \tag{2.3.1}$$

was proven in Sect. 2 only for a particular sequence of the inverse temperature $\beta_k = 2^k\beta_0$. The limit (2.3.1) in principle can also depend on the initial β_0 in the chosen sequence. With a more detailed proof we show that the limit (2.3.1) is well defined and how it depends on the trial wavefunction ψ_T.

For this purpose we introduce two definitions which are standard in linear algebra (see for example [37]).

A subspace $\mathcal{D}$ of $\mathcal{H}$ is called invariant under a family of operators $\{\hat{O}_i\}$ if $\hat{O}_i\psi \subset \mathcal{D}$ for each operator O_i of the given family and all $\psi \in \mathcal{D}$.

An invariant subspace $\mathcal{D}$ (under the family $\{O_i\}$) is called irreducible if the only invariant subspace contained in $\mathcal{D}$ (under the family $\{\hat{O}_i\}$) are $\{0\}$ and $\mathcal{D}$.

In app.3 it is shown that a subspace of $\mathcal{H}$ is irreducible under the family of all the one body operators $U_\sigma(\beta,0)$ (1.1.22,23) if and only if it is irreducible under the family of all elementary hermitian one body operators which appear in $U_\sigma(\beta,0)$. For the specific HST chosen these operators are the kinetic term $\hat{K}$ and the local magnetic operators m_r used for the HST decoupling of the many body term. The problem of finding the irreducible subspaces of the infinite set of operators $U_\sigma(\beta,0)$ is therefore equivalent to find the irreducible subspaces of the finite set of elementary one body operators m_r and $\hat{K}$. Since all such operators are hermitian, to each irreducible subspace corresponds a complementary invariant subspace $\mathcal{H}-\mathcal{D}$. In this case the total Hilbert space can be written as a direct sum[36]:

$$\mathcal{H} = \mathcal{D}_1 \oplus \mathcal{D}_2 \oplus \ldots \oplus \mathcal{D}_n \tag{2.3.2}$$

where each subspace $\mathcal{D}_i$ is irreducible (and therefore invariant) under all the elementary operators that appear in $U_\sigma(\beta,0)$. From app.3 these subspaces are irreducible also under all the family of propagators U_σ. We notice that an irreducible subspace of any elementary operator (m_r and K) is also an invariant subspace of the Hamiltonian (1.1.1–3). In fact this Hamiltonian is simply written in terms of the kinetic term $\hat{K}$ and m_r:

$$H = K - \frac{U}{2}\sum_r m_r^2 + cost. \tag{2.3.3}$$

and of course an invariant subspace for all such elementary operators is also an invariant subspace of H. Hence the decomposition of the Hilbert space (2.3.2) also factorizes the hamiltonian $\hat{H}$ in invariant subspaces containing one or more energy levels.

The decomposition of the Hilbert space in the form (2.3.2) is useful to understand the dependence of the limit (2.3.1) on the trial wavefunction ψ_T.

In any irreducible subspace $\mathcal{D}$, defined with dimension $d \leq D$, we can consider a complete set of orthogonal vectors $\{\Phi_i\}$. For convenience we introduce more manageable "pseudo" partition functions defined in this subspace by means of the chosen complete set $\{\Phi_i\}$:

$$Q_M^*(\beta) = \max_{i,j} Q_{ij}^M(\beta) \tag{2.3.4}$$

where:

$$Q_{ij}^M = \int d\mu_\sigma \, |<\Phi_i|U_\sigma(\beta,0)\Phi_j>| \tag{2.3.5}$$

In app.4(a), we show that $Q_M^*(\beta)$ can be written for sequence of $\beta_k = 2^k\beta_0$ as a bounded function h_M^* times an exponential asymptotic factor:

$$Q_M^*(\beta_k) = h_M^*(\beta_k)e^{-E_{\beta_0}^*\beta_k} \tag{2.3.6}$$

with $h_M^*(\beta_k)$ such that:

$$\frac{1}{d} \leq h_M(\beta_k) \leq 1 \tag{2.3.7}$$

and

$$E^*_{\beta_0} = \lim_{k\to\infty} -\frac{1}{\beta_k} \ln Q^*_M(\beta_k) \tag{2.3.8}$$

In app.4*(b)* we show that the asymptotic energy $E^*_{\beta_0}$ (2.1.7) is independent of the particular choice of β_0 and let's call this energy in the following E^*. Therefore using (2.3.6–7) for $k = 0$ and $\beta_0 = \beta$ arbitrary

$$Q^*_M(\beta) = h^*_M(\beta) e^{-E^*\beta} \tag{2.3.9}$$

with $\frac{1}{d} \leq h^*_M(\beta) \leq 1$. This in fact ensures the convergence of the asymptotic energy:

$$E^* = \lim_{\beta\to\infty} -\frac{1}{\beta} \ln Q^*_M(\beta) \tag{2.3.10}$$

without restriction on a particular sequence of inverse temperature β_k as in (2.1.7). In fact after substitution of (2.3.9) in the limit (2.3.10) the bounded function $h^*_M(\beta)$ gives a contribution that vanishes at least as $\frac{1}{\beta}$. Moreover in app.4*(c)* we show that the value of E^* does not depend on the particular choice of the basis $\{|\Phi_i>\}$ in $\mathcal{D}$ and this basis is not restricted to be an orthonormal basis.

At this point we need to relate the limit (2.3.10) with the original one (2.3.1) defined with a given trial wavefunction ψ_T. In app.5 we show that if ψ_T belongs to a given irreducible subspace $\mathcal{D}$ the limit (2.3.1) we are interested in, exists and converges to the same value E^* previously considered in (2.3.10). Thus since E^* does not depend on ψ_T in $\mathcal{D}$ the limit (2.3.1) does not depend on the trial

wavefunction too. In general if the trial wavefunction has non zero component in more than a single irreducible subspace we can write ψ_T as a sum:

$$\psi_T = \sum_i |\Phi_i > \tag{2.3.11}$$

with each $|\Phi_i >$ belonging to a definite irreducible subspace. Since the propagator U_σ always leaves orthogonal wavefunctions which belong to different irreducible subspaces, $Q_M(\psi_T)$ can be expressed as a simple sum:

$$Q_M^\beta(\psi_T) = \sum Q_M^\beta(\Phi_i) \tag{2.3.12}$$

The limit (2.3.1) still is well defined and converges to the minimum possible energy E_i^* corresponding to each irreducible subspace where ψ_T has non vanishing component:

$$E_M = \lim_{\beta\to\infty} -\frac{1}{\beta} \ln Q_M^\beta(\psi_T) = \min_i E_i^* \tag{2.3.13}$$

This property is analogous to the convergence property of the "pseudo" partition function Q. It is in fact dominated, as it is easily seen in in (2.1.1), by the minimum possible eigenvalue of $\hat{H}$ such that ψ_T has non vanishing overlap with the corresponding eigenstate. It should be noted however that, since U_σ mixes many different states with different symmetries conserved by the hamiltonian H, the decomposition of the Hilbert space in irreducible subspace is usually trivial ($\mathcal{H} = \mathcal{H}$) or at most containing only a few different subspaces which are therefore much less than the total number of energy levels. The chosen HST (1.1.14) obviously conserves the total number of particles and the total magnetization along the z–axis. However it is very interesting that another kind of conserved quantity is useful to classify the different irreducible subspaces. In fact the charge

conjugation symmetry, also described later (2.4.14), applied only to the spin up particles:

$$d^{+}_{i\uparrow} = (-1)^i c_{i-\uparrow} \tag{2.3.14}$$

turns the magnetic operators into density like operators $m_r = 1 - n^d_r$, if the d operators are used (d–representation). On the other hand, due to the factor $(-1)^i$ in (2.3.14) the kinetic term remains unchanged under the considered transformation. In the d-representation it is easy to realize that the elementary operators K and $1 - n^d_r$ appearing in U_σ are spin independent and therefore the total spin $(S^d)^2$ and S^d_z are conserved. Going back to the original c–representation we find that correspondingly $(S^d)^2$ turns into a special kind of operator which commutes with the hamiltonian:

$$(S^d)^2 = (S^d_z)^2 + \frac{1}{2}\sum_{ij}(-1)^{i+j}\left\{c_{i\uparrow}c_{i\downarrow}c^{+}_{j\downarrow}c^{+}_{j\uparrow} + c_{i\downarrow}c_{i\uparrow}c^{+}_{j\uparrow}c^{+}_{j\downarrow}\right\} \tag{2.3.15}$$

where S^d_z is simply $\frac{N_a - N}{2}$. Hence the irreducible representations of the chosen HST can be labelled by the following quantum numbers: the total number of particles N, the total magnetization $N^{\uparrow} - N^{\downarrow}$ and the total spin $s^d(s^d+1)$ corresponding to spin up holes and spin down particles. As an example in a 4×4 Hubbard model with 10 electrons and without z–magnetization the number of eigenstates of H is $\binom{16}{5}^2 \simeq 2\,10^7$, while the number of irreducible subspaces is equal to to the number of different eigenvalues of $(S^d)^2$, in the d–representation:

$$s^d(s^d+1) \quad with \quad s^d = 3, 4, \ldots, 8 \tag{2.3.16}$$

2.4 Some tractable examples

For some particular tractable cases it is possible to state rigorously if the average sign saturates for infinite β (case (b) in 2.1.14) or it vanishes exponentially (case (a) in 2.1.13).

Case (a)

1 *Trial wavefunction orthogonal to the ground state*

After all we give a simple example characterized by the exponential decay of the average sign. The ground state of $\hat{H}$ is assumed non degenerate and, as usual, we indicate with E_1 the first excited energy level.

As noted in the previous section the decomposition of the Hilbert space in irreducible subspaces $\mathcal{D}_i$ also factorizes the Hamiltonian $\hat{H}$ in invariant subspaces containing one or more energy levels. Therefore within the factorization (2.3.2) there exists an irreducible subspace $\mathcal{D}_0$ containing ψ_0 the ground state of $\hat{H}$. In most cases this irreducible subspace $\mathcal{D}_0$ contains several vectors, namely his dimension d_0 is greater than one. In fact if the opposite were true $U_\sigma(\beta,0)\,|\psi_0>$ would be always proportional to ψ_0. This means that the ground state of $\hat{H}$ would be an eigenstate of all the possible one–body propagators $U_\sigma(\beta,0)$. Of course the latter circumstance is very unlikely and trivial. For the chosen HST (1.1.14) this indeed occurs for $U=0$ or for the completely filled case with two electrons per site. In this case the Hilbert space contains only one independent vector. Hereafter it is therefore assumed that $d_0 > 1$.

Then we can choose a trial wavefunction ψ_T orthogonal to the ground state ψ_0 but still having a non-zero component in $\mathcal{D}_0$.

Since ψ_T is orthogonal to the ground state the "pseudo" partition function Q (2.1.1) behaves asymptotically at most as:

$$Q(\beta) < e^{-E_1\beta} \tag{2.4.1}$$

Therefore for a trial wavefunction orthogonal to the ground state and having some component in the irreducible subspace $\mathcal{D}_0$, the average sign given by $< S >_\beta = \frac{Q}{Q_M^\beta}$ decays exponentially with an exponent Δ that is greater than 0, namely from (2.4.1) and (2.1.15):

$$\Delta \geq E_1 - E_0 \tag{2.4.2}$$

This result shows that in the Q functional (1.1.20) the more stable components of the ground state are cancelled out due to the sign changes of $< \psi_T U_\sigma \psi_T >$. However in the $Q_M - Q_N$ ensemble these cancellation cannot occur and they behave exponentially with a larger exponent. This in turns determines the vanishing of the average sign $\frac{Q}{Q_M}$ as $\beta \to \infty$.

We remark at the end of this section that it is a very important property of the HST to preserve the antisymmetry of the propagated wavefunction. In fact we can consider the fermion Hilbert space as a particular subspace of the many body Hilbert space of distinguishable particles and define U_σ in this larger Hilbert space. It is a non trivial property that the fermion subspace is left invariant by U_σ for any σ–configuration —the fermion subspace is an invariant subspace for all the family of one body propagators U_σ—. In fact a Slater determinant remains a Slater determinant trough the one–body propagation U_σ, that is the antisymmetry is always preserved. From the linear property of U_σ, the same holds for any generic

antisymmetric wavefunction. This property seems to be the basic advantage of the HST compared with other fermion QMC[14-16,19] methods. As an example in the GFMC the resulting exponential instability is determined by an energy scale Δ (similar to 2.4.2) given by the difference between the boson and the fermion ground state energy. On the contrary in the HST formulation the boson subspace is always orthogonal to $U_\sigma \psi_T$ and a possible exponential instability in the method is by no means determined by the attraction to the underlying boson ground state.

Case (b)

In the following we describe a list of cases satisfying the condition (b) in (2.1.14) i.e. the average sign is always bounded by a constant $< \psi_0 | \psi_T >^2$. For all the cases (half filled, small U, one dimension, negative U Hubbard models) we will show that:

for any element of a properly chosen complete set of wavefunctions $\{\Phi_i\}$, $Q_M^\beta(\Phi_i)$ *does not grow faster than* $\exp(-\beta E_0)$:

$$Q_M^\beta(\Phi_i) \leq \exp(-\beta E_0) \ \forall \Phi_i \tag{2.4.3}$$

This in fact ensures that for any trial wavefunction ψ_T *non orthogonal to the ground state, the quantity* $S_M(\beta)$ *is always bounded.*

In fact let us consider a generic trial wavefunction ψ_T with non-zero overlap with the ground state and the Q_N "pseudo" partition function, introduced in the previous section. In the integrand of $Q_N^\beta(\psi_T)$ we can express the trial wavefunction

as a linear combination of vectors of the chosen basis $\psi_T = \sum a_i |\Phi_i>$:

$$Q_N(\psi_T) = \int d\mu_\sigma \left\| \sum_i a_i U_\sigma(\beta,0)|\Phi_i> \right\|. \tag{2.4.4}$$

So using the triangular inequality in the integrand of Q_N^β and that $Q_N(\psi_T) \geq Q_M(\psi_T)$, $Q_M^\beta(\psi_T)$ satisfies the following bound:

$$Q_M^\beta(\psi_T) \leq Q_N^\beta(\psi_T) \leq \sum |a_i| Q_N^\beta(\Phi_i) \tag{2.4.5}$$

Since by assumption $Q_M(\Phi_i) \leq e^{-\beta E_0}$, from (2.16) each $Q_N^\beta(\Phi_i)$ in the RHS of the previous inequality is smaller than a constant times $e^{-\beta E_0}$.

This means that the energy scale E_M defined in (2.3.1) is not lower than E_0. This together with the opposite bound (2.1.15) gives:

$$E_0 = E_M \tag{2.4.6}$$

for any trial wavefunction non orthogonal to the ground state. Finally using the result of Sect.2 (2.1.14) $S_M(\beta) \geq <\psi_0|\psi_T>^2$ for any β.

In principle this condition is not enough to ensure that the correlation functions can be calculated by differentiating E_M with respect to some external parameter as in (1.2.8). In fact the average sign could vanish as soon as the perturbation $\lambda \hat{O}$ is added to the kinetic term in U_σ^λ.

Whenever $S_M(\beta) \geq <\psi_0|\psi_T>^2$ is satisfied a sufficient condition for calculating correlation functions even in case $<S> < 1$ is that
(i) the trial wavefunction ψ_T belongs to the irreducible subspace D_0 containing the ground state ψ_0, and

(ii) D_0 *is also an irreducible subspace for all the family of propagators* U_σ^λ.

If $\mathcal{D}_0$ is irreducible under all the family of propagators $U_\sigma^\lambda(\beta,0)$ (see 1.1.22) and ψ_T belongs to $\mathcal{D}_0$, $E_M(\lambda)$ does not depend on the particular chosen trial wavefunction in D_0, as shown in Sect.3. In particular $E_M(\lambda)$ will remains unchanged even using ψ_0 as a trial wavefunction and:

$$\left.\frac{\partial E_M(\lambda)}{\partial\lambda}\right|_{\psi_T}^{\lambda=0} = \left.\frac{\partial E_M(\lambda)}{\partial\lambda}\right|_{\psi_T=\psi_0}^{\lambda=0} \tag{2.4.7}$$

On the other hand for any finite β one has (1.2.8):

$$\left.\frac{\partial E_M}{\partial\lambda}\right|_{\psi_T=\psi_0}^{\lambda=0} = < E_0(\sigma) >_M \ . \tag{2.4.8}$$

Since, $S_M(\beta) = 1$ from eq.(2.1.14), for $\psi_T = \psi_0$ the Q_M average denoted by $<>_M$ is exactly equivalent to the true average. Then for infinite β (2.4.8) gives the ground state expectation value of the desired operator and therefore by (2.4.7):

$$\left.\frac{\partial E_M(\lambda)}{\partial\lambda}\right|_{\psi_T}^{\lambda=0} = \left.\frac{\partial E_M(\lambda)}{\partial\lambda}\right|_{\psi_T=\psi_0}^{\lambda=0} \rightarrow < \psi_0 \hat{O} \psi_0 > \tag{2.4.9}$$

In the following in order to satisfy condition (2.4.3) we choose a basis set of states Φ_i in the Hilbert space of fixed number of spin up $N_\uparrow$ and spin down $N_\downarrow$ particles. Without loss of generality we choose each vector Φ of this basis, as a product of a spin up and a spin down part

$$\Phi = \psi_\uparrow \otimes \psi_\downarrow \tag{2.4.10}$$

where

$$\psi_\alpha = \sum f_\alpha(x_1, x_2, \ldots, x_{N_\alpha})\, c^+_{x_1,\alpha} \ldots c^+_{x_{N_\alpha},\alpha} |O_\alpha > \qquad (2.4.11)$$

and $|O_\alpha >$ is the vacuum state of spin–α particles. Since U_σ is a simple product of one spin component operators $U_\sigma = U^\uparrow_\sigma U^\downarrow_\sigma$ the integrand in (1.1.20) can be written as:

$$< \Phi\, U\, \Phi > = < \psi^\uparrow\, U^\uparrow_\sigma\, \psi^\uparrow > < \psi^\downarrow\, U^\downarrow_\sigma\, \psi^\downarrow > \qquad (2.4.12)$$

Using the statement (2.4.3) we are going to examine separately each case where the sign does not vanish for infinite β for any trial wavefunction non orthogonal to the ground state.

1 *Half filled case in a bipartite lattice*

The basis set of states Φ_i are in this case the complete set obtained by all the possible Slater determinants made up by orbitals defined in a given site: ψ_α in this case is

$$\psi_\alpha = c^+_{r_1\alpha} \ldots c^+_{r_{N_\uparrow}\alpha} |O_\alpha > \qquad (2.4.13)$$

where the corresponding f_α (2.4.11) is non vanishing only for particular values of x_i. In particular the states belonging to this complete set which do not contain double occupancy are invariant under the following charge conjugation transformation which is possible for a bipartite lattice:

$$d^+_{i\sigma} = (-1)^i\, c_{i\,-\sigma} \qquad (2.4.14)$$

Here in (2.4.14) it is understood that the factor $(-1)^i$ has definite sign on each of the two different sublattices. Moreover in (2.4.13) the vacuum in the c–representation must be substituted by the vacuum in the d–representation

$$|O_\alpha >_d = \prod_{i=1}^{N_\alpha} c^+_{i\alpha} |O_\alpha > \tag{2.4.15}$$

More generally the previous transformation is defined in the Hilbert space of fixed number of spin up $N^\uparrow$ and spin down $N^\downarrow$ particles only when the condition $N_\uparrow + N_\downarrow = N_a$ (half filled case) is fulfilled. Note that the hamiltonian $\hat{H}$ after this transformation remains unchanged (apart for constant in this Hilbert space), therefore the transformation (2.4.14) is a discrete symmetry of the considered half filled Hubbard Hamiltonian.

By applying the transformation (2.4.14) to each spin up and spin down component of $<\Phi\, U_\sigma\, \Phi>$ it is easily verified that for the invariant states without double occupancy:

$$<\psi^\uparrow U^\uparrow_\sigma \psi^\uparrow> = \exp \sum_{r,l} \sigma_{r,l} \; <\psi^\downarrow U^\downarrow_\sigma \psi^\downarrow>$$

$$<\psi^\downarrow U^\downarrow_\sigma \psi^\downarrow> = \exp -\sum_{r,l} \sigma_{r,l} \; <\psi^\uparrow U^\uparrow_\sigma \psi^\uparrow> \tag{2.4.16}$$

and it follows that for such states the integrand in Q is always positive definite, in fact:

$$<\Phi\, U_\sigma\, \Phi> = \exp -\sum \sigma_{r,i} \; <\psi_\uparrow U^\uparrow \psi_\uparrow>^2 = \exp \sum \sigma_{r,i} \; <\psi_\downarrow U^\downarrow_\sigma \psi_\downarrow>^2 \tag{2.4.17}$$

Hence

$$Q^\beta_M(\Phi_i) = Q^\beta(\Phi_i) \leq e^{-E_0\beta} \tag{2.4.18}$$

for any element of the basis $\{\Phi_i\}$ not containing double occupancy.

Let us consider now a generic element of the chosen basis Φ_i without restriction about double occupancy. Any element of the basis is not in general invariant under the transformation (2.4.14). In fact given an arbitrary determination of the spin up (spin down) part $\psi^\uparrow$ ($\psi^\downarrow$), in order to have a symmetric state the $\psi^\downarrow$ ($\psi^\uparrow$) part is univocally defined by (2.4.14) in the sites which are not occupied by the spin up (spin down) particles. In the following we formally indicate with $\psi_\downarrow = c\psi^\uparrow$ ($\psi^\downarrow = c\psi^\uparrow$) the spin down (up) part of the state (2.4.10) obtained by applying the previous transformation (2.4.14) to the spin up (down) part of the state (2.4.10). $\psi^\uparrow \otimes c\psi^\uparrow$ and $c\psi^\downarrow \otimes \psi^\downarrow$ are states without double occupancy and therefore satisfying (2.4.18). Now it is shown in app.6 that for any state Φ_i of the form (2.4.10–13) the "pseudo" partition function Q_M is bounded by the "pseudo" partition function Q of corresponding states with no double occupancy:

$$Q_M(\psi^\uparrow \otimes \psi^\downarrow) \leq \sqrt{Q(\psi^\uparrow \otimes c\psi^\uparrow)Q(c\psi^\downarrow \otimes \psi^\uparrow)} \tag{2.4.19}$$

Then, using (2.4.18), condition (2.4.3) is satisfied for any element of the chosen basis.

2 $U < 0$ *with* $N_\uparrow = N_\downarrow$

Even in this case we apply the statement of this section for the particular basis of Slater determinants Φ_i containing only localized orbitals.

The chosen Hubbard–Stratonovich transformation for $U < 0$ (see eqs. 1.1.11–13) determines a propagator $U_\sigma = U_\sigma^\uparrow U_\sigma^\downarrow$ which acts in the same way on both

the spin components. So we have that those states of the form (2.4.10) such that $\psi_\uparrow$ and $\psi_\downarrow$ are defined in the same sites (the opposite case with respect to the half-filled case) always determine a positive integrand in Q . In fact in this case:

$$< \psi_T \, U_\sigma \, \psi_T > = < \psi^\uparrow \, U_\sigma^\uparrow \, \psi^\uparrow >^2 \tag{2.4.20}$$

is always positive for such trial wavefunctions. Analogously to the preceeding case (see app.3), since $Q_M(\psi^\uparrow \otimes \psi^\downarrow) \leq \sqrt{Q(\psi^\uparrow \otimes \psi^\uparrow) Q(\psi^\downarrow \otimes \psi^\downarrow)}$, (2.3.14) is verified too for any element of the chosen basis.

3 *1D case*

For wavefunctions of the form (2.3.8) we define f_α in such a way that in the region described by:

$$1 < x_1^\alpha < x_2^\alpha < \ldots < x_{N^\alpha}^\alpha \tag{2.4.21}$$

f is always positive. All the other regions of the space are obtained by antisymmetric permutation. So we restrict f_α to have a given "nodal surface". We will show in the following that U_σ^α does not modify such nodal surface of f_α and one has that $< \psi^\alpha \, U_\sigma \, \psi^\alpha >$ is always positive for any field configuration. In fact U_σ^α is a product of operators diagonal in real space, that clearly do not change the nodal surface of f_α and kinetic short time propagators $e^{-\Delta\tau \hat{K}}$ that in principle could change this nodal surface. However it is possible to show that, in 1D with periodic boundary conditions, if both $N^\uparrow$ and $N^\downarrow$ are odd, $-\Delta\tau \hat{K} f_\alpha$ is always positive when f_α is positive.

In fact after the application of $-K\Delta\tau$ to a function of the form (2.4.10) the

corresponding f_α changes as (Lieb and Wu[37]):

$$f'_\alpha = D\tau \sum_{i=1}^{N_a} \sum_{s=\pm 1} f_\alpha(x_1 \dots x_{i+s} \dots x_{N^\alpha}) \tag{2.4.22}$$

Since the kinetic term is local the only possible change of sign in the RHS of (2.4.22) occurs when the kinetic term hops electrons at the boundary $x_1^\alpha = 1$ or $x_N^\alpha = N_a$. In this case the change of sign is completely determined by $N^\alpha - 1$ permutation to obtain the same order: i.e. $(-1)^{N^\alpha - 1}$. From the Taylor expansion of the propagator $e^{-\Delta\tau\hat{K}}$ it also follows that $e^{-\Delta\tau\hat{K}} f_\alpha$ is always positive in the region (2.4.21) if f_α is positive. Hence we finally get that $U_\sigma^\alpha \psi_\alpha$ has always the same nodal surface and the overlap $<\psi_\alpha U_\sigma^\alpha \psi_\alpha>$ is clearly positive for any σ.

It is in general possible to choose a complete set of states of the form (2.4.10) with the restriction that $f_\alpha \geq 0$ in the region (2.4.21). For example we can choose the complete set of localized states Φ_i considered before and pay attention to the phase determination of each Φ_i in order to satisfy $f_\alpha \geq 0$. Also in this case $Q_M(\Phi_i) = Q(\Phi_i) \leq e^{-\beta E_0}$ for any element of the basis and condition (2.4.3) is verified.

Clearly the same statement holds for even number of $N_\uparrow$ and $N_\downarrow$ particles with antisymmetric boundary conditions or for any filling but with open chains.

In conclusion in one dimension, the possible vanishing of the average sign only depend on the boundary conditions and therefore has no important physical meaning.

4 small U for "closed shell"

In the following we restrict our analysis to cases where:

i) The HST is real. This can be always obtained for general real fermion hamiltonian with two body interaction (see app.1).

ii) The auxiliary fields used in the HST decomposition of the two body term are defined in a bounded region $|\sigma| < \Lambda$ as for the particular HST (1.1.18–19). Λ is arbitrary small for sufficiently weak interaction and fixed Trotter discrete time $\Delta\tau$ as in (1.1.15) and (1.1.16).

iii) The ground state of the kinetic term is non degenerate. This is the case for particular number of electrons that, for a fixed size, fill the outermost "shell" of the kinetic term. Hence we define $\Delta_K > 0$ as the gap between the first excited energy and the ground state E_K of the kinetic term $\hat{K}$.

We will show in the following that, if the previous conditions are satisfied, the normalized propagated wavefunction $\frac{U_\sigma(\beta,0)|\psi_T>}{\|U_\sigma(\beta,0)|\psi_T>\|}$ is always close to the state ψ_K if the trial wavefunction ψ_T is close to ψ_K and U is sufficiently small.

If:

(iv)

$$\|\psi_T - \psi_K\| < \frac{\sqrt{2}}{4} \tag{2.4.23}$$

and

(v)

$$\frac{2\sqrt{\Lambda N_a}}{1 - e^{\frac{-\Delta_k \Delta\tau}{2}}} < \frac{\sqrt{2}}{4} \tag{2.4.24}$$

which is possible from (ii) for sufficiently small U

then

$$\left\| \frac{U_\sigma|\psi_T>}{\|U_\sigma|\psi_T>\|} - \psi_T \right\| < \sqrt{2} \tag{2.4.25}$$

or equivalently since the distance between two unit vectors is simply related to their overlap one has that:

$$<\psi_T|U_\sigma|\psi_T> > 0 \tag{2.4.26}$$

for any field configuration and ψ_T satisfying (iv). It is clear that in a neighborhood of ψ_T it is always possible to choose a complete set of independent vectors $\{\Phi_i\}$ and for such wavefunctions we have from (2.4.26) that $Q_M(\Phi_i) = Q(\Phi_i)$ and (2.4.3) is satisfied too.

The propagation $\frac{U_\sigma(\beta,0)|\psi_T>}{\|U_\sigma(\beta,0)|\psi_T>\|}$ at each trotter time slice $\{i\}$ can be iteratively calculated by applying a systematic evolution due to the kinetic term:

$$|\psi_{2i+1}> = \frac{\exp -\Delta\tau K|\psi_{2i}>}{\|\exp -\Delta\tau K|\psi_{2i}>\|} \tag{2.4.27}$$

and a stochastic evolution produced by the fields $\sigma_{r,i}$:

$$|\psi_{2i+2}> = \frac{\exp \sum \sigma_{ri} m_r |\psi_{2i+1}>}{\|\exp \sigma_{ri} m_r |\psi_{2i+1}>\|} \tag{2.4.28}$$

The assertion (2.4.25) is essentially based on the stability of the imaginary time evolution in the sphere of unit real vectors. After the application of an imaginary time propagator as $e^{-\beta\hat{K}}$ any real wavefunction non orthogonal to the ground state of $\hat{K}$ tends to become parallel to it in an exponential way. It is clear therefore (see app.7) that, after the application of the iteration (2.4.27) and, if ψ_{2i}

and ψ_K are sufficiently close, the distance between ψ_{2i+1} and ψ_K decreases by a factor α with respect to the distance between ψ_{2i} and ψ_K:

$$\|\psi_{2i+1} - \psi_K\| < \alpha \|\psi_{2i} - \psi_K\| \tag{2.4.29}$$

with $\alpha < e^{-\frac{\Delta_K}{2}\Delta\tau}$ if:

$$<\psi_{2i}|\psi_K>^2 > \frac{1}{2} \tag{2.4.30}$$

It is remarkable that this property does not hold for complex wavefunction because after the propagation this wavefunction can acquire an extra phase factor. This is the reason why we need a real HST (i) because in this case we can limit ourselves to a real basis and a real trial wavefunction.

Using the property (2.4.29–30) we first show that the distance between the ground state of K and the propagated wavefunction remains always small during the propagation for sufficiently small value of the interaction. In fact suppose that at a given time slice i

$$<\psi_{2i}|\psi_K>^2 > \frac{1}{2} \tag{2.4.31}$$

Then from the triangular inequality:

$$\|\psi_{2i+2} - \psi_k\| \leq \|\psi_{2i+2} - \psi_{2i+1}\| + \|\psi_{2i+1} - \psi_K\| \tag{2.4.32}$$

Using the property (2.4.29–30) the second term in the RHS of the previous relation is easily bounded:

$$\|\psi_{2i+1} - \psi_K\| \leq e^{-\frac{\Delta}{2}K\Delta\tau}\|\psi_{2i} - \psi_K\| \tag{2.4.33}$$

We now have to estimate the first term in (2.4.32). The variables $|\sigma_r|$ are always bounded by Λ defined in (1.1.16) which is proportional to $\sqrt{U\Delta\tau}$, and therefore

the operator $\exp \sum \sigma_r m_r$ appearing in (2.4.28) has a maximum ($< \exp \Lambda N_a$) and a minimum positive eigenvalue ($> \exp -\Lambda N_a$). Hence in the expression (2.4.32) the distance $\|\psi_{2i+2} - \psi_{2i+1}\|$ is easily estimated:

$$\begin{aligned} \|\psi_{2i+2} - \psi_{2i+1}\|^2 &= 2 - 2\frac{<\psi_{2i+1} \exp \sum \sigma_r m_r \psi_{2i+1}>}{<\psi_{2i+1} \exp 2\sum \sigma_r m_r \psi_{2i+1}>^{\frac{1}{2}}} \\ &\leq 2 - 2\exp -2\Lambda N_a < 4\Lambda N_a \end{aligned} \tag{2.4.34}$$

Using the two previous bounds the inequality (2.4.32) now becomes a linear relation that can be conveniently iterated:

$$\|\psi_{2i+2} - \psi_K\| \leq e^{-\frac{\Delta_K}{2}\Delta\tau}\|\psi_{2i} - \psi_K\| + 2\sqrt{\Lambda N_a} \tag{2.4.35}$$

In fact if U satisfies (v) one can apply the previous relation for each Trotter slice i provided (iv) is satisfied by the initial trial wavefunction, namely after l iterations with $\psi_{i=0} = \psi_T$:

$$\begin{aligned} \|\psi_{2l} - \psi_K\| &\leq \exp -\frac{\Delta_K}{2}\Delta\tau l \, \|\psi_T - \psi_K\| + 2\sqrt{\Lambda N_a}\sum_{j=0}^{l-1} \exp -\frac{\Delta_K}{2}\Delta\tau j \\ &\leq \|\psi_T - \psi_K\| + \frac{2\sqrt{\Lambda N_a}}{1 - \exp -\frac{\Delta_K}{2}\Delta\tau} \leq \frac{\sqrt{2}}{2} \end{aligned} \tag{2.4.36}$$

where in the latter inequality we have used (iv) and (v).

Finally the main statement (2.4.25) and (2.4.24) follow from the triangular inequality and (2.4.36), in fact:

$$\|\psi_{2l} - \psi_T\| \leq \|\psi_{2l} - \psi_K\| + \|\psi_K - \psi_T\| \leq \frac{\sqrt{2}}{2} + \frac{\sqrt{2}}{4} < \sqrt{2} \tag{2.4.37}$$

For any imaginary time l.

From (2.4.26) the exponential instability ($\Delta \neq 0$) in the HST formulation is surely not present for sufficiently small U say $U \leq U_c$ and

$$E_M = E_0 \quad for \ \ all \ \ U \leq U_c. \tag{2.4.38}$$

Therefore E_M has *the same perturbative expansion* of the true ground state energy. This is a very remarkable property. In fact if for some $U > U_c$ the exponential instability appears, it is a non perturbative effect that may be related to some interesting feature of strongly correlated systems.

Chapter III

Stochastic approach and Langevin dynamic

3.1 Importance sampling

The problem of evaluating a multidimensional integral with a stochastic approach is based on the idea of importance sampling.

A general integral

$$I = \int [d\sigma]\, P(\sigma) \tag{3.1.1}$$

can be decomposed in a product of a weight function $w(\sigma)$ time another function $A(\sigma)$:

$$P(\sigma) = A(\sigma)\, w(\sigma) \qquad with \int [d\sigma]\, w(\sigma) = 1 \tag{3.1.2}$$

The decomposition $P(\sigma) = A(\sigma)w(\sigma)$ is arbitrary and $w(\sigma)$ could be chosen as a uniform distribution. However in order to improve the efficiency of the numerical calculation, it is important that w is large when the value of P is large. In this way the configurations "randomly generated" of σ are concentrated in the region

where w, and hopefully P, is large. This is the so-called "importance sampling" strategy.

Thus the problem is the evaluation of a classical thermal average :

$$I = \frac{\int [d\sigma]\, e^{-\frac{V}{T}}\, E(\sigma)}{\int [d\sigma]\, e^{-\frac{V}{T}}} \qquad (with\, T = 1) \tag{3.1.3}$$

where the potential V is defined up to a constant: $V = -\ln w(\sigma) + const$ and T is an effective temperature of the classical system. With a statistical method we can generate configuration of σ according to the probability function $w(\sigma)$. For this purpose one can use either a Monte–Carlo algorithm or a molecular–dynamics strategy: one simply consider the system with σ-degrees of freedom in the fictitious classical potential V. As it will be discussed in Sect.3.2 a convenient algorithm consist in considering the variables σ to be function of a formal continuous time variable s. Then the relevant σ configurations are generated by integrating the Langevin equations (LE), i.e.:

$$\frac{d\sigma_i}{ds} = -\frac{\partial V}{\partial \sigma_i} + \eta_{\sigma_i} \tag{3.1.4}$$

and η_{σ_i} are gaussian random variables with zero mean and variance:

$$< \eta_{\sigma_i}(s)\, \eta_{\sigma_j}(s') > = \; 2T\delta_{ij}\delta(s - s') \tag{3.1.5}$$

Using this property, the statistical evaluation of classical expectation values of estimators $E(\sigma)$ depending on the variables σ can be expressed as a temporal average.

$$< E(\sigma) > = \frac{\int [d\sigma] w(\sigma) E(\sigma)}{\int [d\sigma] w(\sigma)} = \lim_{s \to \infty} \frac{1}{(s - s_0)} \int_{s_0}^{s} E(\sigma_s) ds \qquad (3.1.6)$$

where s_0 is the time needed to reach equilibrium for the LD dynamic eqs. or the MC scheme. The rational behind this approach, first suggested by Parisi[38], is that to the stochastic evolution described by (3.1.4,5) is associated a Focker–Plank (FP) equation:

$$\partial_s P(\sigma) = T \Delta P + \nabla \cdot (\nabla V(\sigma)) P$$

where $P(\sigma)$ is the probability that the stochastic trajectory associated to the LD equations (3.1.4,5) generates a configuration $\{\sigma\}$. In the limit $s \to \infty$ $P(\sigma) \to e^{-\beta V}$ and one can use this property to sample the Boltzmann factor. For infinite time s equ.(3.1.6) would lead to zero statistical error. In the practice however this is not possible and one has to consider statistical errors. A naive estimation would give

$$\Delta E \simeq \frac{\left(< E^2 > - < \bar{E} >^2 \right)^{\frac{1}{2}}}{\sqrt{p}} \qquad (3.1.7)$$

where p is the number of sampled configurations. However strong correlation exists between successive configurations.

In order to correct for this, one usually measures the average interval q between the statistically independent configurations. This should correct (3.1.7) in the form

$$\Delta E \simeq \frac{\left(< E^2 > - < E >^2\right)^{\frac{1}{2}}}{\sqrt{\frac{p}{q}}} \tag{3.1.8}$$

The underlying hypothesis is that at equilibrium $E(\sigma)$ is gaussianly distributed. For our QMC calculations this is not always the case, and we measure the error by dividing the measure into segments of sufficient length and comparing the averages obtained in these intervals.

If the segments are long compared to the correlation time of the simulation the sub-averages are roughly gaussian distributed, due to the central limit theorem. An estimate of the error using (3.1.7), where p now represents in (3.1.7) the number of sub-averages, is therefore correct and ensures the 68% of probability of finding the exact value of E within the calculated uncertainty.

3.2 A STABILIZED DISCRETIZATION OF THE LANGEVIN DYNAMIC EQUATIONS

The most important step for the practical solution of the L.D.E. is how to introduce in a convenient way a discrete dynamical time which maps the

dynamics of the $\{\sigma\}$ variables onto a standard iterative scheme which can be easily implemented. The simplest approach is to integrate the LDE between s and $s + \Delta s$:

$$\int_s^{s+\Delta s} \dot{\sigma} = \int_s^{s+\Delta s} -\left(\frac{\partial V}{\partial \sigma}\right)_{s'} ds' + \int_s^{s+\Delta s} \eta_\sigma(s')ds' \tag{3.2.1}$$

and neglects in the integration terms of order $o(\Delta s^2)$:

$$\sigma_i(s + \Delta s) = \sigma_i(s) + \left(-\frac{\partial V}{\partial \sigma}\right)_s \Delta s + z_i(s)\sqrt{2\Delta s} \tag{3.2.2}$$

where $z_i(s)$ are defined in terms of the variables η_σ appearing in (3.1.5) as:

$$\int_s^{s+\Delta s} \eta_{\sigma_i}(s')ds' = \sqrt{2\Delta s} z_i(s) \tag{3.2.3}$$

From the definition (3.2.3), $z_i(s)$ for discrete $s = k\Delta s$ are therefore uncorrelated normal distributed numbers with mean $< z_i(s) > = 0$ and variance $< z_i(s)^2 > = 1$. These variables can be easily obtained by a deterministic machine, using the so called "pseudo" random generator routines[39]. It is possible also to improve the accuracy of the scheme (3.2.2) with better approximations of the first term in the RHS of eq.(3.2.1). As shown by Gunsteren and Berendsen[40] one can formally take a Taylor expansion in Δs of the RHS of eq.(3.2.1) and proceed as is usually done for deterministic differential equations. In this case however, since the random force η_σ appearing in (3.1.4) generates random trajectory which are not continuously differentiable, these methods are not expected to give accurate results as far as the sampling of the weight is concerned.

A better approach was obtained by several authors[41,42] by optimizing the error, due to discretization, on the sampling of the weight instead of finding

improved approximation of the single LD trajectory which is clearly difficult. In practice for large Langevin time s, even though the exact continuous ($\Delta s \to 0$) trajectory is completely different from the discretized one, this can give statistical property of an effective weight $\tilde{w}(\sigma)$ which differ by $o(\Delta s^2)$ with respect to the desired weight. In some calculation we have used this approach, while more recently we have developed a new method described below.

The necessity of developing new methods for integrating LE arises from the need to overcome some difficulties pointed out by Wilkins et al. These authors have noted that if the weight is positive semi-definite —that is $w(\sigma) = 0$ for some configuration— the potential $V(\sigma)$ becomes infinite. Since a strict dynamical classical motion cannot cross (for $\Delta s \to 0$) an infinite potential barrier there may be problems of sampling "ergodically" all the phase space. Moreover when the potential has some singular behavior in a surface of the phase space (and this is the case when $w(\sigma)$ is semi–positive definite) the discretized dynamic of the LDE may be unstable close to this region showing also severe problems of equilibration (Wilkins and White[42]). We anticipate that a solution to this problem can be simply obtained with an adaptive time step integrator of the LDE. This is in fact useful because a very small time step Δs has to be used only when the LD trajectory is very close to the mentioned singular region.

In order to avoid these possible drawbacks of the LD sampling, we start, to find convenient approximations of the corresponding FP dynamic. We note that the FPE is quite similar to the time dependent Schrodinger equation in imaginary time of interacting particles:

$$\partial_t \psi = -\hat{H}\psi \tag{3.2.4}$$

where the hamiltonian $\hat{H}$ is the sum of a kinetic term $\hat{K}$ which is diagonal in momentum[43] space $\hat{K} = \frac{-\hbar^2}{2m}\Delta$ and a potential term $V(x)$ which is diagonal in real space. A useful method[43] to solve the SE from a given initial condition $\psi_{t=0} = \psi_T$ is to consider both the simpler cases when $\hat{V} = 0$ or $\hat{K} = 0$. In these cases the time dependent SE is easily solved by using the appropriate basis which diagonalizes the corresponding Hamiltonian $\hat{H}$ in (3.2.4). Then in order to calculate $e^{-\hat{H}t}\psi_T$, which is the formal solution of (3.2.4), the propagator $e^{-(K+V)t}$ is divided in terms of short time propagators containing only the kinetic term or the potential one, as it is also shown in chapter I:

$$\psi_t = \lim_{n\to\infty} (\exp -\Delta\tau_n V \exp -\Delta\tau_n K)^n \psi_T \tag{3.2.5}$$

where $\Delta\tau_n = \frac{t}{n}$ and in this form the Trotter error vanishes as n^{-1}. In fact it is easily verified that the short time propagator

$$e^{-\Delta\tau_n V} e^{-\Delta\tau_n K} = I - \Delta\tau_n(K+V) + o(\Delta\tau_n^2) \tag{3.2.6}$$

differs by $o(\Delta\tau_n^2) \propto n^{-2}$ respect to the desired $e^{-\Delta\tau_n(K+V)}$. This approach is quite general and is convenient if each propagation $e^{-\Delta\tau_n V}$ or $e^{-\Delta\tau_n K}$, taken separately, can be efficiently applied to any given wavefunction.

Systematic improvement of the Trotter approximation are also possible, e.g.

$$e^{-\Delta\tau(K+V)} = e^{-\frac{\Delta\tau}{2}V} e^{-\Delta\tau K} e^{-\frac{\Delta\tau}{2}V} + o(\Delta\tau^3) \tag{3.2.7}$$

but for reason of simplicity we restrict in the following to the simplest Trotter decomposition. However the following analysis can be easily generalized for more accurate decomposition.

We now apply the same kind of approximation for solving the FPE because there are two limits for it that can be easily understood as in the mentioned SE (3.2.4). In fact one can identify the probability density as a sort of wavefunction:

$$P(\sigma, s) = \psi$$

the kinetic term of the SE with the corresponding diffusive term of the FPE

$$\hat{K} = -T\Delta \tag{3.2.8}$$

and the analogous of the potential term as the operator

$$\hat{V} = -\Delta V_\sigma - \nabla V_\sigma \cdot \nabla \tag{3.2.9}$$

appearing in the FPE. This operators now act on probability functions instead of wavefunctions and conserve separately the total probability.

Inspired by the methods of solution of time dependent SE we calculate the evolution of $P(\sigma, s)$ as:

$$\psi_s(\sigma) = \lim_{n\to\infty} \left(e^{-\Delta s_n V} e^{-\Delta s_n K}\right)^n P(\sigma, 0) \tag{3.2.10}$$

where $\Delta s_n = \frac{s}{n}$, which is valid at $o(\Delta s^2)$ and expresses the total evolution as product of elementary evolutions under the alternate action of the operator

$$e^{-\Delta s_n K} \quad and \quad e^{-\Delta s_n V}. \tag{3.2.11}$$

The first one $(e^{-\Delta s_n K})$ gives the evolution of a FP eq. without potential term. To it one can then associate a purely stochastic LE of the type

$$\dot{\sigma}_i = \eta_{\sigma_i}(s) \tag{3.2.12}$$

which can be exactly integrated to give

$$\sigma_i(s+\delta s) = \sigma_i(s) + \sqrt{2T\Delta s} z_i(s). \tag{3.2.13}$$

The evolution $e^{-\Delta s V}$ instead corresponds to a FPE where the diffusive (kinetic) term is missing. In this case the associated LE is a purely deterministic[42] first order differential equation (see 3.1.4,5 for $T = 0$).

$$\dot{\sigma}_i = -\frac{\partial V}{\partial \sigma_i} \tag{3.2.14}$$

There are several methods, which have been well established in literature, to obtain a first or higher order approximation of eqs.(3.1.4) with respect to the discretization time Δs. One of this is the simple discretization

$$\sigma_i(s+\Delta s) = \Delta s \left(-\frac{\partial V}{\partial \sigma_i}\right)_s + \sigma_i(s) \tag{3.2.15}$$

Analogously up to $o(\Delta s)$, average quantities as in (3.1.6) can be written as:

$$\frac{1}{\Delta s} \int_s^{s+\Delta s} E(s')ds' = E(\sigma_s) + o(\Delta s) \tag{3.2.16}$$

where now the error has a well defined meaning since all the time derivatives of the trajectory $\sigma(s)$ are defined and depend only on the shape of the potential V_σ in the neighborhood of $\sigma(s)$. They do not depend in fact on the random force which can in principle have arbitrary large variation in the short time Δs.

Strictly speaking, as soon as the systematic equations (3.2.14) are discretized it always remains a finite step error in representing the change of the probability P produced by the operator $e^{-\Delta s V}$. However the described change of variables (3.2.15) can be thought as acting on the same probability distribution $P(\sigma, s) \rightarrow P(\sigma, s + \Delta s)$ by means of an effective operator which differ by $o(\Delta s^2)$ from the continuous evolution operator $e^{-\Delta s V} P(\sigma, s)$. Again within this approximation, due to discretization, the scheme remains a first order algorithm in the time step Δs. In fact the approximation (3.2.16) remains to the same order if one substitutes to the operator $e^{-\Delta s \hat{V}}$ another one differing at most by $o(\Delta s^2)$.

At this point we note that, combining eq.(3.2.15), for the systematic evolution with eq.(3.2.13), for the diffusive motion of the variables, we get in a natural way the first order discretization of the LDE (see eq.3.2.2).

Since the potential V_σ may be not well behaved for some σ configurations —when for example $w(\sigma) = 0$ in (3.2.2)— it is convenient to use during the systematic evolution (3.2.14) an adaptive integration scheme. The interval $s, s+\Delta s$ is divided in many different subintervals

$$(s, s+\Delta s) = (s, s+\Delta s_1), (s+\Delta s_1, s+\Delta s_1+\Delta s_2), ..., (s+\Delta s_1+\ldots \Delta s_{n-1}, s+\Delta s) \tag{3.2.17}$$

with the condition that

$$\Delta s_n = \max_i \left| \frac{\partial V}{\partial \sigma_i} \right| \leq c \Delta s \tag{3.2.18}$$

and in each interval an integration scheme like (3.2.15) is followed. A similar condition was already used by several authors in the solution of the LDE[33,34].

However we think that this trick can be rigorously applied only during the systematic evolution and not in presence of the random force. Only in this case in fact the error due to the discretization in the short time interval Δs is systematically controlled by the adaptive condition (3.2.18). The constant c has to be chosen conveniently. For $\Delta s \to 0$ the LDE and consequently the FPE are exactly integrated with an error which scales as (Δs).

This FPE, discretized using the Trotter approximation, would give an equilibrium distribution for $s \to \infty$ differing by $o(\Delta s^2)$ from the desired one. To this FPE we can finally associate discrete LDE for evolving the variables $\{\sigma\}$ from the time s to the time $s + \Delta s$. These can be calculated in two different steps, where we put $T = 1$ for simplicity:

(1) Firstly apply the diffusive term:

$$\sigma_i' = \sigma_i(s) + \sqrt{2\Delta s} z_i(s) \tag{3.2.19}$$

(2) Solve adaptively up to $o(\Delta s^2)$ the 1^{st} order differential eqs.:

$$\dot{\tilde{\sigma}} = -\left(\frac{\partial V}{\partial \tilde{\sigma}}\right). \tag{3.2.20}$$

from s to $s + \Delta s$ with the initial condition $\tilde{\sigma}_i(s) = \sigma_i'$.

In principle expectation values of physical quantities have to be calculated even during the random evolution (3.2.20) but after equilibration for $s \to \infty$ it is not important when to calculate them and we preferred to update expectation values only during the systematic evolution. This way of performing averages can have some advantage if the potential V_σ is singular in some region of the phase

space. This singular behaviour can be conveniently regularized using the adaptive scheme described before (3.2.18). In fact when for example $\frac{\partial V}{\partial \sigma}$ is very large at some time s the corresponding contribution to the expectation value of A is weighted by a factor of the order of $\frac{1}{\frac{\partial V}{\partial \sigma}}$.

In order to show the efficiency of the present discretization of the LDE we apply it to the weight $w(\sigma) = | < \psi_T U_\sigma \psi_T > |$ described in (1.1.16–19). For the 2D Hubbard model the weight $w(\sigma)$ used is not positive definite and can vanish for some configuration $\{\sigma\}$. Even in this case however the previously described scheme works very efficiently and accurately as it is shown in fig.3.1 for some interesting exact results.

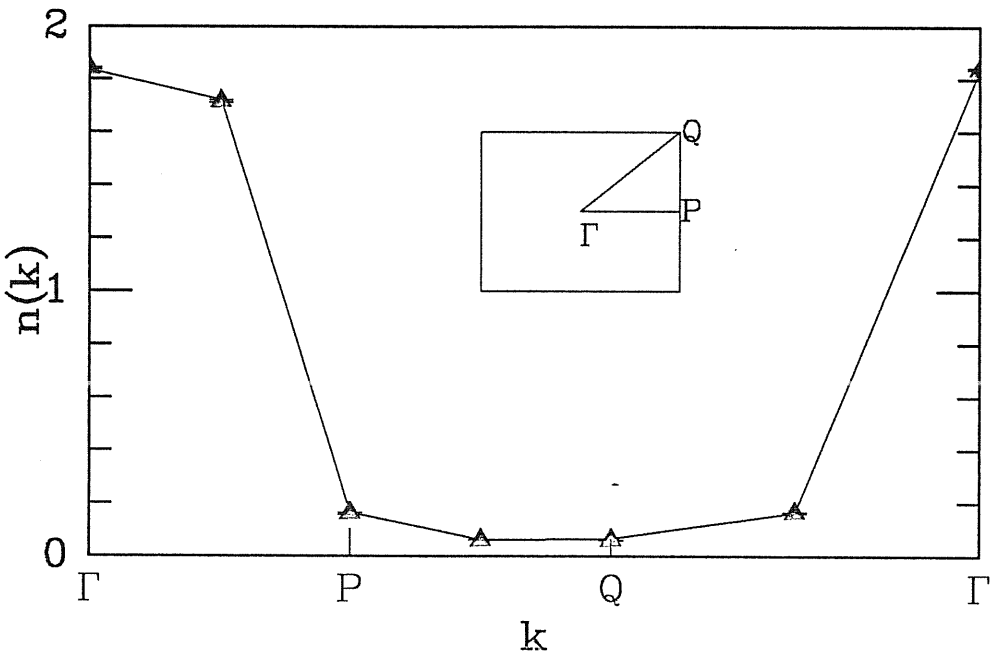

Figure 3.1. Momentum distribution of the doped (6 holes) 2D 4×4 Hubbard model with U=8. The continuous line connect the exact results obtained by direct diagonalization[1] and the triangles are the results of the simulation for β=10. The time step chosen for the discretization of the LDE was Δs=0.1 The path in the Brillouin zone is shown in the insect

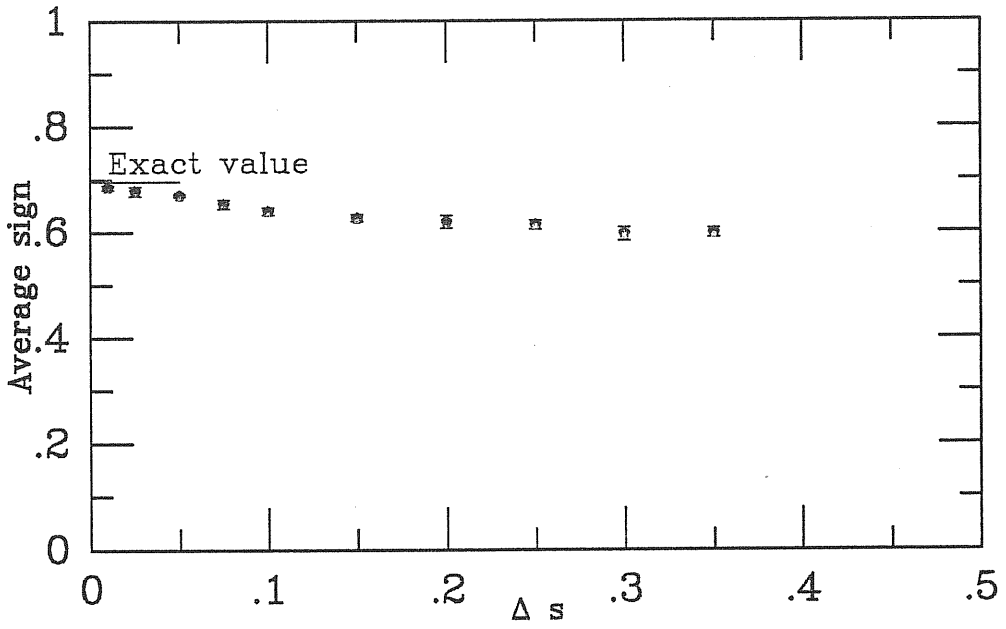

Figure 3.2. Average sign as a function of the discretization time Δs for the toy model discussed in the text. The black dots are the results of the statistical simulation, using the adaptive first order algorithm (3.2.23-24).

In fig.3.2 we plot the average sign as a function of Δs for a singular weight

$$w(\theta) = (1 - 2\cos\theta) \tag{3.2.21}$$

We see that using the scheme described in Ch.IV one can also use the Langevin dynamic for sampling weight with negative sign.

A better approximation of the Trotter formula as in (3.2.7) is not convenient because requires the calculation of the forces several times for each short time interval propagation Δs and when the weight is non positive definite we expect to have little or worse behaviour in the region of the nodal surface $w(\sigma) \simeq 0$ with an higher order algorithm.

In conclusion we have shown that the problem of the large moves occurring

during the LD evolution when the potential has some singular behaviour can be simply and rigorously solved by using the present adaptive scheme. As far as the possible lack of ergodicity of the LDE, it is enough to note that during the diffusion motion, (3.2.20) for any finite Δs, there is always a finite probability for the variables $\{\sigma\}$ to reach an arbitrary configuration of the phase space. This of course means that the discretized LDE are always ergodic and at most the algorithm can become slower when $\Delta s \to 0$ if the probability to cross different regions separated by infinite potential barriers becomes smaller and smaller as $\Delta s \to 0$. In this case it is enough to use a Langevin simulation time that for any fixed Δs is much longer than the average time to cross the barriers.

Chapter IV

The algorithm

In this chapter we present a newly developed scheme for sampling the weight $w(\sigma)$ described in the previous chapters, using the Langevin dynamic approach. As also pointed out in ref.[41] Langevin updating proves to be ideal here, largely because the entire space–time lattice is updated simultaneously, rather than link by link or site by site as in Monte Carlo calculations.

We found a way to calculate the forces which is stable and fairly convenient since the most expansive part in the calculation of the forces grows quadratically with the system size for fermions and linearly for bosons. It should be mentioned, however, that there exist methods, developed in QCD[35,41] demanding a computational cost growing only linearly with the size. For QCD it seems not important to reach very low temperatures while it is essential in condensed matter physics to reach temperatures well below the *Fermi* one. We think therefore that these schemes used in QCD are unstable for low temperatures. In fact an essential part to stabilize the calculation of the forces in the present approach

is obtained by using the orthogonalization technique, which has considerably improved the stability of existing Monte Carlo calculations based on the HST[24,25]. This procedure (described in sect. (4.2)) is computationally quite expensive but has to be used necessarily for a stable simulation of Fermions at low temperatures. In fact dynamical methods based on the QCD approach[35] are limited to very high temperature so far. On the other hand our algorithm can be improved efficiently using the so called Fourier accelerator and more efficient ways of orthogonalizations.

4.1 Calculation of the forces

We now describe how to calculate the forces, corresponding to the weight (1.1.20) in an efficient way. For a dynamical method of sampling based on forces we have found that the most convenient way to perform the HST is to use the distribution (1.1.19), because with this choice the fields $\{\sigma\}$ fluctuates in a finite range

$$|\sigma_\tau| < \Lambda \tag{4.1.1}$$

with $\Lambda = \sqrt{2U\Delta\tau}\left[1 + \frac{U\Delta\tau}{16} + o(\Delta\tau^2)\right]$. In fact the imaginary time evolution in this case is clearly more stable, because the operator $e^{\sigma_\tau m_\tau}$ is always close to the identity for sufficiently small Trotter time interval. After the change of variables:

$$\sigma_{rl} = \Lambda \cos\theta_{r,l} \tag{4.1.2}$$

the weight in consideration assumes a particular simple form in which the constraint (4.1.1) —which would be difficult to approximate with a dynamical method— is no more present for the angular variables $\theta_{r,l}$. In fact the weight appearing in (1.1.20) can be written as:

$$Q = \int d\mu_\theta \; w(\theta) \tag{4.1.3}$$

where $d\mu_\theta$ from (1.1.21) is:

$$d\mu_\theta = \prod_{l=1}^{P} \prod_{i=1}^{N_a} \left(\frac{d\theta_{rl}}{2\pi} \right) \tag{4.1.4}$$

and the weight is simply given by:

$$w(\theta) = <\psi_T U_{\sigma(\theta)} \psi_T> \tag{4.1.5}$$

where U_σ is defined in (1.1.22) and (1.1.23). Using this angular variables $\theta_{r,l}$ and, the LDE described in chapter 3, the forces needed for sampling the weight $w(\theta)$ are given by:

$$F_r(l) = -\frac{\partial}{\partial\theta_{r,l}} V(\sigma(\theta)) = \frac{\partial}{\partial\theta_{r,l}} \ln <\psi_T \,|\, \hat{U}_{\sigma(\theta)} \,|\, \psi_T> \tag{4.1.6}$$

We consider, for the trial wavefunction ψ_T a single Slater determinant made up by $N^\uparrow$ spin up and $N^\downarrow$ spin down orbitals. As mentioned before, $\hat{U}_\sigma$ acts independently on spin up states $\varphi^\uparrow_m$ and on spin down states $\varphi^\downarrow_m$.

$$|\varphi^\uparrow_m> \quad |\varphi^\downarrow_n> \tag{4.1.7}$$

Therefore we can write:

$$<\psi_T|\hat{U}_\sigma|\psi_T>=\det<\varphi_m^\uparrow|\hat{U}_\sigma|\varphi_n^\uparrow>\det<\varphi_m^\downarrow|\hat{U}_\sigma|\varphi_n^\downarrow> \tag{4.1.8}$$

and the problem of computing the forces is completely decoupled in spin space. As a consequence:

$$F_r(l) = \frac{\partial}{\partial\theta_r(l)}\ln det\ <\varphi_m^\uparrow\,|\,\hat{U}_{\sigma(\theta)}\,|\,\varphi_n^\uparrow> + \frac{\partial}{\partial\theta_r(l)}\ln det\ <\varphi_m^\downarrow\,|\,\hat{U}_{\sigma(\theta)}\,|\,\varphi_n^\downarrow> \tag{4.1.9}$$

The derivative in the last expression affects only the propagator U_σ at the time slice i. Such derivative, if calculated in the most straightforward way, requires the computation of at least one determinant for each of the LN_a degrees of freedom amounting to a total of LN_aN^3 operations. However the total number of operations can be significantly reduced by means of the following considerations.

Since the calculation is similar for both the spin component we will omit in the following the spin labels $\uparrow$ and $\downarrow$ for the orbitals. Let us consider the matrix:

$$A_{m,n}(\theta) =<\varphi_m\,|\,\hat{U}_{\sigma(\theta)}\,|\varphi_n> \tag{4.1.10}$$

Its determinant appearing in (4.1.9) can be formally written as:

$$\det\ A = e^{\mathrm{tr}\ln A}. \tag{4.1.11}$$

Therefore the terms appearing in the R.H.S. of eq.(4.1.9) for the calculation of forces become:

$$-\frac{\partial tr\ \ln A}{\partial\theta_r(l)} = -tr\,\frac{\partial A}{\partial\theta_r(l)}A^{-1} = -\sum_{m,n}\left[\frac{\partial A}{\partial\theta_r(l)}\right]_{mn}A^{-1}_{nm} \tag{4.1.12}$$

The derivative $\frac{\partial}{\partial\theta_r(l)}A$ can be explicitly calculated by introducing the back and forth propagated orbitals at time $\left(l-\frac{1}{2}\right)\Delta\tau$

$$\varphi_{>}(l) = e^{+\frac{\Delta\tau}{2}K}\tilde{\varphi}_{>}(l\,\Delta\tau)$$

$$\varphi_{<}(l) = e^{-\frac{\Delta\tau}{2}K}\,\tilde{\varphi}_{<}(l\Delta\tau) \tag{4.1.13}$$

where $\tilde{\varphi}_{<}$ and $\tilde{\varphi}_{>}$ are the back and forth propagated orbitals for integer times:

$$\tilde{\varphi}_{>}(l\Delta\tau) = U_{\sigma}(l\Delta\tau, 0)\varphi_{0,m}$$

$$\tilde{\varphi}_{<}(l\Delta\tau) = U_{\sigma}(l\Delta\tau, \beta)\varphi_{0} \tag{4.1.14}$$

and $\varphi_m(0)$ are the one particle orbitals corresponding to the trial function $|\psi_T>$. These propagated functions, as well as $\tilde{\varphi}_{>}(\Delta\tau l)$ $\tilde{\varphi}_{<}(\Delta\tau l)$ can be calculated using iterative formulae:

$$\varphi_{>,m}(l) = e^{\sum_r \Lambda \cos\theta_{r,l}\,\hat{c}_r^{+}\hat{c}_r}\, e^{-\Delta\tau K}\,\varphi_{>,m}(l-1) \tag{4.1.15}$$

$$\varphi_{<,m}(l-1) = e^{-\Delta\tau\hat{K}}\, e^{\sum_r \Lambda\,\cos\theta_{r,l}\,\hat{c}_r^{\dagger}\hat{c}_r}\,\varphi_{<,m}(l) \tag{4.1.16}$$

$$\varphi_{<,m}(L) = e^{-\frac{\Delta\tau}{2}\hat{K}}\,\varphi_m(0)\ and\ \varphi_{>,m}(0) = e^{\frac{\Delta\tau}{2}\hat{K}}\varphi_m(0) \tag{4.1.17}$$

Since $\hat{K}$ contains operator diagonal in fourier space and the the random fields acts over operator diagonal in real space a way to evaluate such iterative propagations is obtained using the Fast Fourier Transform[43]. Another convenient way to apply the kinetic propagation $e^{-\Delta\tau\hat{K}}$ to the orbitals can be obtained using the locality of the kinetic term. In fact by approximating $e^{-\Delta\tau\hat{K}}$ with

$$I - \Delta\tau K_0 + \frac{\Delta\tau^2}{2} K^2. \tag{4.1.18}$$

we still remain with a second order Trotter error and the propagation is efficient because involves only multiplication of sparse matrices containing only few non zero elements.

By the knowledge of the back and forth propagated orbitals (4.1.15) and (4.1.17) we thus find:

$$\left[\frac{\partial}{\partial\theta_r(l)} A \right]_{m,n} = -\Lambda \sin\theta_{r,l} \; <\varphi^{\uparrow}_{<,m}(l)\, \hat{c}^{+}_{r}\, \hat{c}_r\, \varphi^{\uparrow}_{>,n}(l)> \tag{4.1.19}$$

Such expression for each m, n becomes simply calculated in real space where it is the product of two real functions at the site point $\underline{r}$.

In conclusion in order to compute the forces we need N^3 operations to evaluate A^{-1},LN_aN to propagate the orbitals for evaluating eq.(4.1.19), and finally N^2LN_a operations to assemble this quantity into eq.(4.1.12). Therefore we have gained a factor of N relative to the direct approach. A further gain can be obtained by rearranging the calculation as follows:

$$\frac{\partial tr\, \ln A}{\partial\theta_r(l)} = \sum_m -\Lambda \sin\theta_r(l) \; <\varphi^{A^{-1}}_{<,m}(l)|\, \hat{c}^{+}_{r}\, \hat{c}_r\, |\varphi_{>,m}(l)> \tag{4.1.20}$$

where

$$\varphi^{A^{-1}}_{<,m}(l) = \sum_n A^{-1}_{m,n}\, \varphi_{<,n}(l) \tag{4.1.21}$$

Since this is a linear transformation $\varphi^{A^{-1}}_{<}$ can be obtained by propagating backwards the vectors

$$\varphi^{A^{-1}}_{m}(0) = \sum_n A^{-1}_{m,n}\, \varphi_n(0) \tag{4.1.22}$$

as in formula (4.1.16). This transformation will reduce the number of operations needed in the calculation of the trace in (4.1.12) from N^2LN_a to NLN_a at the only cost of adding N^2N_a operations to evaluate $\varphi^{A^{-1}}(0)$. When all this factors are taken into account we end up with an estimate of only $N^3 + N^2N_a + NLN_a$ operations to compute the forces with an overall gain of a factor NL with respect to a brute force approach.

We write the explicit expression of the forces using eqs. (4.1.6, 4.1.20) and taking in mind the discussed propagation scheme

$$F_{r_j}(l) = \Lambda \sin\theta_{rl} \left[\left(\sum_k < \varphi^{\uparrow\, A^{-1}}_{<,k}(i) \mid \hat{c}^{+\uparrow}_{r_j} \hat{c}^{\uparrow}_{r_j} \mid \varphi^{\uparrow}_{>,k}(i) > \right) \right.$$

$$\left. + \left(< \varphi^{\downarrow\, A^{-1}}_{<,k}(i) \mid \hat{c}^{+\downarrow}_{r_j} \hat{c}^{\downarrow}_{r_j} \mid \varphi^{\downarrow}_{>,k}(i) > \right) \right] \qquad (4.1.23)$$

4.2 Numerical Stability by Gram–Schmidt Orthogonalization

Following the preceding steps the computer time required for the evaluation of the forces is very much reduced but the numerical stability is not taken into account. The imaginary time propagation is not unitary and the orthonormality conditions, initially satisfied by the orbitals, are not preserved during such propagation. Therefore after repeating many times the step (4.1.15–16) an orthogonal basis set $\varphi_i(r)$ $i = 1, \ldots, N$ will no longer remain orthogonal. This

circumstance can produce a numerical instability of the algorithm. In fact suppose the orbitals are independently propagated through an imaginary time one–body propagator $e^{-\hat{h}t}$. The fermionic ground state can be considered as an excited state (with the right symmetry) of a many–body hamiltonian; its true ground state being a boson–symmetric wavefunction. When the orbitals freely propagate, after long time, they are spontaneously led to the bosonic ground state of $\hat{h}$. In this way the numerical information of the fermionic state is gradually lost until the Slater determinant exactly vanishes when the N orbitals of the Slater determinant are no longer linear independent within the given computer precision. Therefore, in order to have a stable propagation, we have to rewrite, any few steps, the Slater determinant which is at the time t:

$$|\psi>^t = \det\ \varphi^t_m(r_j) \tag{4.2.1}$$

in terms of an orthogonal basis set. This is always possible with a transformation

$$\varphi^t_m = \sum_n U_{m,n}\,\tilde{\varphi}_n \tag{4.2.2}$$

where the matrix $U_{m,n}$ is chosen in such a way that $<\tilde{\varphi}_m|\tilde{\varphi}_n>= \delta_{m,n}$. The matrix $U_{m,n}$ is not univocally determined by the previous condition (4.2.2). A convenient choice is to use the Gram- Schmidt orthogonalization scheme because, in this case, $U_{m,n}$ is a triangular matrix.

Now from (4.2.1) and (4.2.2) $|\psi^t>$ can be written as

$$|\,\psi> = \ det\ \left[\sum_n U_{m,n}\,\tilde{\varphi}_n(r_j)\right] \ = \ det(U)\,det\ \left[\varphi^t_n(r_j)\right] \tag{4.2.3}$$

where the latter equality simply follows by expanding the determinant of the product of two square matrices: $U_{m,n}$ and $\varphi^T_n(r_j)$. Hence we easily get that

the Slater determinant can be written, up to a constant, by means of orthogonal orbitals. Such a constant affects only the value of the propagated wavefunction which can be independently updated. Therefore we again have to propagate a Slater determinant, made up by orthogonal orbitals, and one can proceed as before until the numerical stability will require another orthogonalization. Numerically such a strategy is very useful and we can propagate for long time any function without any numerical problem. However the computation time increases because of the orthogonalization of the orbitals which costs an amount of $N^2\,N_a$ floating point operations. Moreover the formulas obtained in the previous section for the calculation of the forces where derived under the assumption that the orbitals freely propagate. Then eqs.(4.1.20–4.1.22) can only be used between two contiguous orthogonalizations.

In fig.4.1 we plot a simple example to show the efficiency of the stabilization technique which allows to perform stable imaginary time propagation.

In this fig.4.1 we see that without the orthogonalization technique the logarithm of the determinant tends to increase with a faster exponent than the true one and this happens because the matrix A becomes ill conditioned for large imaginary time.

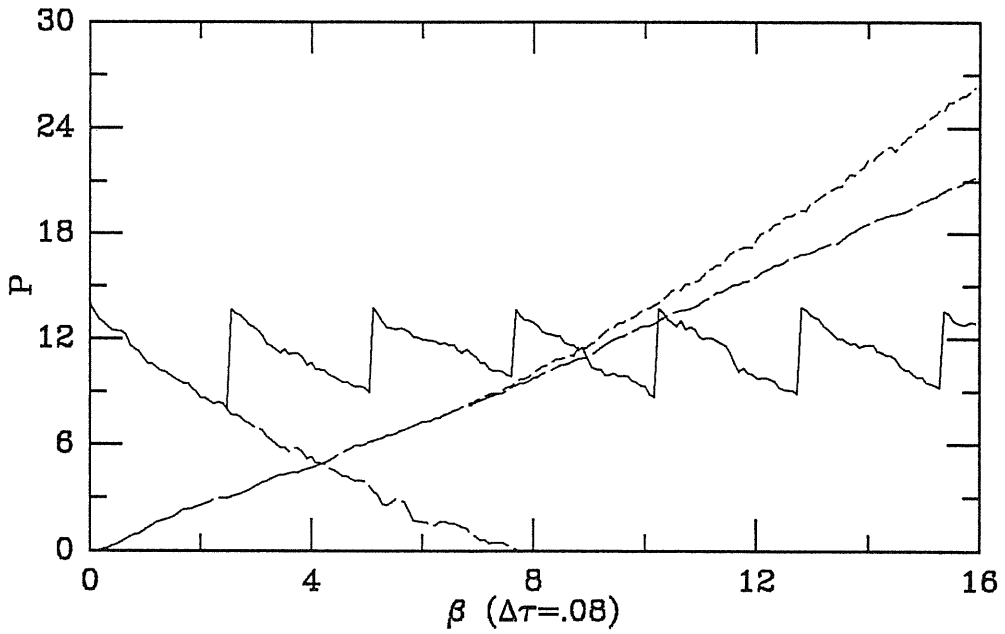

Figure 4.1. Estimated number of significant digits P in the calculation of the logarithm of the determinant as a function of the imaginary time β. The continuous and the long dashed lines indicate evaluations of P with or without the stabilization technique described in the test. The dotted line is the evaluation of $1/10(log_{10}\ det)$ without stabilization and the short dashed represent the same quantity calculated with the stabilized algorithm. The data refer to a sample calculation for the 2D doped 6 holes Hubbard model in a 4×4 lattice for U=8.

4.3 Ground State Expectation Value of Operators

The ground state expectation value of arbitrary operators $\hat{O}$ can be calculated using the fundamental relation (1.1.18), (1.1.2), (1.2.3). After performing the differentiation with respect to the external perturbation a well defined estimator $E_0(\sigma)$ is obtained. This can be calculated by taking the imaginary time average

of independent measurements at a fixed imaginary time t:

$$E_0(\sigma) = \frac{1}{\beta}\int_0^\beta dt\, E_0^t(\sigma) \tag{4.3.1}$$

where

$$E_{\hat{O}}^t(\sigma) = \frac{<\psi_T \,|\, U_\sigma(\beta,t)\,\hat{O}\,U_\sigma(t,0)\,|\,\psi_T>}{<\psi_T \,|\, U_\sigma(t,0)\,|\,\psi_T>} \tag{4.3.2}$$

The expectation value of the operator $\hat{O}$ is then obtained from the statistical average for the estimator $E_{\hat{O}}(\sigma)$ over the weight $< \psi_T U_\sigma(\beta,0)\psi_T >$. In our approach this statistical average is obtained by a temporal average over the LD dynamics as in eq.(3.1.6).

Notice that in the evaluation of the estimator with the imaginary time average (4.3.1) the contribution coming from imaginary time measurements close to the initial $t = 0$ and the final imaginary time produce a slow convergence of the physical quantities with respect to the inverse temperature. In fact such measurements are too close to the trial wavefunction and give contribution which vanishes as β^{-1}. It is possible to improve systematically such convergence in β in the following way. Instead of averaging over all the imaginary time slices an average over an interval which is far apart from the initial $t = 0$ and the final time $t = \beta$ is considered. In our calculations we used estimators given by:

$$E_{\hat{O}}(\sigma) = \frac{2}{\beta}\int_{\frac{\beta}{4}}^{\beta-\frac{\beta}{4}} E^t(\sigma)\, dt \tag{4.3.3}$$

This kind of estimator can be formally obtained by taking the logarithmic derivative of the partition function $Q = <\psi_T e^{-\beta H}\psi_T>$:

$$\frac{\partial}{\partial\lambda} - \frac{2}{\beta}\ln < \psi_T e^{-\beta\hat{H}}\psi_T > \tag{4.3.4}$$

where λ acts as a time dependent perturbation $H \rightarrow H + \lambda_t \hat{O}$:

$$\begin{cases} \lambda_t = \lambda & \frac{\beta}{4} \leq \lambda \leq \beta - \frac{\beta}{4} \\ \lambda = 0 & otherwise \end{cases}$$

and this gives as well for $\beta \rightarrow \infty$ the ground state expectation value $< \psi_0 O \psi_0 >$ with an exponential convergence in β.

Let us now consider two points equal time Green's function. The corresponding operator $\hat{O}$ reads:

$$\hat{O} = \hat{c}_{j\alpha} \hat{c}^{\dagger}_{k\alpha} \tag{4.3.5}$$

In this case eq.(4.3.2) can be easily written as:

$$E^t_{\hat{O}}(\sigma) = \frac{< c^{\dagger}_{\alpha j} U_\sigma(t,\beta)\, \psi_T \mid c^{\dagger}_{\alpha k} U_\sigma(t,0)\, \psi_T >}{< U_\sigma(t,\beta)\, \psi_T \mid U_\sigma(t,0)\, \psi_T >} \tag{4.3.6}$$

Therefore if ψ_T is a N–state single Slater determinant, eq.(4.3.6) involves the scalar products of two $N+1$–state determinants. Using the definition of the forward and backward propagated wavefunction $\tilde{\varphi}^{<}$ and $\tilde{\varphi}^{>}$ (4.1.14) for integer times and that the scalar product of two Slater determinants is the determinant of the corresponding overlap matrix, eq.(4.3.6) becomes

$$E_{\hat{O}}(\sigma) = \frac{det\, \underline{A}^{\alpha}(j,k)}{det\, A^{\alpha}} \tag{4.3.7}$$

where $\alpha = \uparrow$ or $\downarrow$, $\underline{A}_\alpha(j,k)$ is a $(M+1) \times (M+1)$ matrix indexed by the single particle wavefunction components with up or down spin projection:

$$\underline{A}_{m,n} = \begin{pmatrix} \delta_{j,k} & \tilde{\varphi}^{>}_n(r_k) \\ \tilde{\varphi}^{<}_m(r_j) & A_{m,n} \end{pmatrix} \tag{4.3.8}$$

and $A_{m,n}$ is the $N \times N$ overlap matrix:

$$A_{m,n} = < \tilde{\varphi}_m^< | \tilde{\varphi}_n^> > \tag{4.3.9}$$

By letting the indices j and k assume all the possible values, we obtain N_a^2 matrices of the form (4.3.8). Therefore the full calculation of the two points Green's function requires the evaluation of $2N_a^2$ determinants of order $(N+1)$.

At first sight this would seem an impossible task. However the problem can be greatly simplified by noting that the N_a^2 matrices differ one from another simply by the exchange of one row and one column. It is convenient to formulate all the calculation in terms of the quantities:

$$B(j,k) = \sum_{m,n} \tilde{\varphi}_m^>(r_k)\, A_{m,n}^{-1}\, \tilde{\varphi}_n^<(r_j) \tag{4.3.10}$$

It is well known that a determinant remains unchanged if one adds to a column any linear combination of others. Hence we may add to the first column of the matrix $\underline{A}$ a linear combination of the other columns, in order to make vanishing all the elements of the first column but the one in the first row.

$$det \begin{pmatrix} \delta_{j,k} & \tilde{\varphi}_n^>(r_k) \\ \tilde{\varphi}_m^<(r_j) & A_{m,n} \end{pmatrix} = det \begin{pmatrix} \delta_{j,k} - \sum_n c_n\, \tilde{\varphi}_n^>(r_k) & \tilde{\varphi}_n^>(r_k) \\ \tilde{\varphi}_m^<(r_j) - \sum_n A_{m,n}\, c_n & A_{m,n} \end{pmatrix} \tag{4.311}$$

where in order to have:

$$\tilde{\varphi}_m^<(r_j) - \sum_n A_{m,n}\, c_n = 0 \tag{4.3.12}$$

one must take:

$$c_m = \sum_n A_{m,n}^{-1}\, \tilde{\varphi}_n^<(r_j). \tag{4.3.13}$$

Substituting (4.3.13) in the R.H.S. of (4.3.11) and using the definition (4.3.10) one obtains:

$$det \begin{pmatrix} \delta_{j,k} & \tilde{\varphi}^{>}_{n}(r_k) \\ \tilde{\varphi}^{<}_{m}(r_j) & A_{m,n} \end{pmatrix} = \begin{pmatrix} \delta_{j,k} - B(j,k) & \tilde{\varphi}^{>}_{n}(r_k) \\ 0 & \\ 0 & \\ 0 & A_{m,n} \\ \vdots & \end{pmatrix} = det\, A\ (\delta_{j,k} - B(j,k)) \tag{4.3.14}$$

In the calculation of $E_{\hat{O}}(\sigma)$ in (4.3.6) the factor $\det A$ cancels out in eq.(4.3.14) with the denominator, yielding:

$$E^{t}_{c_j\, c^{\dagger}_{k}}(\sigma) = [\,\delta_{j,k} - B(j,k)\,] \tag{4.3.15}$$

Summarizing, the ground state expectation value of any operator $\hat{O}$ deriving from a suitable contraction of the 2–point equal–time Green's function can be obtained from the thermal statistical average of a classical field operator $E_{\hat{O}}(\sigma)$ (estimator of the operator $\hat{O}$) expressed in terms of the elements of two $N_a \times N_a$ matrices $B^{\uparrow}$ and $B^{\downarrow}$ at each time slice t.

The computation (4.3.10) of the matrices $B^{\uparrow}$ and $B^{\downarrow}$ requires the inversion of two $\frac{N}{2} \times \frac{N}{2}$ matrices $A^{\uparrow}$ and $A^{\downarrow}$ amounting N^3 operations, a change of basis $A^{-1}\varphi^{<}$ ($N^2 N_a$ operations) and remaining N multiplications for each different couple of lattice sites (N_a^2) for which the matrices $B^{\alpha}(i,j)$ are defined. In this way the matrices B^{α} can be updated with less than $o(N_a^3)$ operations.

For higher order correlation functions, by using standard properties of determinants as before, it is easy to verify that Wick's theorem applies and that all the estimators $E_O(\sigma)$ can be also expressed in terms of the matrices B^{α} at the time t, i.e.:

$$< c_i^\dagger \, c_j \, c_k^\dagger \, c_l > = < c_i^\dagger \, c_j > < c_k^\dagger \, c_l > \; + \; < c_i^\dagger \, c_l > < c_j \, c_k^\dagger > \, . \qquad (4.3.16)$$

Here the brackets means the quantum expectation value over a fixed configuration of σ fields at a fixed time t and each pair average in the R.H.S. is calculated by means of eq.(4.3.15).

Chapter V

Numerical results

5.1 – Half Filled 2D Hubbard Model

The Hubbard model, already described in chapter I, represents a truly interacting system. Without interaction ($U = 0$) one obtains a pure band behaviour due to the small but finite overlap of the atomic wavefunctions. In the atomic limit ($t = 0$) the particles are localized. So the Hubbard Hamiltonian describes a system which allows for both these limits naturally, the intermediate regime ($t \sim U$) is of particular interest, as in this range of parameters the competition between band effects and localization due to the correlation is most important. So far only the one–dimensional case has been solved exactly[36,44,45]. One finds a Mott transition in the ground state having strong antiferromagnetic correlation[45]. For higher dimension only approximation[46] exists besides a few

exact results within perturbation theory[9,10]. Of particular interest are also some exact result about the limit $d \rightarrow \infty$[47,48] where d is the physical dimensionality.

A major development in the understanding the physics of the Hubbard model has been provided by use of computer simulation techniques. At half filling Hirsch[24,29] has shown, using a Hubbard–Stratonovich formulation, that it is possible to study the half filled Hubbard model without any "Fermion sign problem". He found that, in agreement with spin wave theory the ground state of the half filled Hubbard model is likely an antiferromagnetic insulator for all U. Moreover he found a very simple description of his numerical results which we describe briefly in the following.

The Hartree Fock spin density wave theory (HF) of the Hubbard model predicts a value of the staggered magnetization m that for small U behaves as:

$$m_{HF} \propto \frac{t}{U} e^{-2\pi\sqrt{\frac{t}{U}}} \tag{5.1.1}$$

An important point is that within the HF theory there is a very simple relation between the gap of the charge excitations Δ_{ch} and the value of the magnetization

$$\Delta_{ch} = Um \tag{5.1.2}$$

This simple relation is expected by Hirsch to remain valid even for the correlated system.

For the 2D Half filled Hubbard model Hirsch found[19], (and quite recently[23] confirmed) that the value of the staggered magnetization at a given U can be obtained by using the HF result and correcting it only by a factor α independent of U

$$m = \alpha\, m_{HF}. \tag{5.1.3}$$

For $U \to \infty$ the Hubbard model becomes a Heisenberg model and the value of m for this model is quite well established ($m = 0.60$). Using this result together with the assumption (5.1.3) the HF results can be scaled by a factor $\alpha = .60$ in the intermediate regime as well. Then, according to Hirsch, the physical properties of the half filled model can be easily understood by a simple mean field spin density wave picture, corrected only for spin–wave fluctuations.

We present here a numerical work on this subject, using the newly developed technique presented in the previous chapters. At half filling, as it is proved in chapter I, one can use, instead of the partition function

$$Q = \int d\mu_\sigma \; < \psi_T U_\sigma(\beta, 0) \psi_T > \tag{5.1.4}$$

coming from a straightforward application of the Hubbard–Stratonovich transformation, a well behaved partition function

$$Q_N(\beta) = \int d\mu_\sigma \; \| \bar{U}_\sigma |\psi_T > \| \tag{5.1.5}$$

useful for the Langevin dynamics sampling (the weight is strictly positive definite). As shown in Sect.(2.4) the quantity

$$E_N = \lim_{\beta \to \infty} -\frac{1}{\beta} \ln Q_N^\beta(\psi_T) \tag{5.1.6}$$

is exactly the ground state energy for $\beta \to \infty$ and any trial wavefunction non orthogonal to the half filled ground state. Furthermore, by the Hellmann–Feynmann theorem, average expectation values of operators $< \psi_0 \hat{O} \psi_0 | >$ can be

calculated by differentiating the ground state energy of the Hamiltonian H in presence of the perturbation $\lambda\hat{O}$ with respect to λ. Then we get a well defined estimator of any given operator $\hat{O}$

$$< \psi_0 O \psi_0 > \; = \; \lim_{\beta \to \infty} \; < E_0(\sigma) >_N^{\beta} \tag{5.1.7}$$

where the estimator $E_0(\sigma)$ is:

$$E_0(\sigma) \; = \; \frac{\partial}{\partial \lambda}\bigg|_{\lambda=0} \; - \frac{1}{\beta} \ln \| U_\sigma^\lambda \| \tag{5.1.8}$$

and U_σ^λ is obtained in (5.1.8) by adding the perturbation λO to the kinetic term. If at half filling ψ_T is invariant under the charge conjugation transformation it is also true that average quantities (5.1.7) converge to the desired ground state expectation value.

Using numerical methods based on finite systems calculations the staggered magnetization m can be evaluated by studying the spin–spin correlation function for clusters of increasing size $L \times L$

$$m \; = \; \lim_{L \to \infty} \sqrt{3\, C\left(\frac{L}{2}, \frac{L}{2}\right)} \tag{5.1.9}$$

or from the Fourier transform $S(q)$ of the spin–spin correlation function $C(\underline{r})$

$$m \; = \; \lim_{L \to \infty} \sqrt{\frac{3S(\pi, \pi)}{L^2}} \tag{5.1.10}$$

where C in our units is defined as:

$$C(r) \; = \; \frac{4}{3} \; < \vec{S}_{r'} \, \vec{S}_{r' + \underline{r}} > \tag{5.1.11}$$

and the factor $\frac{4}{3}$ is used to match our convention with the usual definition. In fact it is commonly used[20,24] as a spin correlation function $C(r) = < m_{r'}\, m_{r'+r} >$ where only local magnetic operators along the z–axis appear. The two previous definitions are equivalent for a singlet ground state but we used the symmetric expression to reduce statistical errors in our calculation.

For a finite size scaling estimation of m by means of eqs.(5.1.9,10) it is useful to have a guess about the finite size corrections on the mentioned quantity. This is indeed possible because, according to spin-wave theory, the finite size corrections to the staggered magnetization are expected[20] to vanish as L^{-1}.

In order to perform an accurate finite size scaling of the 2D Hubbard model we restrict our simulations to the particular value of $U = 3$. Moreover we worked with tilted lattices, as discussed by Oitmaa and Betts[2], rotated by 45^0 with respect to the normal coordinate axis. The number of sites was fixed $2l^2$ where l is an odd integer. This is convenient because the $U = 0$ solution at half filling is in this case non degenerate and this allows more stable numerical simulations at least for small U. We choose for this simulation a Trotter discrete time $\Delta\tau = .08$ and $\Delta\tau = .16$ as a test for the convergence, while the Langevin dynamic equations were discretized with $\Delta s = \frac{\sqrt{2}}{10}$. The last choice has been checked to produce systematic error, that for all quantities studied, are negligible compared with the statistical errors. A careful analysis has been performed for the convergence in the inverse temperature β. For each size we made several runs with different temperatures until convergence has been reached within statistical error.

In fig.5.1 we plot the quantity $C(\frac{L}{2}, \frac{L}{2})$ and $\frac{S(\pi,\pi)}{L^2}$. The data fit quite good a quadratic extrapolation in $\frac{1}{L}$, and this indicates an important size dependence of these quantities on top of the spin–wave behaviour L^{-1}. After extrapolation,

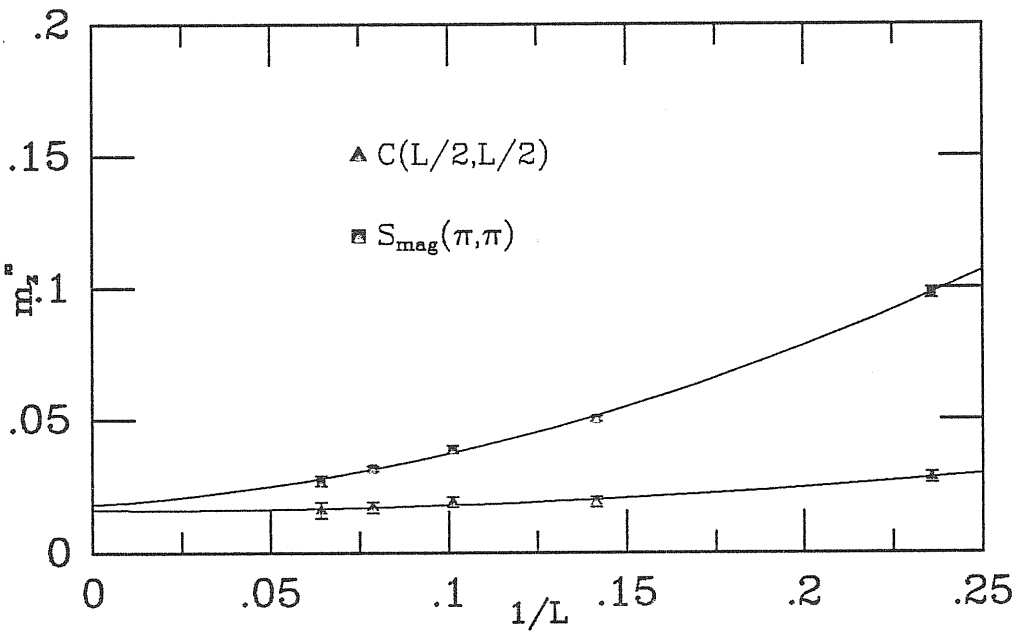

Figure 5.1. A plot of $\frac{S(\pi,\pi)}{L^2}$ (squares) and $C(L/2,L/2)$ (triangles) against L^{-1} for the 2D Half filled Hubbard model for U=3. The intercept is equal to $m_z^2=m^2/3$ where m is the value of the staggered magnetization. The curves are quadratic fits of the data.

which is fairly consistent for both measured quantities, we obtain a finite value of the staggered magnetization (see eqs. 5.1.3 and 5.1.4)

$$m = .24 \pm .02 \qquad for\ U = 3 \tag{5.1.12}$$

The value (5.1.12) is somewhat lower than the corrected HF theory described before (see eq.5.1.3) which would give $m = .35$. Hence spin density wave HF theory, even corrected with the empirical spin wave factor α, is not very accurate. A possible mechanism in originating this decrease of magnetization is associated with a finite charge gap Δ_{ch} for finite U. Charge quantum fluctuations–somewhat similar to doping– cause a reduction of this gap from its HF value. In view of the qualitative connection (5.1.2), this can cause a further reduction of m.

This close relation between spin–related and charge–related properties suggests the necessity of studying the latter, which seems largely unexplored in the 2D hubbard model. As a first step we have performed a detailed size scaling analysis of the momentum distribution function, in order to characterize the metallic or non metallic property of the ground state, which, as well known, are directly related to the presence or the absence of a Fermi surface in the thermodynamic limit of the momentum distribution:

$$n_k = \sum_\alpha c^\dagger_{\alpha,k} c_{\alpha,k} \tag{5.1.13}$$

For this study we have used a special analysis of data that we briefly describe below and that can be obviously extended even away from half filling(see next section) or in higher dimensionality. For reason of simplicity, we neglect in this exposition the further complication that our cells are rotated.

As well known in 2D or in higher dimensionality the resolution in k space increases very slowly with the size of the system and it is difficult to reach a reasonable size to distinguish whether a Fermi surface is really defined for the infinite system. Instead of considering directly the momentum distribution we found convenient to consider the following related quantity:

$$n_\epsilon = \frac{\int \frac{d^2k}{(2\pi)^2} n_k \, \delta\left(\epsilon(k) - \epsilon\right)}{\int \frac{d^2k}{(2\pi)^2} \, \delta\left(\epsilon(k) - \epsilon\right)} \tag{5.1.14}$$

where $\epsilon(k) = -2\,cos(k_x) - 2\,cos(k_y)$ is the Fourier transform of the hopping matrix. For a finite system all the vectors of the Brillouin zone can be divided into different groups with a defined $\epsilon(k) = \epsilon$ (see fig.5.2). For each group we calculate the average value of the momentum distribution and represent it as a function of ϵ.

It is clear that for infinite size this function can be obtained by a surface integral over surfaces $S_\epsilon = \{k \mid \epsilon(k) = \epsilon\}$ for $-4 \leq \epsilon \leq 4$ as in (5.1.14).

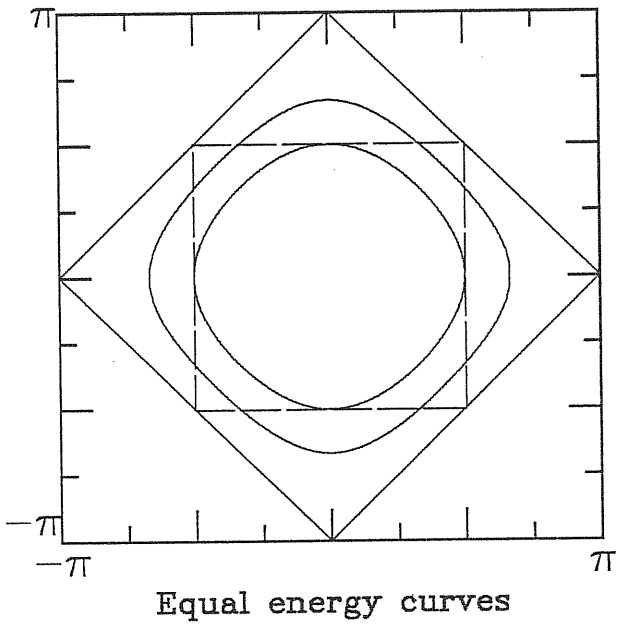

Figure 5.2. Locus of k-points S_ϵ (continuous lines) with equal kinetic energy for a two-dimensional Hubbard model with nearest-neighbour hopping only. ϵ=−2,−1,0 starting from the inner surface. The dashed line represents an idealized Fermi surface at an arbitrary filling.

An illustrative example of this function n_ϵ is given by the HF spin density wave results where the solution is possible[49]:

$$n_\epsilon = \frac{1}{2}\left(1 - \frac{\epsilon}{\sqrt{\epsilon^2 + (\frac{\Delta_{ch}}{2})^2}}\right) \tag{5.1.15}$$

Within HF theory n_ϵ is a smooth function of ϵ even at the Fermi energy $\epsilon = 0$, thus indicating the disappearance of the Fermi surface in the momentum distribution. In fact in this case n_k is easily related, in HF theory, to n_ϵ:

$$n_k = n_{\epsilon(k)} \tag{5.1.16}$$

The derivative γ of n_ϵ at the Fermi energy is finite and is simply related to the gap Δ_{ch}:

$$\gamma = -\frac{\partial n_\epsilon}{\partial \epsilon} = \frac{1}{\Delta_{ch}} \tag{5.1.17}$$

By doping the system, n_ϵ vanishes in a finite range of energy $|\epsilon| \leq |\epsilon_F|$, thus showing the same discontinuity of n_k at the Fermi surface.

More generally, without restricting ourselves to mean field theory, if n_k has a Fermi surface that coincides with one of the possible surfaces S_ϵ for say $\epsilon = \epsilon_F$, as it is the case in the previous example, the function $n(\epsilon)$ will exhibit a jump in the thermodynamic limit. On the other hand if by increasing ϵ the surfaces S_ϵ touch the Fermi surface only in some points, as it is the case for the dashed surface shown in fig.5.2, n_ϵ will be discontinuous only in its first derivative. In this way, by studying the property of this function for increasing size systems, it is possible to understand the appearance of a Fermi surface with a much better resolution $\left(\propto \frac{1}{size}\right)$, with respect to a direct analysis of the momentum distribution in k-space. In fact in the interval $-4 \leq \epsilon \leq 4$ the number of possible values of the discrete energies ϵ is proportional to the finite size of the system.

We plot in fig.5.3 the function n_ϵ for all different sizes studied. The picture show that this quantity, even for large system, smoothly depends on size and does not appear to be singular for any value of ϵ still in agreement with the absence of a Fermi surface, typical of an insulating behaviour.

In order to describe systematically this property, for a finite system with size L we consider the finite difference $n(-\epsilon_L) - n(+\epsilon_L)$ of the function $n(\epsilon)$ in the two symmetric values of the discrete energies $\pm\epsilon_L$ closest to 0. We plot in fig.5.4 this quantity as a function of the finite energy resolution $2\epsilon_L$ and we see that this finite size jump clearly approaches 0 in a linear fashion for $L^2 > 78$. This

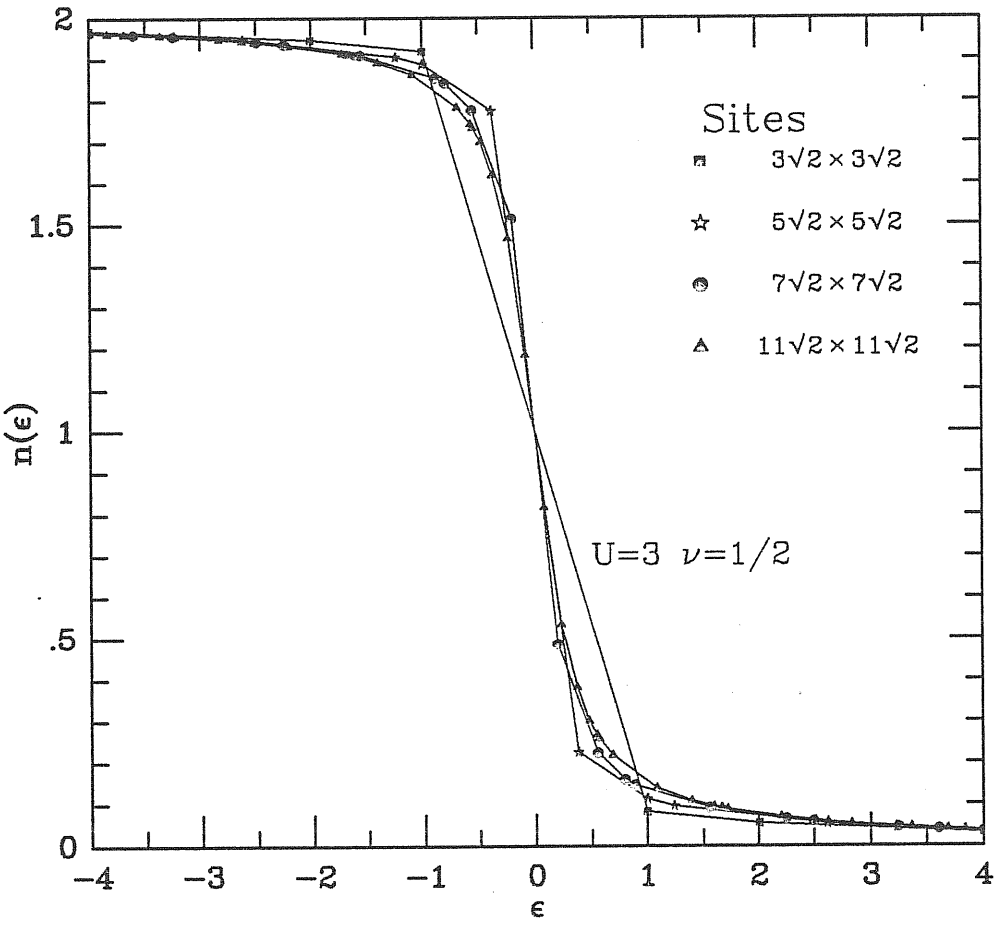

Figure 5.3. A plot of $n(\epsilon)$ for different sizes for a 2D Hubbard model at half filling

indicates that that the sharp nested Fermi surface occurring at $U = 0$ disappears for large enough size due to the interaction. In the same picture it is also shown for comparison the size dependence of the jump of $n(k)$ in the (1,0) direction. Of course in this way, that is choosing a direction and studying the size dependence of n_k, requires a much larger size to detect a Fermi surface discontinuity. This is the reason why we preferred to study the possible singularity of $n(\epsilon)$ (5.1.14).

Moreover this size scaling analysis shows a finite slope γ of n_ϵ for $\epsilon = 0$ (see fig.5.4), which as discussed before is consistent with the simple HF theory

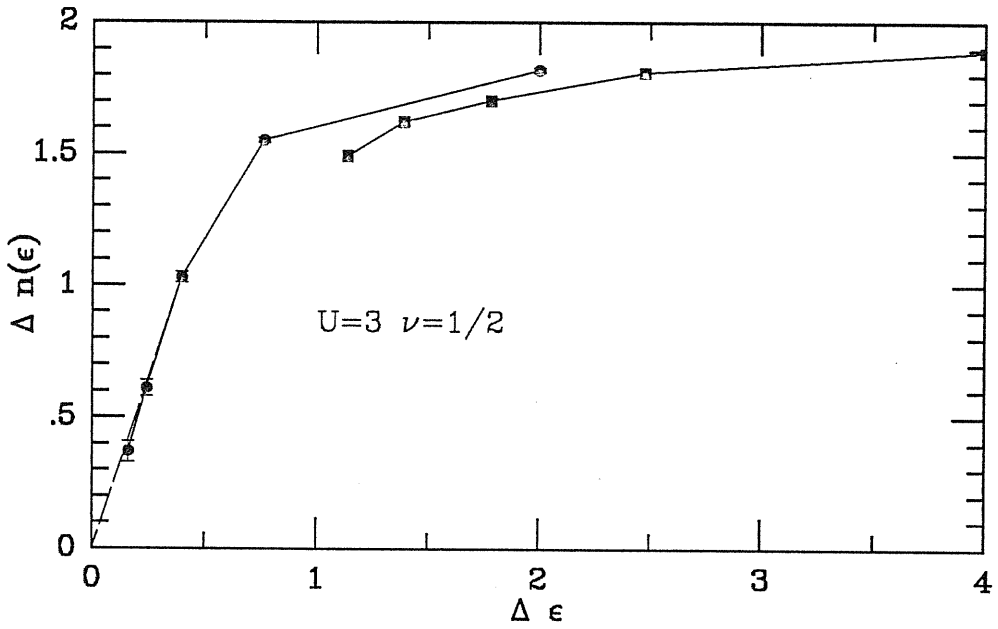

Figure 5.4. Plot of the maximum jump (full dots) of the function $n(\epsilon)$ described in the text as a function of the finite size resolution in energy for a 2D Half filled Hubbard model. The squares indicates the plot of the jump of n_k in the (1,0) direction as a function of the corresponding difference of kinetic energies for the chosen k values.

(eq.5.1.17). Using the values shown in fig.5.4 we can estimate the value of this slope, which is

$$\gamma \simeq 2.3. \tag{5.1.18}$$

This compared with the HF value $\gamma = \simeq .6$ suggests, in view of eq.(5.1.17), a very strong suppression of the charge gap due to quantum fluctuations.

We may compare this value (5.1.18) with the one obtained by the simple relation $\Delta_{ch} = Um$, using the calculated value of $m = .24$ and, naively identifying γ with $\frac{1}{\Delta_{ch}}$ (see 5.1.17). This gives

$$\gamma \simeq 1.5 \tag{5.1.19}$$

Although the previous calculation of γ (given m) applies only within mean field theory, the value obtained in this way is fairly in agreement with the previous

independent estimate (5.1.18). This in turns shows that a corrected mean field theory gives reasonable quantitative relations in this case.

In summary we described QMC results confirming that the half filled Hubbard model is an antiferromagnetic insulator. The main new result concern 1) accurate finite size scaling for the magnetism, which turns out to be, for $U = 3$, more like $0.4\frac{\Delta_{ch}^{SDW}}{U}$ that $0.6\frac{\Delta_{ch}}{U}$ as previously suggested[10,11]; 2) a study of the momentum distribution, and of the jump at the Fermi level, which is shown to scale to zero, as expected for an insulator; 3) the effective (renormalized) charge gap Δ_{ch}, which for $U = 3$ is $\sim \frac{1}{4}$ of its Hartree–Fock value Δ_{ch}^{SDW}.

5.2 Doped 2D Hubbard model

The physical properties of the Hubbard model away from half filling are of extreme current interest also because of its possible relevance for understanding the mechanisms responsible for high T_c superconductivity.

It is generally believed that antiferromagnetic long-range order disappears for $\nu \neq 1$, but the nature of the resulting state is at present controversial. In particular, according to Anderson, a superconducting RVB phase should appear in some region of doping δ ($\delta = 1-\nu$) as a result of large fluctuations in the number of singlet pairs made possible by the presence of holes[50]. Numerical simulations by Hirsch have failed to detect any other significant feature than the breakdown of antiferromagnetism away from $\delta = 0$ [26,28]. In particular Hirsch's work seems to suggest the existence of an ordinary paramagnetic metallic phase as soon as

$\nu \neq 1$. However, existing simulations of the ground state of interacting fermions are affected by a number of uncertainties due to *i)* small system size, *ii)* non zero temperature making extrapolation to the ground state problematic, and *iii)* non positiveness of the statistical weight. Very recently the first two difficulties are almost been solved by using stabilized and faster algorithms but the last one still remains the main difficulty in Monte Carlo schemes, as we have discussed in detail in Chapter II. We have seen that using the weight obtained with the HST, there may be problems because the average sign can exponentially vanish as the "effective" temperature β^{-1} approaches the $0K$ limit. On the other hand, according to the statements (2.1.13) and (2.1.14), it is also possible that the sign changes of this weight depend only on the particularly chosen trial wavefunction and the average sign approaches a constant for infinite β. In this case, no matter how small this constant is, numerical simulations are possible without sampling directly the sign changes. Therefore the sampling of the sign is in fact not necessary in this case (as is discussed in Ch. II). Since it is not possible to establish a "priori" the behaviour of the average sign one has to rely only on numerical simulation.

We have studied a number of small cluster for which an exact diagonalization has been successfully obtained. In table 5.1 we show exact ground state expectation values of different operators compared with results of numerical simulation by neglecting the sign (i.e. using the Q_N ensemble see eq.1.2.10). Quite surprisingly we found a quite good agreement with exact results with very few exception as it can be seen in table 5.1. It is noteworthy that even for two holes (non closed shell case) total and kinetic ground state energy are correctly predicted. However the magnetization is grossly underestimated. Also for 10 electrons in 16 sites the kinetic energy is slightly off. In spite of the overall encouraging pattern

Size	# el	U	E/N	E_{kin}/N	$S_{magn.}(\pi,\pi)$
2×2	4	4	-1.406(5) (-1.414)	-1.880(6) (-1.867)	1.92(8) (1.93)
3×3	10	4	-0.700(1) (-0.699)	-1.626(6) (-1.626)	
4×4	10	4	-1.227(3) (-1.224)	-1.414(5) (-1.408)	0.73(1) (0.73)
4×4	10	8	-1.088(6) (-1.094)	-1.255(8) (-1.272)	0.76(2) (0.75)
4×4	16	4	-0.848(5) (-0.8514)	-1.324(6) (-1.3118)	3.4(2) (3.64)
4×4	14	4	-0.988(3) (-0.9840)	-1.331(4) (-1.3366)	1.60(7) (2.14)

Table 5.1. Comparison of the HST simulation and of exact diagonalization (in brackets) results. E/N and E_{kin}/N represent the total and kinetic energy respectively. S_{mag} is the magnetic structure factor. These results refer to ground state properties only.

the few exception found can only be explained with appearance of a finite Δ in the $\beta \to \infty$ limit (see eq.(2.1.13)). However table 5.1 indicates that, using the HST, the fermion sign problem is considerably less severe than expected, so that it can be considered a good approximation of the ground state properties to neglect the sign. We don't know whether this approximation is indeed exact away from half filling, unless for very small U and closed shell (as shown in Sect. 2.4), but in all numerical works it is not possible to distinguish if a quantity is exactly 0. It is only possible to estimate a bound from above. Moreover even in case the average sign exponentially vanishes one can relate exact ground state average of operators to the averages of estimators (1.2.3) with the approximation of neglecting the sign.

In fact from $E_M = E_0 - \Delta$ and the Hellman–Feynman theorem, we have that:

$$<\psi_0 \hat{O} \psi_0> \; = \; \frac{\partial E_0}{\partial \lambda} - \frac{\partial \Delta}{\partial \lambda} \tag{5.2.1}$$

Now if Δ smoothly depend on the external coupling λ we can get good approximation of ground state expectation values without sampling the sign. Within this approximation, we now describe some of the results concerning the physical property of the Hubbard model away from half filling. Then we make an independent calculation, although for smaller but comparable sizes, by considering the sign in the weight, and verify how good is the mentioned approximation.

The 2D antiferromagnetic order is readily destroyed by doping. In Fig.5.5 we display the spin-spin correlation function C in the 16×16 lattice at $U = 4$ for $\nu = \frac{226}{256}$ ($\delta = 12\%$) and for $\nu = \frac{74}{256}$ ($\delta = 71\%$). These results have been obtained using a paramagnetic trial wavefunction. The same results are also recovered starting from an antiferromagnetic wavefunction. However in this case a longer Langevin simulation is needed to reach equilibrium and melt the magnetic order.

The results of Fig.5.5 confirm the suggestion by Hirsch that away from $\nu = 1$ the magnetic order is destroyed in the 2D Hubbard model. The question whether spin correlations in this system decay exponentially or as a power law is however difficult to answer within the present numerical accuracy. In fact, the corresponding spin–spin correlations for the $U = 0$ Fermi–liquid look quite similar.

In order to test the further conjecture that the disappearance of magnetic order signals the onset of paramagnetic metallic behavior, we have measured the momentum distribution $n(k)$ for three values of the doping $\delta = 1 - \frac{N}{N_a}$. Our results, which are displayed in Fig.5.6, show that the momentum distribution for the half–filled case is a smooth function consistent with the insulating character

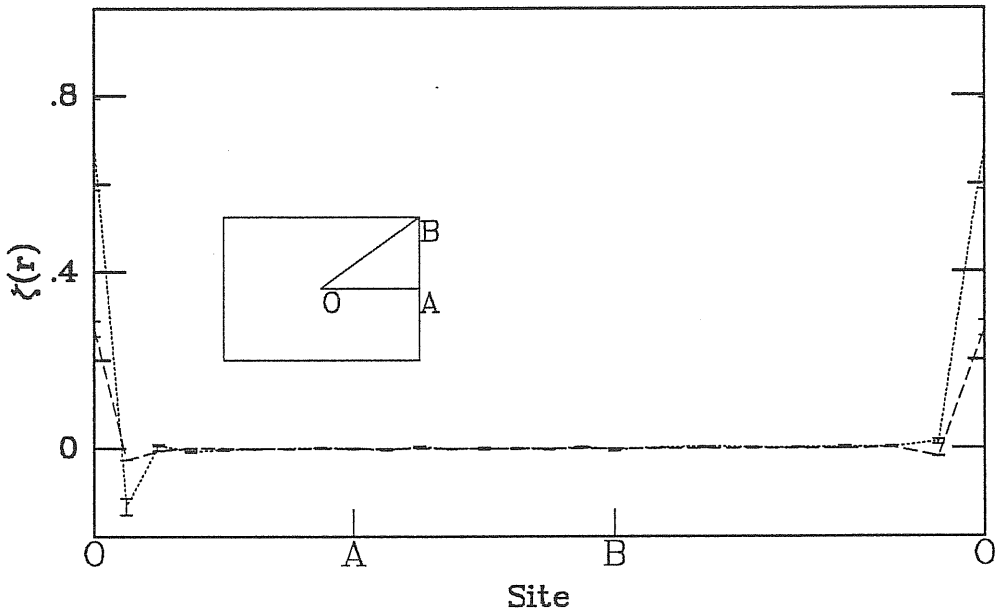

Figure 5.5. Spin-spin correlation function of a 2D 16×16 Hubbard model for U=4, $\nu=\frac{226}{256}$ (continuous line) and $\nu=\frac{74}{256}$ (dashed line). The path in the unit cell is shown in the inset.

of the antiferromagnetic state. The momentum distribution of the half–filled AF Hartree–Fock state, shown by the dashed line of Fig.5.7, is in fact rather similar to that of the true ground state of Fig.5.6. The situation changes completely with moderate doping, $\delta = 12\%$. The new HF state displays a sharp dip corresponding to a Fermi surface (Fig.5.7). The true ground state $n(k)$ shown in Fig.5.6, however, has no such dip, and roughly looks as though some kind of insulating character were preserved, in spite of the fact that magnetic order is destroyed. For heavy doping, finally ($\delta = 71\%$) a sharp Fermi surface is clearly recovered.

After these results were obtained with the approximation that neglects the sign we have considered tilted shell at 10% doping case with tilted PBC. For the sequence of site numbers 20,100,180 and orientation $tan(\theta) = \frac{1}{2}, \frac{3}{4}, \frac{1}{2}$ respectively, the kinetic term is non degenerate, and this ensures, as shown previously in

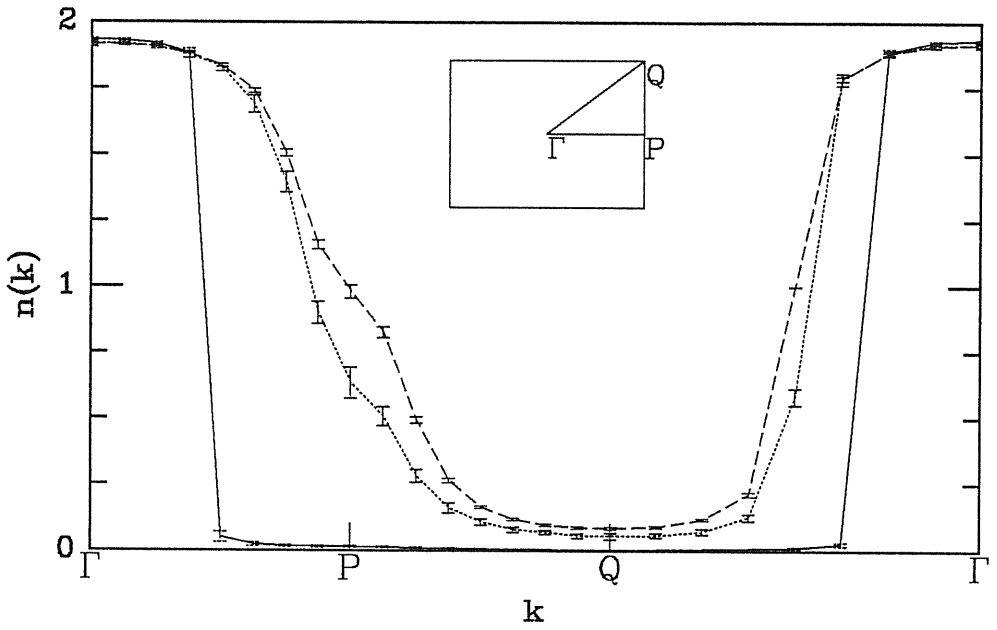

Figure 5.6. Momentum distribution of the 2D 16×16 Hubbard model with U=4,for $\nu=\frac{256}{256}$ (dashed line), $\nu=\frac{226}{256}$ (dotted line), and $\nu=\frac{74}{256}$ (continuous line). The path in the Brillouin zone is shown in the inset. The imaginary time was T=12 (half filled) and T=24 (less than half filled).

chapter II, that for sufficiently small U the average sign is never vanishing exponentially. Also at larger U we expect the sign problem to be less severe once the degeneration of the kinetic energy term has been removed. Moreover in order to improve the convergence in the inverse temperature we used the Gutzwiller wavefunction as a trial wavefunction. This Gutzwiller wavefunction[6,47,48] is expected to be closer to the true ground state than a simple Slater determinant and it is defined as follows:

$$\psi_{GW} = e^{-\frac{\alpha}{2}\left(\sum n_{i\uparrow} n_{i\downarrow}\right)} |\psi_T> \tag{5.2.2}$$

with α chosen in such a way to minimize $\frac{<\psi_{GW} H \psi_{GW}>}{<\psi_{GW}|\psi_{GW}>}$ and ψ_T is still a chosen Slater determinant wavefunction. In fact within the HS formulation it is very

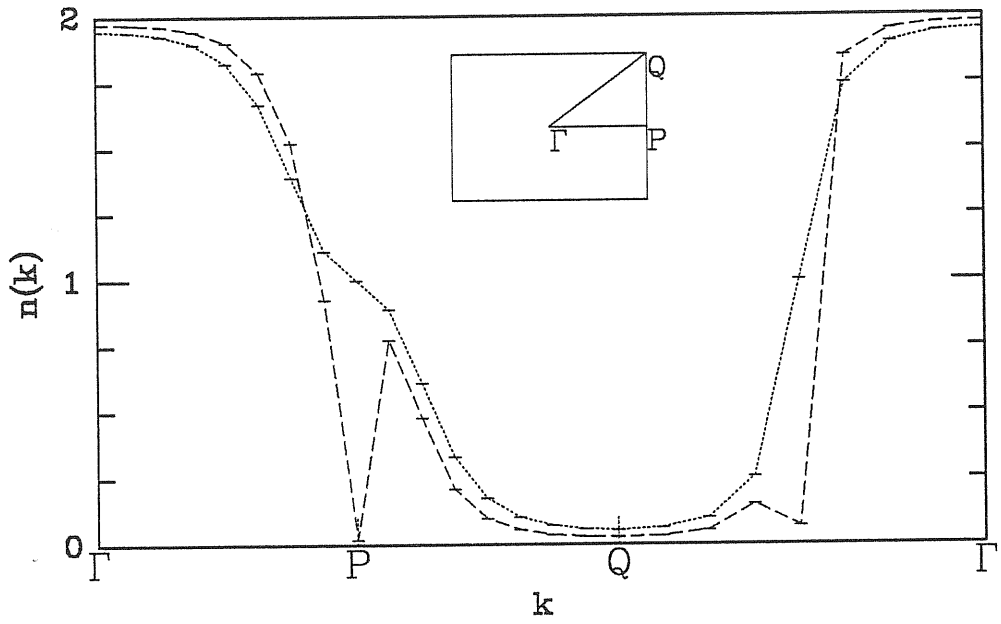

Figure 5.7. Momentum distribution of the Hartree-Fock AF solution of the 2D 16×16 Hubbard model with U=4. The dashed line correspond to half filling, whereas the continuous line corresponds to $\nu=\frac{226}{256}$.

simple to build the Gutzwiller operator $\exp -\frac{\alpha}{2}\sum n_{i\uparrow}n_{i\downarrow}$ in terms of auxiliary fields exactly in the same way as the many body term is treated in (1.1.14):

$$e^{-\hat{V}\Delta\tau} = e^{-(U\Delta\tau)\sum n_{i\uparrow}n_{i\downarrow}} \qquad (5.2.3.)$$

After all a Gutzwiller wavefunction can be used as a trial wavefunction by adding further $2N_a$ auxiliary variables in the propagator U_σ defined in (1.1.23) at the first and at the last discrete imaginary time slice. We considered in the numerical calculation two different Gutzwiller trial wavefunctions with or without antiferromagnetism in the free electron part ψ_T of ψ_{GW} (5.2.2). The convenience of the Gutzwiller wavefunction is illustrated in fig.5.8 where it is shown that the estimated energy converges very soon to the ground state energy. In fact the Gutzwiller variational parameter α remarkably improve the value of the energy

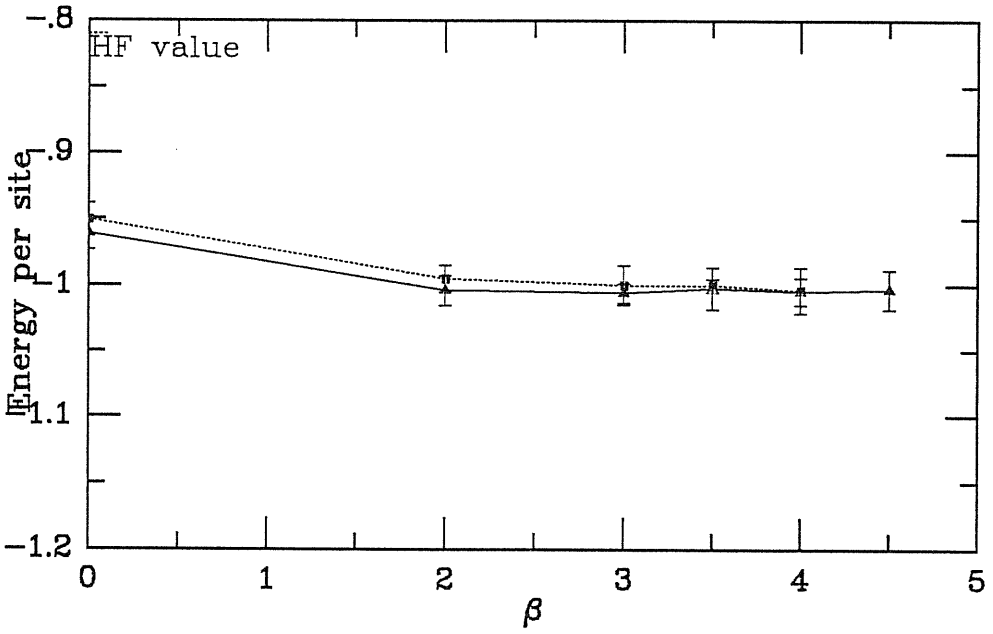

Figure 5.8. Ground state energy per site for the doped (10 holes) 2D Hubbard model in a 8^2+6^2 100-sites tilted lattice as a function of the effective inverse temperature. The triangles correspond to simulations with a paramagnetic Gutzwiller trial wavefunction with α=1.0. The squares are instead obtained with an antiferromagnetic Gutzwiller trial wavefunction with the same α. In the last case the value of the staggered magnetization was fixed to 1/2 the mean field value. The corresponding Hartree Fock paramagnetic energy is indicated for comparison

with respect to the uncorrelated part. $E_{HF} = -.815$, $E_{GW} \simeq= -.94$ while the estimated ground state energy is around $-1.00 \pm .03$.

In order to show the instability of the AF order obtained with a little amount of doping, we show in fig.5.9. the dependence of the magnetic structure factor at $Q = (\pi, \pi)$ as a function of our "effective" temperature β^{-1}, for the two trial wavefunctions considered. We clearly see in this picture that the temperature dependence of $S(\pi, \pi)$ is much more stable when the trial wavefunction is the paramagnetic one, thus suggesting disappearance of AF order. Remarkable is the comparison on the same system of the value obtained with the norm–

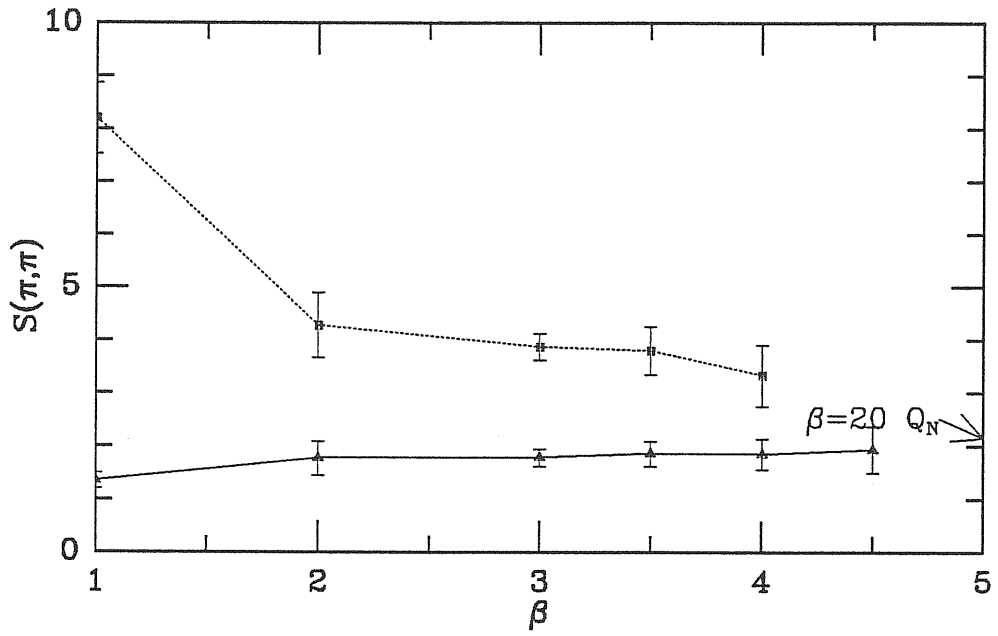

Figure 5.9. Magnetic structure factor $S(q)$ at $q=(\pi,\pi)$ for the doped (10 holes) 2D Hubbard model in a 8^2+6^2 100-sites tilted lattice as a function of the effective inverse temperature. The triangles correspond to simulations with a paramagnetic Gutzwiller trial wavefunction with α=1.0. The squares are instead obtained with an antiferromagnetic Gutzwiller trial wavefunction with the same α. In the last case the value of the staggered magnetization was fixed to 1/2 the mean field value. The corresponding value obtained at low temperature, using the Q_N ensemble is indicated for comparison

approximation described before.

As far as the momentum distribution function is concerned we show in fig .5.10 the value of the jump $n_{\epsilon_+} - n_{\epsilon_-}$ at the Fermi energy. From fig.5.10 it is apparent that the Gutzwiller wavefunction implies a finite jump in the Fermi surface even in the thermodynamic limit. More difficult is to reach any definite conclusion on the ground state obtained by HST simulation, due to statistical errors and insufficiently large sizes and β values. The jump is much smaller than Gutzwiller, but it is otherwise not clear what value it will take in the thermodynamic limit. The fact that the maximum jump in $n(\epsilon)$ occurs at the same value for which a

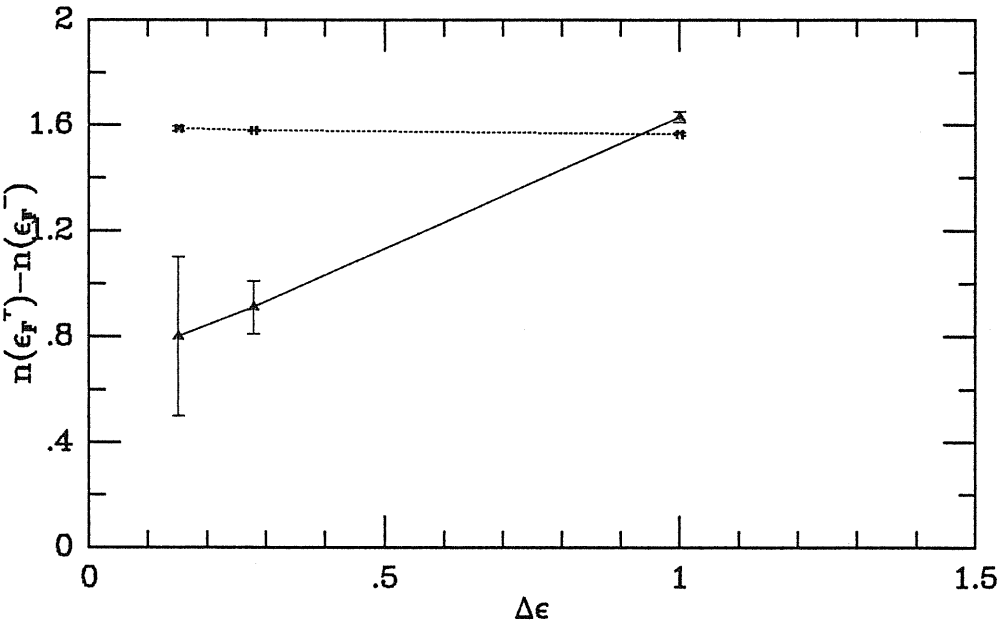

Figure 5.10. Plot of the maximum jump of the function $n(\epsilon)$ described in the text as a function of the finite size resolution in energy for a 2D 10% doped Hubbard model(continuous line). The dotted line gives the corresponding jump for the Gutzwiller wavefunction, where $\alpha = 2$ and the single particle determinant is paramagnetic.

free particle state at $\nu = .9$ has its largest discontinuity would indicate that, if the Fermi surface survives at finite U its shape remains approximately inaltered. Recent numerical studies[25] are in agreement with this scenario.

For the 2D 10% doped Hubbard model however it is not possible to understand the metallic or non metallic behaviour of the ground state since larger size are prohibitive to simulate due to "sign problem " for low temperatures and smaller ones do not belong to the same class of "closed shell" filling.

In conclusion the ground state of the Hubbard model away from half filling may show peculiar and interesting properties (as also shown by exact diagonalization results in the next section), that makes still difficult its representation in terms of classical Hubbard–Stratonovich variables. However further technical im-

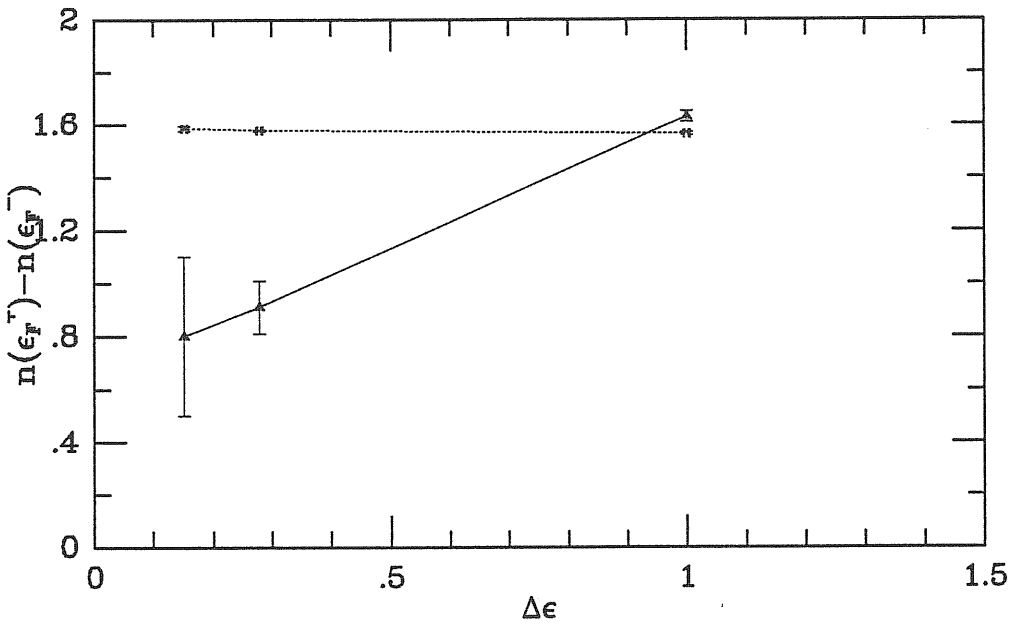

Figure 5.10. Plot of the maximum jump of the function $n(\epsilon)$ described in the text as a function of the finite size resolution in energy for a 2D 10% doped Hubbard model(continuous line). The dotted line gives the corresponding jump for the Gutzwiller wavefunction, where $\alpha = 2$ and the single particle determinant is paramagnetic.

free particle state at $\nu = .9$ has its largest discontinuity would indicate that, if the Fermi surface survives at finite U its shape remains approximately inaltered. Recent numerical studies[25] are in agreement with this scenario.

For the 2D 10% doped Hubbard model however it is not possible to understand the metallic or non metallic behaviour of the ground state since larger size are prohibitive to simulate due to "sign problem " for low temperatures and smaller ones do not belong to the same class of "closed shell" filling.

In conclusion the ground state of the Hubbard model away from half filling may show peculiar and interesting properties (as also shown by exact diagonalization results in the next section), that makes still difficult its representation in terms of classical Hubbard–Stratonovich variables. However further technical im-

provements of the convergence in temperature or by a very good choice of the trial wavefunction may lead to the final understanding of this very important topic.

5.3 D-WAVE, DIMER AND CHIRAL STATES IN THE 2D HUBBARD MODEL

Here we study the states of two holes in the 2D Hubbard model. This is the only section where a method different from QMC is used. The reason is the need for extreme accuracy ($< 10^{-3}t$) which is not permitted by the fermion sign problem, and general convergence problems. We show, by detailed analysis of a small size system, namely a 4×4 Hubbard lattice with 14 electrons, that very interesting information on the possible ground states is foreshadowed by the properties of the low–lying states of the two–hole problem.

In particular, we find three uniform and one density–wave state within a very small energy difference of one another. Among the possible uniform states, one closely resembles a dimer phase while another can be interpreted as a kind of flux phase, or chiral spin liquid. We also find that all these and exclusively these low lying states can be given an approximate representation in terms of linear combinations of "Fermi level" hole creation operators acting onto the half filled ground state. This form suggests new approximate wavefunctions for the 2D Hubbard model at small but finite doping.

We seek the lowest eigenvalues of the 4×4 Hubbard model with PBC by a power method:

$$|\psi_0 >= \lim_{k\to\infty} \frac{(\Lambda - H)^k |\psi_T >}{\|(\Lambda - H)^k |\psi_T > \|} \tag{5.3.1}$$

where Λ is a sufficiently large, but otherwise arbitrary energy shift, and ψ_T is a trial wavefunction. The iterative search for the ground state is supplemented by a few Lanczos steps at the end in order to improve accuracy. This method, although rather slow, minimizes memory requirements which are at present the major limiting factor for this kind of calculations.

Special coding of the wavefunction and memory access techniques were used to make the calculation feasible. In this calculation we have restricted our search to the subspace of $S_z = 0$ and even total spin, whose size is $\frac{M(M+1)}{2}$ where $M = \binom{N_a}{N_\uparrow}$. In the present case $N_a = 16$, $N_\uparrow = 7$, the size is $\sim 7 \times 10^7$. No explicit use has been made of the spatial symmetries of the lattice. The initial vector ψ_T of our iterative procedure has been taken to be an appropriate *random* superposition of eigenvectors of the total momentum. This device permits the simultaneous study of all possible symmetries and k-vectors. Each of them is singled out after convergence by using a symmetry projector. We find that all the low lying states, within our even S manifold, are singlets.

In Table 5.2 we show the resulting energies for each total k–vector along with the magnetic structure factor $S_{mag}(\pi,\pi)$, the density structure factor $S_{den}(\pi,\pi)$, the single particle off–diagonal density matrix ρ_n (where n denotes the n-th neighbor) and, where defined, the rotational symmetry of the state. The energy improvement upon doping, which is seen by comparison with the undoped case in Table 5.2, is basically a kinetic energy gain, as indicated also by ρ_1. Although this is not surprising, it is interesting to note that the ground state does not have

ν	16/16			14/16			
Q	$(0,0)$	$(0,0)$	$(0,\pi)$	(π,π)	$(\pm\frac{\pi}{2},\pm\frac{\pi}{2})$	$(\pi,\frac{\pi}{2})$	$(0,\frac{\pi}{2})$
g	s	d		p			
E/N	-0.8514	-0.9840	-0.9840	-0.9839	-0.9839	-0.922	-0.922
E_{kin}/N	-1.3118	-1.3366	-1.3366	-1.3375	-1.3375	-1.24	-1.24
$S_{mag}(\pi,\pi)$	3.64	2.14	2.18	2.18	2.16		
$S_{den}(\pi,\pi)$	0.385	0.4242	0.4242	0.4245	0.4245		
ρ_1	0.164	0.167	0.168	0.167	0.167		
ρ_2	0.0	$5.4\ 10^{-2}$	$-7.8\ 10^{-4}$	$-7.4\ 10^{-4}$	$-7.7\ 10^{-4}$		
ρ_3	0.0	$-5.6\ 10^{-2}$	$5.5\ 10^{-2}$	$5.4\ 10^{-2}$	$-7.4\ 10^{-4}$		
ρ_4	$-4.8\ 10^{-2}$	$-5.0\ 10^{-2}$	$-5.1\ 10^{-2}$	$-5.1\ 10^{-2}$	$-5.0\ 10^{-2}$		
ρ_5	0.0	$-5.1\ 10^{-2}$	$-5.1\ 10^{-2}$	$-5.1\ 10^{-2}$	$-5.1\ 10^{-2}$		

Table 5.2. Exact diagonalization results for a 4×4 2D Hubbard model for different filling and physical quantities (see text). The value of the on-site Hubbard interaction is fixed to U=4. These results refer to ground state properties only except in the $\nu \doteq \frac{14}{16}$ where the lowest excited states have been identified.

the best kinetic energy. Clearly doping has a depressing effect on the magnetic $S_{mag}(\pi,\pi)$, but do not affect so much the density response at the same wavevector.

The ground state is threefold degenerate $(0,0)$, $[(0,\pi), (\pi,0)]$. This agrees well with the existing $t-J$ model calculations.

The extra, non–rotational, degeneracy between $(0,0)$ and $(0,\pi)$ is due to an

additional symmetry of the Hubbard hamiltonian, specific to the 4×4 lattice. A new striking feature is the presence of extremely low–lying excited states with $(\pm\frac{\pi}{2}, \pm\frac{\pi}{2})$ and at (π, π). By contrast states at $(0, \frac{\pi}{2})$, $(\pi, \frac{\pi}{2})$ are found to be much higher in energy. The density matrix indicates that electron hopping within the same sublattice, strictly forbidden by charge conjugation symmetry at half–filling, is allowed in a substantial amount in presence of holes.

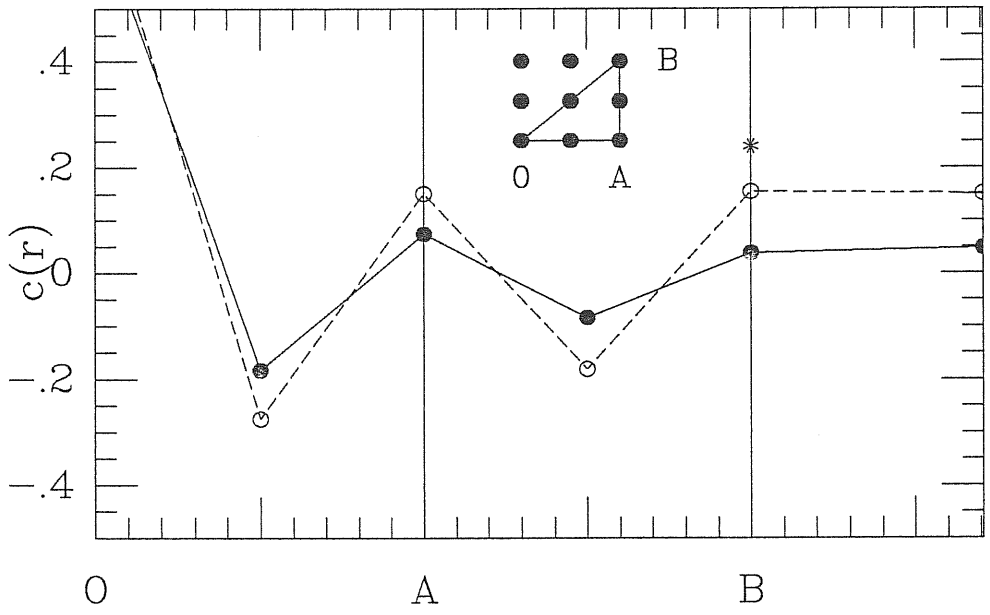

Figure 5.11. Spin–spin correlations for U=4 along the path shown in the inset. Dashed line: half filling. Solid line: two holes in the (0,0) state. The star at the maximum distance indicates the corresponding Heisemberg value for the same lattice size.

We have also studied charge-charge and spin-spin correlation functions for all the low-lying states. Rather surprisingly we find that all the low lying states have similar correlations. The spin correlation $c(R) =< S_z(0)S_z(R) >$ all show evidence of tendency towards antiferromagnetic ordering which is however substantially weakened with respect to the half filled case (see Fig.5.11 and

also $S_{mag}(\pi,\pi)$ in Table 5.2). Remarkably, the hole–hole correlations $h(R) = <(1-n^{\uparrow}(0))(1-n^{\downarrow}(0))(1-n^{\uparrow}(R))(1-n^{\downarrow}(R))>$ are slightly "repulsive" and not much structured (Fig.5.12), i.e. the two holes tend to stay apart in all cases. Previous t-J model studies found a crossover between repulsion and attraction for increasing J, but seem to attach importance only to the attractive regime. In view of existing suggestions that long range hole–hole correlations should show overall indifference if not repulsion[50] or instead attraction[8,9] it would be desirable to remove the short range hole–hole hard core. If we take the undoped $h(R)$ as representative of these "bare" correlations then one would conclude (see Fig. 5.12) that the additional correlations are repulsive at short range and seem to turn attractive at the largest available distance.

In order to extract more information we analyse in detail the nature of the low lying states.

$(0,0)$: This state is even under x and y reflections and changes sign under $\frac{\pi}{2}$ rotation. Therefore the two holes are in a $d_{x^2-y^2}$ relative state. The symmetry of this state is the same as that of one of the proposed d–wave RVB states. However we have not calculated the overlap between the exact ground state and this class of functions. It is interesting to note that the d_{xy} state is instead pushed up at higher energy $\Delta E \simeq .3\,t$.

$(0,\pi);(\pi,0)$: This doublet can be combined to break translational invariance, while restoring rotational symmetry. The states thus obtained exhibit neither charge nor spin density wave spatial modulation. Rather, an order parameter distinguishing the two inequivalent states of the doublet can be identified as a *current fluctuation*

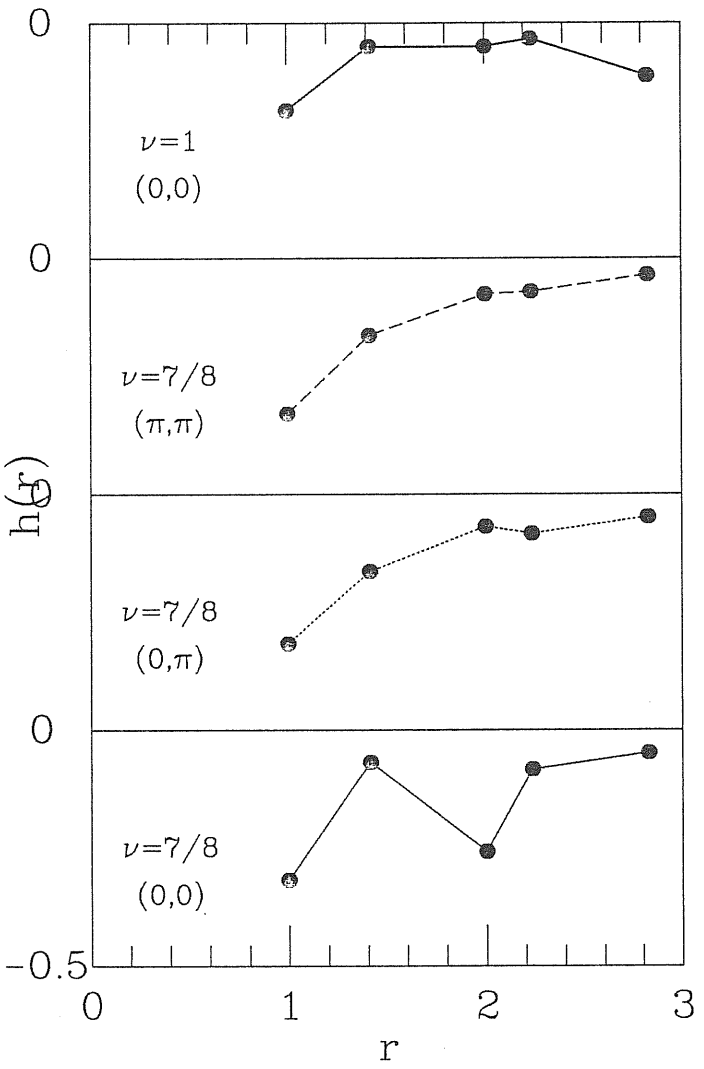

Figure 5.12. Hole–hole correlations for half filling and for the three uniform states at ν=7/8. Note that the two holes tend to stay apart (*repulsivecorrelations*).

operator: we find an interesting non homogeneous current pattern which can be identified by measuring $< \chi_{ij}\chi_{jk}\chi_{kl}\chi_{li} >$, the circulation along the elementary square plaquettes of the operator $\chi_{ij} = \sum_{\sigma} c_i^{+\sigma} c_j^{\sigma}$. This gives 0.18 and -0.008 along two non equivalent neighboring plaquettes. This result rather resemble the pattern one

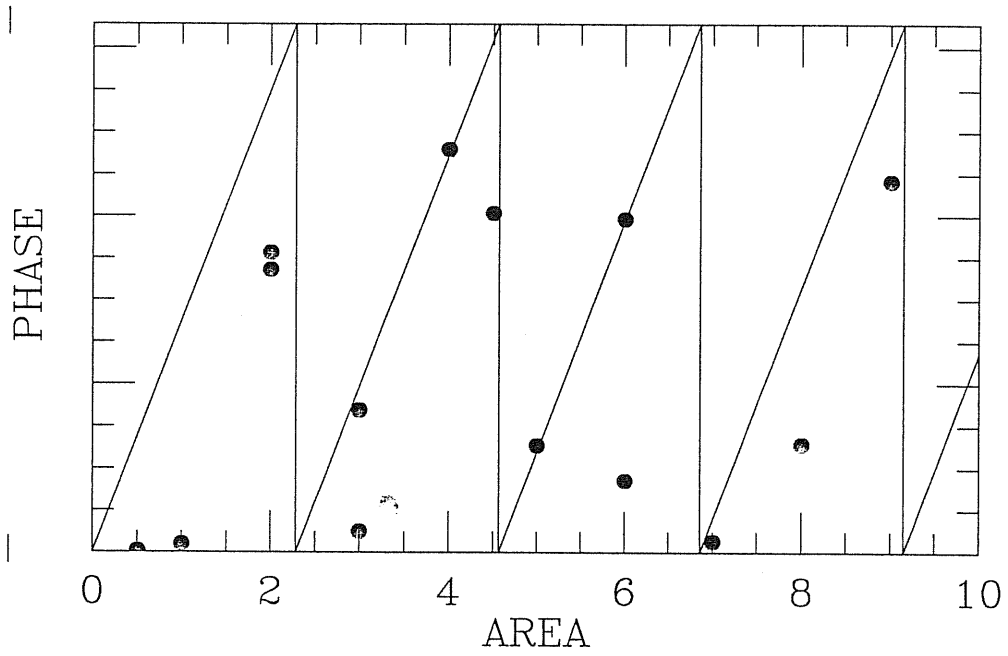

Figure 5.13. Phases associated with several plaquettes of different areas (•) as found in the (π,π) chiral state. The phase expected for a flux state with 1/2 flux per electron is also shown (solid line).

could expect for some superposition of *dimer* phases.

$(\pm\frac{\pi}{2},\pm\frac{\pi}{2})$: This quartet of states can also be combined to give translationally non invariant states with uniaxial symmetry. One thus finds two pairs of states characterized by a weak CDW ($\Delta n/n = 6.5\,10^{-3}$) arranged to form a two sublattice structure. Another feature of this state is a weak asymmetry between $< \chi_{i,j} >$ at right angles: $< \chi_{i,i+x} >= 0.3340, < \chi_{i,i+y} >= 0.3347$.

(π,π): This is a doublet of translationally invariant states with p–like rotational symmetry. The circularly polarized combination $p_x \pm ip_y$ have well defined chiralities. Therefore this state is a natural candidate for a finite size realization of a "chiral spin liquid". We have investigated the circulation dependence on the plaquette area.

For a long range chiral ordered state of the type proposed by Wen, Wilczek and Zee, the phase of the circulation should increase with the area. The flux states first introduced by Affleck and Marston and by Kotliar imply 1/2 flux quantum per electron. The phase of a flux state is predicted to depend upon doping in the simple manner $\phi = \nu\pi A$. The results for our (π, π) state given in Fig. 5.13 do show an increase of phase with plaquette area which compares rather well, though not exactly, with the flux state values. This state is characterized by a non zero chiral order parameter: $< P(R) >=< \mathbf{S}_i \cdot \mathbf{S}_j \times \mathbf{S}_k >= 1.3 \times 10^{-2}$, where i, j, k label the vertices of the elementary triangle centered at R. This provides a first indication of the rather small amount of *parity symmetry breaking* to be expected for a Hubbard model as opposed to more "ad hoc" hamiltonians. If, as it seems possible, the chiral long range order still shows up in the thermodynamic limit, then statistical transmutation would necessary follow. We have also studied the spatial correlations $< P(0)P(R) >$, and found them still large, of order 10^{-2} for the largest distance in the cluster ($R = \sqrt{8}$). Note that the uncorrelated value would be ($< P(0) >^2 = 1.7\,10^{-4}$).

This exhausts the set of low lying states of the two holes. It seems remarkable that, in spite of the obvious size limitation, so many different kinds of states already show up in the two holes problem. It is clearly desirable at this stage to have a simple description and rationalization of these states. A crucial clue is provided by

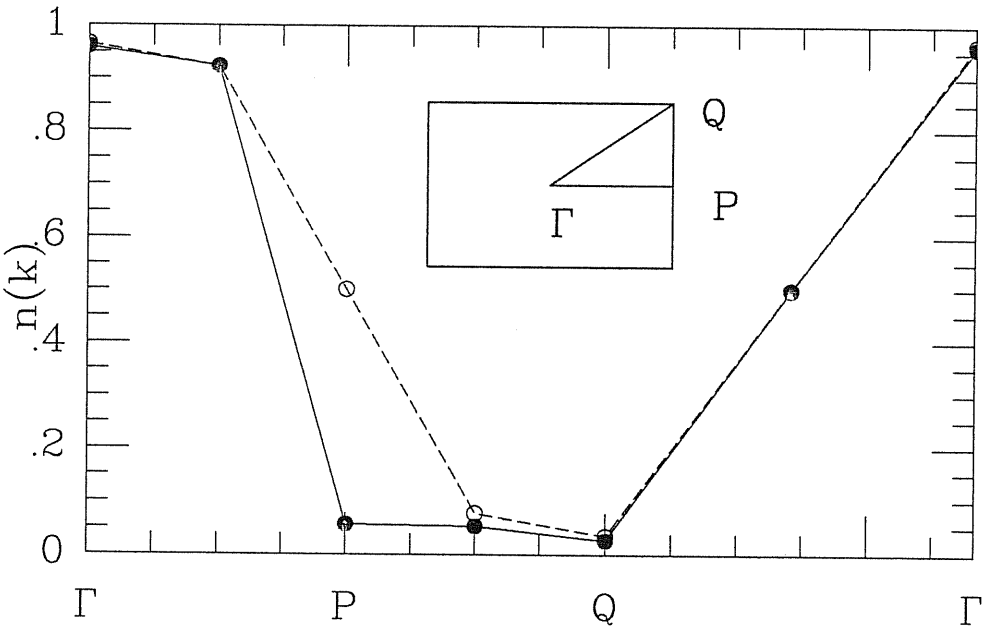

Figure 5.14. Momentum distribution $n(k)$ for the two hole state (0,0) (•) as compared with the half filled, zero hole, state (o).

the change in the momentum distribution function $n(k)$ which we observe upon doping. As exemplified in the $(0,0)$ case $\delta n(k)) = n(k)|_{\nu=16/16} - n(k)|_{\nu=14/16}$ shown in Fig. 5.14 is a very strongly peaked function at $(0,\pi)$ $(\pi,0)$ suggesting that the main ingredients in this state are two holes at these k-vectors. This turns out to be a general property for all the low lying states. For all of them, the true eigenfunction can, approximately but accurately, be described by the form:

$$|\psi_{\frac{N}{2}-2}> = \sum_{\mathbf{k}_1,\mathbf{k}_2} \Phi(\mathbf{k}_1,\mathbf{k}_2) c^{\uparrow}_{\mathbf{k}_1} c^{\downarrow}_{\mathbf{k}_2} |\psi_{\frac{N}{2}}> \tag{5.3.2}$$

where $|\psi_{\frac{N}{2}}>$ is the half filled ground state. The form of $\Phi(\mathbf{k}_1,\mathbf{k}_2)$ is uniquely determined by the following requirement: (i) $\mathbf{k}_1$ and $\mathbf{k}_2$ should lie on the outermost shell of the $U = 0$ Fermi surface at half filling, (ii) $\mathbf{k}_1 + \mathbf{k}_2$ should equal the total momentum of the state, (iii) the holes form a singlet state, (iv) the holes

cannot sit on the same site. The latter two requirements prevent the holes from being in a relative s–like state (i.e. $\Phi(r_1 = r_2) = 0$). Although very simple, the wavefunctions (2) reproduce very well the properties of all the true low-lying states. It is to be noted that most of the correlations in $|\phi_{\frac{N}{2}-2}>$ derive from those already present in the parent half filled state $|\phi_{\frac{N}{2}}>$.

For the 4×4 lattice the Fermi surface consists of 6 points $(\pm\frac{\pi}{2}, \pm\frac{\pi}{2})$, $(0,\pi)$, $(\pi,0)$. Out the 36 pair hole states that can be formed, 15 are triplets and 21 singlets. Out of the latter, 10 states satisfy the above criteria. We find that nine of them are good approximations to the low lying states described above, as anticipated.†

Summing up, the above analysis shows how to build approximate but accurate, two–hole states, starting from the knowledge of the ground state at half filling. It seems possible, although clearly speculative, at this stage, to generalize this result to the many–hole, dilute limit. One such generalized wavefunction could be, for example,

$$\Psi = \exp\left(\sum_{<\mathrm{k}_1,\mathrm{k}_2>} \Phi(\mathrm{k}_1,\mathrm{k}_2) c^+_{\mathrm{k}_1} c^+_{\mathrm{k}_2}\right) \left|\psi_{\frac{N}{2}}\right\rangle \tag{5.3.3}$$

where the pair envelope function $\phi_{k_1 k_2}$ can be determined variationally, but must obey the same rules as described above for two holes. The richness of different states found in a tiny range of energy suggests that in the infinite size limit

† The 10^{th} state has $k = (0,0)$ and it has symmetric d_{xy} combination of holes $(\pm\frac{\pi}{2}, \pm\frac{\pi}{2})$. A state of this symmetry has been found among the excited states at a considerably higher energy ($\Delta E \sim 0.3t$). However we have found impossible to represent it as in Eq.5.3.2.

various scenarios are indeed possible. Translational invariance (charge and spin uniformity) is equivalent to regarding $\mathbf{k}_1 + \mathbf{k}_2 = \mathbf{Q} = \mathbf{G}/2$, where $\mathbf{G}$ is a reciprocal lattice vector. The symmetry of $\Phi(\mathbf{k}_1, \mathbf{k}_2)$ will of course be reflected in the overall symmetry of the corresponding Ψ. We do not yet know, however, any other property of these proposed states, including the presence of off-diagonal long–range order. We note, however, a certain similarity of our wavefunction (5.3.3) with the spin–bag proposal by Schrieffer *et al.*[9], which is recovered, in particular, if $|\psi_{\frac{N}{2}}>$ is approximated by a spin density wave state and $\Phi(\mathbf{k}_1, \mathbf{k}_2)$ is peaked around pockets at the corners of the Fermi Surface. An alternative choice, valid for large U, could be to use a Heisenberg state as $|\psi_{\frac{N}{2}}>$ in Eq. (5.3.3).

In summary, we have presented a detailed study of the two hole problem in the 2D Hubbard model, which uncovers a manifold of ground states (or very nearly ground states) including a d–wave state, a dimer–like state and a chiral flux state. From these exact states, approximate wavefunctions are constructed which permit extension to the thermodynamic limit.

5.4 Scaling of the 1D Hubbard model to the Tomanaga–Luttinger model

One of the central issues which have come into focus in the physics of highly correlated electron systems —of particular relevance in the modeling of $H - T_c$ superconductors[51] is the question whether in such systems the electron behaviour is Fermi Liquid or not Fermi liquid like. In a Fermi Liquid, propagating electron quasi–particles are well–defined which implies a) a non–zero quasi–particle pole strength Z_k in the single particle propagator

$$G(k,\epsilon) = \frac{Z}{\epsilon - v_F(k-k_F) + i\delta \ \mathrm{sgn}(k-k_F)} + G_{incoh}(k,\epsilon) \qquad (5.4.1)$$

(with standard notations) and b) a finite jump Δ of the momentum distribution $n_k = < \sum_\sigma c^+_{k\sigma} c_{k\sigma} >$ at $k = k_F$ exactly equal to the quasiparticle amplitude renormalization Z.

The vanishing of Z and then of Δ strongly indicates the need for a new description, replacing the conventional Landau Fermi Liquid[52].

In a system of finite size L $\Delta(L)$ is anyway non–zero. His asymptotic behaviour however can fall into one of three categories:

$$\Delta(L)_{L\to\infty} \to \begin{cases} e^{-L/\zeta} & \text{insulator} \\ L^{-\theta} & \text{marginal conductor (non-Fermi liquid)} \\ const & \text{normal conductor (Fermi liquid).} \end{cases} \qquad (5.4.2)$$

It is therefore in principle straightforward to determine whether a correlated electron conductor model is a Fermi-liquid, provided finite–size scaling can be done on $\Delta(L)$.

Among the models of highly interacting electrons, the Hubbard model (HM) achieved a very special status, for three main reasons. The first reason is of course its ability to provide an idealized prototype for the Mott transition between a metal and an antiferromagnetic insulator[13,46]. A second reason has emerged more recently, and is related with suggestions that the HM could contain the basic ingredients for a new type of superconductivity[50]. The third, and maybe the principal reason is that the HM is one of few hard but well-posed problems (to use Anderson's terms), and has systematically defeated so far all perturbative, simple minded approaches towards its solution.

Apart from its general importance, approximate realizations of the $1D$ HM are found in antiferromagnetic salts like $Cu\ Cl_2$[53,54] as well as in a larger class of organic quasi one dimensional molecular crystals [55].

From a strictly mathematical point of view the *one dimensional* HM can be regarded as exactly solved for all fillings. Lieb and Wu[36] have given the formally exact ground state wavefunction and a scheme for calculating energy and related static quantities[56-60]. The half filling state is an insulator for all U, with strong AF couplings but without LRO. Away from half filling, Lieb and Wu found the $U > 0$ 1D HM to be a "conductor", (vanishing single-particle gap). Later, a scaling to the Tomonaga model strongly suggested that this system could at best be a "marginal" conductor, i.e., one without well-defined quasi particles, and thus not a Fermi-liquid. More recent work, including variational[61,62] and numerical[63,64], while providing much new information on several important quantitative aspects has not been able to attack directly the nature of the Fermi-level singularity in this regime.

In this section we resolve this question, and provide a first numerical

characterization of the non-Fermi liquid behaviour of the repulsive 1D HM, through finite size scaling. This prototype 1D study thus paves the way for the future applications to 2D models, where the Fermi-liquid issue is still entirely open.

The diagonalization method used was a simple power method scheme, in which the operator $\Lambda - H$ is repeatedly applied to $|\psi_T>$. Λ is a sufficiently large, but otherwise arbitrary energy shift.

The ground state properties of the Hubbard hamiltonian (1.1.2-3) for finite size systems consisting of N electrons distributed on N_a sites, have been determined by using either exact diagonalization, or the newly developed quantum Monte Carlo method presented in this thesis.

The convergence of the power method is rather poor, however this is compensated by the reduced storage requirement, which grow very rapidly with the number of electrons. Use of the sparseness of the Hamiltonian matrix and of special memory access techniques has allowed us to treat Hilbert spaces as large as 10^8 states[1].

Each of our small systems is characterized by three parameters: size N_a, filling $\nu = \frac{N}{2N_a}$, and Hubbard repulsion U. We have focused essentially on $U = 8$, although some results are also presented for $U = 4$. Omitting $\nu = \frac{1}{2}$, which is trivial, we have chosen representative values (the low doping regime $\nu \sim \frac{1}{2}$ presents additional difficulties and is omitted here) $\nu = \frac{1}{4}$ ("quarter filled"), and $\nu = \frac{1}{12}$ ("low density" regime). Quite good convergence is achieved with $N_a \leq 36$ for $U = 8$. The convergence of the QMC calculations (with respect to increasing β, reducing $\Delta\tau$, and improving the accuracy of Langevin sampling) has been carefully checked against both diagonalization (whose accuracy is $\Delta E_0/E_0 \leq 10^{-6}$), and against an accurate evaluation of Lieb and Wu's E_0, for the finite system. In all

cases presented here, we have an accuracy of E_{kin} of better than 0.5%.

The typical appearance of the 1D Hubbard momentum distribution away from half filling is shown in Fig.5.15. We notice several bumps, and also a non-monotonic behaviour due to a small but clear feature near $2k_F$.

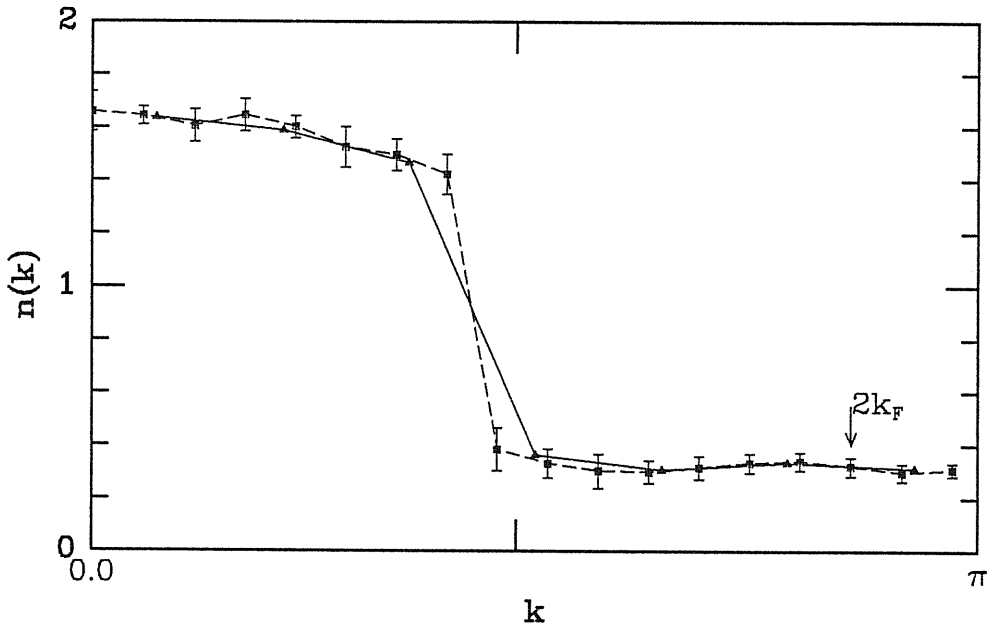

Figure 5.15. Momentum distribution for the 1D Hubbard model with $\nu=\frac{6}{7}$ for a 14 (continuous line) and 35 (dashed) sites ring. The results for the smaller size system were obtained with the power method, while for the larger ring we used the statistical method with a Gutzwiller type trial wavefunction (α=2, see eq.5.2.2) and β=4

Most importantly, there is a very strong jump Δ across k_F. This jump is quite similar to those we have reported before on the same system[31,32]. More recently, the existence of this jump in the finite system has been confirmed by several groups[65−67], It is believed however[65], that the jump $\Delta(L)$ will eventually scale to zero with increasing size L. This is expected to follow from the non-Fermi liquid behaviour predicted by the renormalization group (RG) mapping on the Tomonaga model[68,69].

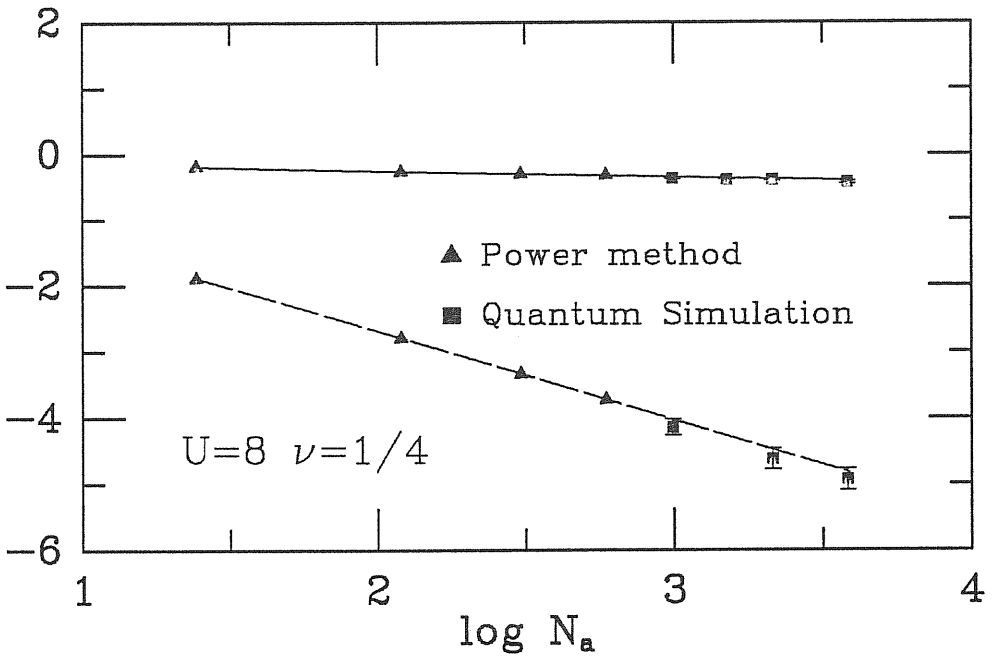

Figure 5.16. Logarithmic plots of the jump of the momentum distribution function at k_F (continuous line) and the density–density correlation functions at $4k_F$ (dashed line). The two curves are fit only of the power method data, using the interpolation described in the text.

In Fig. 5.16 we show by explicit finite-size scaling that this prediction is indeed correct, and that the 1D Hubbard model has non Fermi surface in the thermodynamic limit. In order to extract accurately the exponents, it is necessary to include also the higher order scaling corrections. They can be obtained from the Tomonaga mapping in the form of an expansion in power of $\ln L$.

$$\ln Z(L) = -\theta \ln L + a \ln\ln L + b + c/\ln L + \ldots \qquad (5.4.3)$$

This singular form is required by the especially slow approach of the RG fixed point. From this fit, neglecting the $\ln\ln$ term in (5.4.3) that can be considered approximately a constant, i.e. a redefinition of b, we extract the exponent θ which characterizes the singularity of $n(k)$ near the Fermi level of a marginal

conductor[68,69] in the form:

$$n(k) = A\,|k_F - k|^{\theta}\,\mathrm{sgn}\,(k_F - k) + B \tag{5.4.4}$$

Within RG scaling further logarithmic corrections to the previous expression are also possible, analogously to expression (5.4.3), e.g. $(k - k_F)^{\theta}\ln^{\gamma}(k - k_F)$, but we neglect them in the present analysis.

Using the fit (5.4.3) we obtain (for $U = 8$) $\theta = 0.08$ for $\nu = \frac{1}{4}$ and $\theta = 0.10$ for $\nu = \frac{1}{12}$. Very recently Shiba[67] has provided an accurate evaluation of $n(k)$ for $U = \infty$, and $\nu = \frac{1}{4}$. Fitting his numbers with the form (5.4.3), we obtain $\theta = 0.126$. It is interesting to observe that, inclusion of the higher order terms in the expansion (5.4.3), does make an appreciate difference. Omitting them would yield $\theta = 0.11$, 0.14, and 0.15 instead of 0.08, 0.10, 0.126 in the three cases described.

These results confirm in qualitative agreement with expectations based on RG[65,68,69] and on perturbation theory[70], that θ is an increasing function of $\frac{U}{t}$ and of ν^{-1}. However, the RG second order result $\theta = \frac{v^2}{16}$ where $v = (u/2\pi t\sin(\pi v))$ is clearly off already at $\frac{U}{t} = 8$.

Having thus established a clear quantitative deviation of the single particle properties of the 1D HM from the Fermi-liquid behaviour, it seems interesting to ask to what extent will the two-body correlation functions reflect this property. Quite generally in a 1D conductor one can expect the large distance charge–charge and spin–spin correlation to fall like power laws, neglecting possible logarithmic

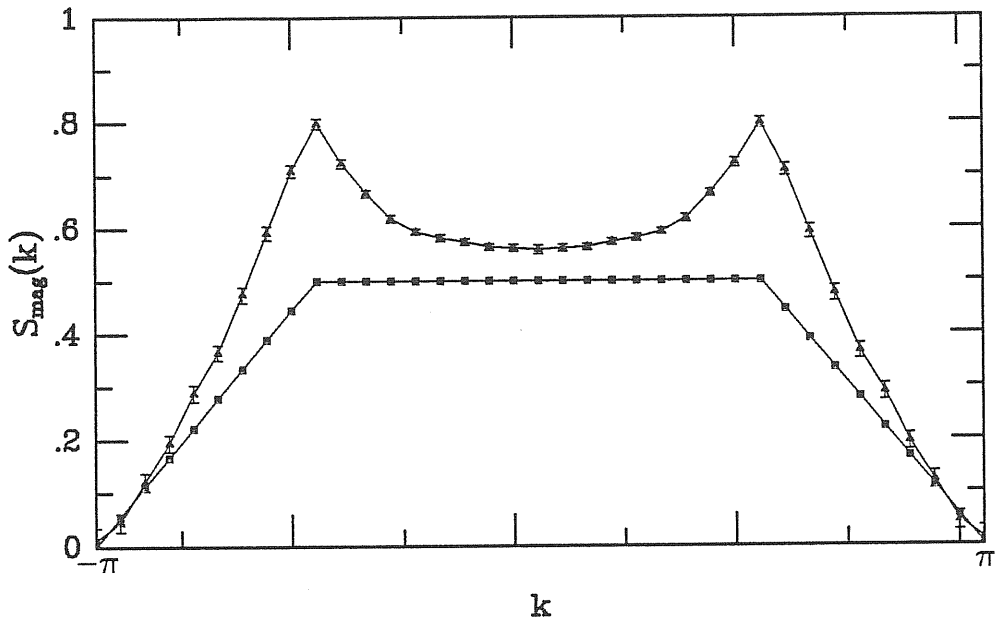

Figure 5.17. Spin-Spin correlation function for the 36 sites quarter filled Hubbard ring for U=0 (lower curve) and U=8 (upper curve). The latter results were obtained with the QMC method for $beta$=20 and $\Delta\tau$=0.03

corrections as before,:

$$\begin{aligned} <\rho(r_0)\,\rho(r)>_{r\to\infty} &\rightarrow K_2 r^{-\alpha}\cos 2k_F r + K_4 r^{-\beta}\cos 4k_F r + \ldots + \\ <\vec{s}(r_0)\cdot\vec{s}(r)>_{r\to\infty} &\rightarrow H_2 r^{-\gamma}\cos 2k_F r \end{aligned} \tag{5.4.5}$$

In the non interacting case ($U = 0$), we have $\alpha = \gamma = 2$, $K_4 = 0$. In order to obtain the exponents for $U > 0$, we can in analogy with the above finite size scaling of $\Delta_{n(k)}$, extract the slopes

$$\gamma_{\pm} = -\frac{d\ln}{d\ln L}(S_{mag}(2k_F) - S_{mag}(2k_F \pm \frac{2\pi}{L})) \tag{5.4.6}$$

and a similar expression for α and β. Here the density and spin structure factor are defined as usual by

$$S_{den}(k) = \frac{1}{N_a} \sum_{ij} e^{ik(n_i - n_j)} (< n_i n_j > - < n_i >< n_j >) \tag{5.4.7}$$

$$S_{mag}(k) = \frac{1}{N_a} \sum_{ij} e^{ik(n_i - n_j)} < m_i m_j > \tag{5.4.8}$$

where $m_i = n_{i\uparrow} - n_{i\downarrow}$, $n_i = n_{i\uparrow} + n_{i\downarrow}$.

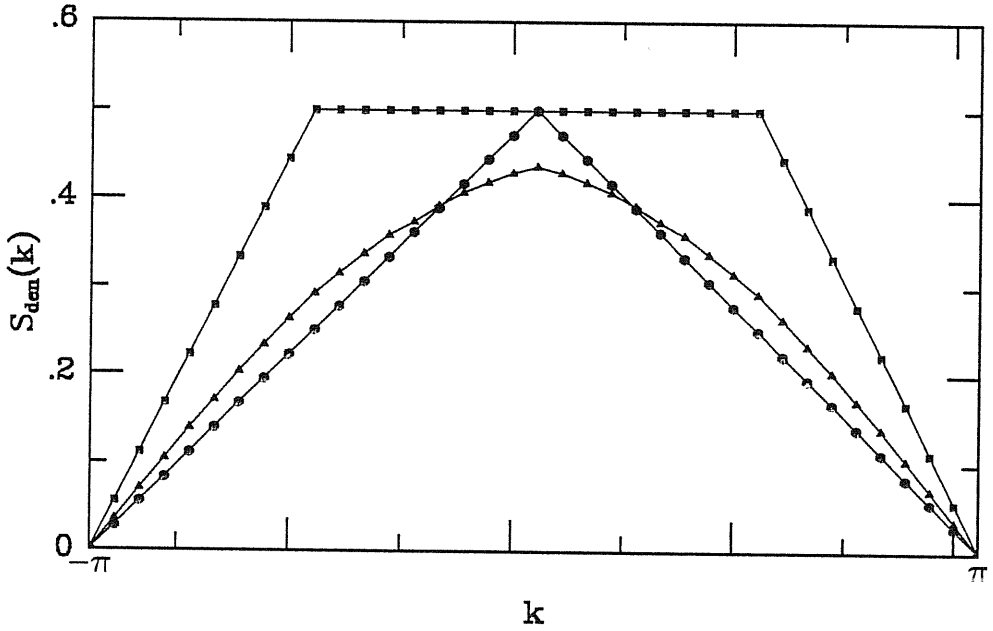

Figure 5.18. Charge–charge correlation function for the 36 sites quarter filled Hubbard ring for U=0 (squares), U=∞ (dots), and for U=8. The latter results were obtained with the QMC method for *beta*=20 and $\Delta\tau$=0.03

As Figs.5.17 and 5.18 show (for $U = 8$, $\nu = \frac{1}{4}$) that a non-zero U strongly depresses the $2k_F$ charge singularity, while enhancing the $2k_F$ spin and the $4k_F$ charge singularities. This qualitative behaviour has been well-known e.g. from QMC work[64]. In Fig.5.16 we also show the finite-size scaling of the $4k_F$ charge

case and that of the $2k_F$ spin case are plotted in Fig.5.19 (the $2k_F$ charge case is not feasible).

We find for $\frac{U}{t} = 8$ and $\nu = \frac{1}{4}\beta = 2.38$. Surprisingly this compares favorably with *lowest order* RG predictions $\beta_{RG} = 4 - v = 2.2$, but (not surprisingly) much less so with the second order result $4 - v + \frac{9}{8}v^2 = 5.89$. The scaling of the spin exponent α is much less clear cut at $\nu = \frac{1}{4}$, (see fig.5.19). This is due to the exceedingly strong size dependence of $S_{mag}(2k_F)$, shown also by Shiba for $U = \infty$. At $U = \infty$, we note that the charge charge correlations must be identical with those of spinless fermions, which implies $\beta = 2$. This result follows from the known factorization into a charge and a spin part of the Lieb and Wu wavefunction for $U \rightarrow \infty$[67]. More work is clearly necessary to clarify this particular aspect.

In summary, finite–size scaling quantitatively demonstrates the non–Fermi liquid nature of the marginal conducting state of the $1D$ Hubbard model away from half filling. Scaling to the Lattinger model appears to be exact for $U = \infty$, and very plausible for all $U > 0$. According to the RG scaling to the Luttinger Tomonaga model, all the exponents are related, in the form:

$$\begin{aligned} \theta &= \frac{1}{2}\left(\frac{1}{\sqrt{1-x^2}} - 1\right) \\ \beta &= 4\left(\frac{1-x}{1+x}\right)^{\frac{1}{2}} \\ \alpha &= \gamma = 1 + \left(\frac{1-x}{1+x}\right)^{\frac{1}{2}} \end{aligned} \tag{5.4.9}$$

For $U \rightarrow \infty$ $\beta = 2$ implies $x = \frac{3}{5}$, hence the prediction is $\theta = \frac{1}{8}$, $\gamma = \frac{3}{2}$. This result for θ is in striking agreement with that obtained from our finite size scaling of Shiba's numbers ($\theta = 0.126$), strongly suggesting that scaling to the Tomonaga

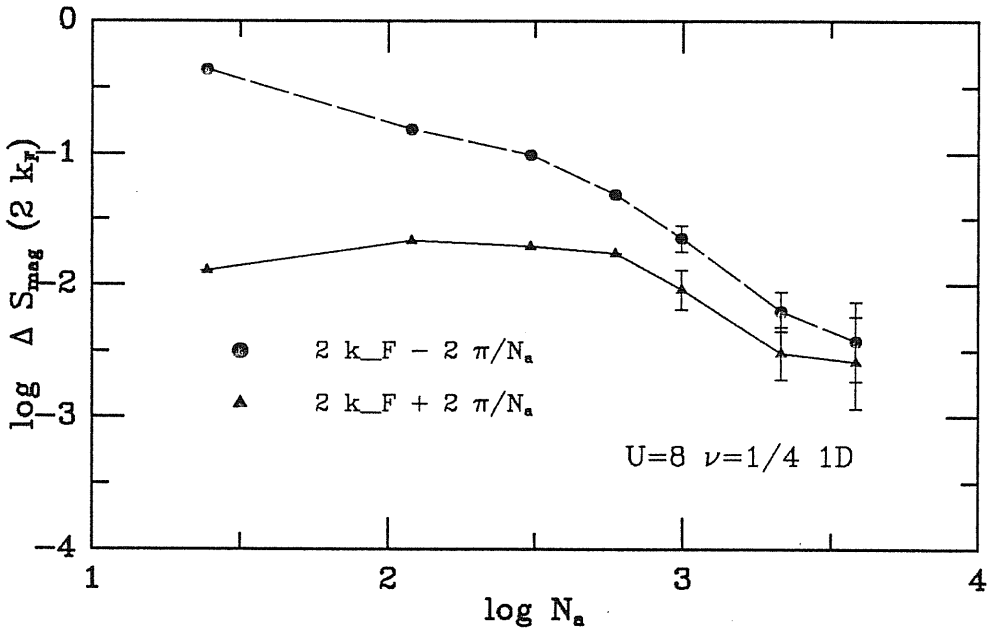

Figure 5.19. Logarithimc plot of the finite difference of the magnetic structure factor S_{mag} relative to the two k values closest to $2k_F$. The results without error bars comes from the power method while the remaining ones are obtained using the statistical simulation.

model is exact, at least for $U = \infty$†.

If we accept that the model is also the exact fixed point for $U < \infty$ we would predict:

$$\theta = \frac{1}{\beta} - \frac{1}{2} + \frac{\beta}{16} \tag{5.4.10}$$

and $\beta = 2.38$ yields $\theta = 0.07$, to be compared with our actual value $\theta = 0.08$ for $U = 8$ and $\nu = \frac{1}{4}$. Similarly $\beta = 2.13$ would imply $\theta = 0.103$, to be compared with $\theta = 0.10$. The agreement seems very good within possible errors due to finite size effects.

In conclusion, it seems at least possible that scaling to the Luttinger model

† An independent proof, based on Lieb and Wu wavefunction is being published separately

is a universal feature for $U > 0$.

Chapter VI

Conclusions

In the present thesis we have described in detail a new method for the simulation of many electrons systems. As in any other method based on the Hubbard–Stratonovich transformation (HST), direct electronic interactions are replaced by coupling to auxiliary bosonic fields. Then, sums over these fields are performed statistically using the determinantal weights to guide the importance sampling. Generally, this type of procedure has a low–T stability problem, due to loss of orthogonality. We have described a recently developed method for stabilizing the calculation at low temperatures, particularly efficient for algorithms based on the HST. This stabilization technique allows to preserve efficiently the spread of different energy scales that in a Fermion problem is particularly wide due to the Pauli principle. As an example, in the one body picture, the electrons occupy levels from the bottom of the band up to the Fermi level and this is basically the physical origin of the so called "ill conditioned" determinants that now it can be considered a solved problem.

Alternative stable algorithms do exist for specialized problems [71,72], but at low temperatures they remain very costly. In contrast, the overhead associated with explicitly maintaining small scales is modest in the HST formulation. It is possible to stabilize a variety of simulation algorithms in this manner. In the present work we choose a particular implementation. We set up a scheme that, using a Force based method of sampling, allows better performances compared to the usual MC schemes, at the non trivial expense to introduce an extra source of systematic error: the integration error of the Langevin Dynamic eqs. (see Ch.3.2). However in all these statistical methods the most important problem is the minimization of the statistical error. A faster algorithm allows a more accurate sampling of the phase space with the same computational effort and consequently it gives smaller statistical error.

Another problem which is usually believed to affect a dynamical way of sampling is that for a dynamical trajectory it is difficult[43] to sample correctly the region around "nodal barriers" which divide the bosonic field space. We have shown in the present thesis that an adaptive Langevin step scheme removes the above difficulties and numerical simulations can be performed even in this case with good accuracy.

In this way we have set up an efficient and stabilized algorithm which in principle allows relatively inexpensive explorations of the low temperature phases of a variety of models of strongly correlated electrons. We have concentrated in particular the Hubbard model in 1D and 2D. In 1D we established quantitatively that the Hubbard model away from half filling shares the same asymptotic behaviour of the Lattinger–Tomonaga model. As was supposed earlier[68], it is always a paramagnetic metal , but with a very peculiar feature common to 1D

systems: namely the absence of a well defined Fermi surface. The possibility of studying the momentum distribution of 1D system was made possible by using the present method.

In 2D, in the half filled case, we confirm that even for small U the system is an antiferromagnetic insulator. As a new contribution we systematically studied the momentum distribution for increasing system sizes and large imaginary time (up to 242 sites with $\beta = 20$). We show that the Fermi jump clearly disappears and is replaced by a seemingly analytic behaviour.

In spite of this successes important algorithmic difficulties remain for the numerical study of fermions. Undoubtedly, the most important of this is the " fermion sign problem", a difficulty which appears also in the HST formulation.

In the present thesis we analyze theoretically the problem of defining a positive statistical weight using the Hubbard–Stratonovich transformation (the weight obtained after a straightforward application of the HST is not always positive definite). The study of this problem is very important not only from a numerical point of view –the difficulty to sample non positive weight is well known in Fermion simulations– but also for the understanding the physics of the Hubbard–Stratonovich transformation.

In the present thesis we have shown rigorously that the average sign of the considered statistical weight is either bounded by a constant depending on the trial wavefunction or it vanishes *exponentially* in the low temperature limit. Whenever this exponential instability occurs, the method faces difficulties which are similar to other Monte Carlo schemes. However in many cases such as a half filled and, or a small positive U, or a negative U, or a 1D case, it is possible to find convenient HST that rigorously allow the mapping of the quantum many body problem onto

the one of simulating a classical system without any kind of instability in the low temperature limit. We speculate, based on these theoretical results, that whenever a mean field approximation is a good starting point of a considered model the sign problem should be irrelevant in the sense described before. Unfortunately in more than 1D and away from half filling, we were not able to find a rigorous proof on the behaviour of the average sign for $\beta \to \infty$. There are however numerical accurate calculations developed by E. Loh et al.[24] implying that for 10 electrons and 14 electrons and 16 sites the average sign exponentially vanishes for an Ising type of HST†. Just away from half filling and for large U, where the physics is particularly interesting, the vanishing of the average sign suggests that no conventional mean field approximation is a good starting point due to the deeply correlated nature of the state. In other words there may be a deep physical reason in the *failure* of the HST when applied in this limit.

All the same we speculate that for a class of models larger than the simple 1D Half filled , small and negative U Hubbard model, the HST can be used for the study of the low temperature properties without any "Fermion sign problem". In fact when the Hubbard–Stratonovich fields couples to physical quantities which describe very well the physics of the system –in the sense that the mean field approximation is a good starting point– it is likely that the sign problem is not important (the average sign being bounded by a constant for $\beta \to \infty$).

The sign problem in the HST is therefore especially baffling at this moment. It has been suggested, for example, that the heart of the mechanism for high$-T_c$ superconductivity could be contained inside the single–band Hubbard model.

† This is also confirmed by our calculations because we found that inequality (2.1.14) is not satisfied in these cases

However, the validity of such a theory cannot be checked yet with our numerical method because, it is just near half filling (the only doping at which the repulsive Hubbard model could superconduct), that the sign problem is worst.

In this regime we cannot hope to perform calculations that are well converged in imaginary time, because of the prohibitive difficulty for sampling an extremely small value of the average sign. Nevertheless in the present approach a possibility to improve that convergence in temperature can be obtained by improving the trial wavefunction. In fact the HST formulation allows the use of a large variety of trial wavefunctions (e.g. the Gutzwiller wavefunctions has been used in Ch. V Sect.3). A good trial wavefunction (that is close to the true ground state) reduces the imaginary time needed for convergence and one can get information about the ground state properties without reaching the region where the average sign is too small.

Following this route we are at the moment systematically improving our calculation away from half filling and larger coupling constant.

APPENDIX I

THE H.S.T. FOR A GENERAL FERMIONIC OPERATOR

Consider a general interaction term :

$$\sum_{i,j} v_{i,j}\, \hat{n}_i\, \hat{n}_j \tag{A1.1}$$

where $\hat{n}_i$ is the density operator of a fermion at a given site and for a defined spin projection. Then, using that $\hat{n}_i^2 = \hat{n}_i$ for a Fermi-operator one can write:

$$\sum_{i,j} v_{i,j}\, \hat{n}_i\, \hat{n}_j \;=\; \sum_{i,j} \left[v_{i,j} \;-\; \lambda\, \delta_{i,j}\right]\, \hat{n}_i\, \hat{n}_j \;+\; \lambda\, \hat{N} \tag{A1.2}$$

where $\hat{N}$ is the total density operator. For λ sufficiently large the matrix $v'_{i,j} = v_{i,j} - \lambda\delta_{i,j}$ in the preceding equation (A1.2) is negative definite. Therefore one can apply the Hubbard–Stratonovich transformation (1.1.12) even in this case. In fact, diagonalizing the symmetric negative-definite matrix (the matrix v can generally be chosen symmetric in a quadratic form like A3.1)

$$v'_{i,j} \;=\; \sum_{k} U_{k,i}\, \alpha_k^2\, U_{k,j} \tag{A1.3}$$

one can decompose the quadratic form

$$\sum_{i,j} v'_{i,j}\,\hat{n}_i\,\hat{n}_j \;=\; \sum_k \;-\,\alpha_k^2\,\hat{O}_k^2 \tag{A1.4}$$

where

$$\hat{O}_k \;=\; \sum_j U_{k,j}\,\hat{n}_j \tag{A1.5}$$

are single particle commuting operators satisfying

$$\left[\hat{O}_k,\,\hat{O}_j\right] \;=\; 0 \quad and \quad \left[\hat{O}_k,\,\hat{N}\right] \;=\; 0 \quad \forall\, k,j \tag{A1.6}$$

Therefore the calculation of

$$e^{-\sum_{i,j} v'_{i,j}\,\hat{n}_i\,\hat{n}_j} \;=\; \prod_k e^{\alpha_k^2\,\hat{O}_k^2} \qquad using\ (A1.6)$$

$$\;=\; \int \prod_k d\sigma'_k\, e^{-\sum_k \sigma'_k \alpha_k\,\hat{O}_k \,-\frac{1}{2}\,\sigma_k'^2} \tag{A1.7}$$

Finally with the further change of variables:

$$\sigma_k \;=\; \sum_j U_{k,j}\,\sigma'_j \tag{A1.8}$$

using eq.(A1.7) and definition (A1.3)

$$e^{\sum_{i,j} v_{i,j}\,\hat{n}_i\,\hat{n}_j} \;=\; \int \prod_k d\sigma'_k\, e^{-\sum_{k,j} \sigma'_j\,(\lambda - v)^{1/2}_{k,j}\,\hat{n}_j} \; e^{\sum_k -\frac{1}{2}\sigma_k'^2} \; e^{\lambda\,\hat{N}} \tag{A1.9}$$

In practice it is convenient to choose λ equal to the maximum eigenvalue of the matrix v. In this case, in fact we need one less integration variable in the previous transformation.

APPENDIX II

Given a set of independent vectors ψ_i which is a complete set in an arbitrary invariant subspace $\mathcal{D}$ of the Hilbert space $\mathcal{H}$ under all U_σ propagators we define the following quantities

the operator

$$\hat{U}^{ij} = \int d\mu_\sigma \text{ sign} < \psi_i \,|\, U_\sigma \,|\, \psi_j > \hat{U}_\sigma \tag{A2.1}$$

and the functionals

$$Q_{ij}^M(\beta) = < \psi_i \, \hat{U}_\beta^{ij} \, \psi_j > = \int d\mu_\sigma \, |< \psi_i \,|\, U_\sigma \,|\, \psi_j >| \,. \tag{A2.2}$$

We show that:

$$\left(Q_{ij}^M(\beta)\right)^2 \leq Q_{ii}^M(2\beta) \tag{A2.3}$$

In fact from the definition (A2.1) and a general property of matrix, since the chosen basis is complete in $\mathcal{D}$:

$$< \psi_i \, U_\beta^{ij} \, \psi_j >^2 \leq < \psi_i \, U_\beta^{ij} \, U_\beta^{+ij} \, \psi_i > \tag{A2.4}$$

one has clearly the bound for Q_{ij}^M:

$$\left(Q_{ij}^M(\beta)\right)^2 = < \psi_i \, U_\beta^{ij} \, \psi_j >^2 \leq < \psi_i \, U_\beta^{ij} \, (U_\beta^{ij})^+ \, \psi_i > \tag{A2.5}$$

Then using the definition of $\hat{U}_\beta^{ij}$ the RHS of the previous inequality reads:

$$\int [d\mu_\sigma] \int [d\mu_{\sigma'}] \; < \psi_i \, U_\sigma(\beta,0) \, U_{\sigma'}(0,\beta) \, \psi_i > \; \text{sign} < \psi_i \, U_\sigma \psi_j > \text{sign} < \psi_i \, U_{\sigma'} \psi_j > \tag{A2.6}$$

that is by a further change of variable (which makes clearly sense even for discrete imaginary time):

$$\tilde{\sigma}(t) = \begin{cases} \sigma'(\beta - t) & 0 \leq t \leq \beta \\ \sigma(t - \beta) & \beta \leq t \leq 2\beta \end{cases} \tag{A2.7}$$

The previous inequality (A2.6) becomes:

$$\begin{aligned} \left(Q_{ij}^M(\beta)\right)^2 &\leq \int [d\mu_{\underline{\sigma}}] \; < \psi_i \, U_{\tilde{\sigma}}(2\beta,0) \, \psi_j > \; \text{sign} < \psi_i \, U_{\tilde{\sigma}}(0,\beta) \, \psi_j > \\ &\quad \text{sign} < \psi_i \, | \, U_{\tilde{\sigma}}(2\beta,\beta) \, | \, \psi_j > \\ &\leq \int [d\mu_{\underline{\sigma}}] \; | < \psi_i \, U_{\tilde{\sigma}}(2\beta,0) \, \psi_j > | \\ &= Q_{ij}^M(2\beta) \end{aligned} \tag{A2.8}$$

And this proves the assertion of this appendix.

Appendix III

A subspace $\mathcal{D}$ of $\mathcal{H}$ is irreducible under the family F_σ of operators $U_\sigma(\beta,0)$ if and only if $\mathcal{D}$ is irreducible under all the family F_e of the "elementary" hermitian one body operators appearing in $U_\sigma(\beta,0)$.

We prove this statement for the particularly chosen HST where F_e is the set of elementary operators $\{m_r\}$ *and* $\hat{K}$. In general for the validity of this statement it is enough that all the elementary operators appearing in U_σ are hermitian.

Proof.

Suppose that $\mathcal{D}$ is irreducible under the family F_σ and it is not irreducible under F_e.

We show that this is impossible, that is, $\mathcal{D}$ is irreducible under the family F_σ if $\mathcal{D}$ is irreducible under the family F_e. In fact if each $\{m_r\}$ and K belonging to the family F_e of operators has an invariant subspace different from $\{D\}$ and $\{0\}$ say $\tilde{\mathcal{D}}$, $U_\sigma(\beta,0)$ has of course such an invariant subspace because is an algebraic composition of operators m_r and K which have this invariant subspace. Hence $\mathcal{D}$ contains an invariant subspace $\tilde{\mathcal{D}}$ under all $U_\sigma(\beta,0)$ therefore $\mathcal{D}$ is not an irreducible subspace under the family F_σ, and this is impossible.

On the other hand suppose that $\mathcal{D}$ is irreducible under the family F_e and $\mathcal{D}$ is not irreducible under the family F_σ. We show again that this is impossible that

together with the previous statement proves the main assertion of this appendix.

In fact if $\mathcal{D}$ is not irreducible under the family F_sigma it is possible to find a subspace $\tilde{\mathcal{D}}$ different from $\mathcal{D}$ and $\{0\}$ which is left invariant by all $U_\sigma(\beta,0)$ defined in (1.1.22,23). In particular $\tilde{\mathcal{D}}$ is an invariant subspace of $e^{\Lambda M}e^{\Delta\tau\hat{K}}$ which is obtained when $U_\sigma(\beta,0)$ defined in (1.1.22,23) contains only one Trotter slice $\beta=\Delta\tau$ and $[\sigma_r=1]_{\forall r}$. Here $M=N^\uparrow-N^\downarrow$ is the to total magnetization which commutes with U_σ.

Now since $\hat{K}$ is an hermitian operator $\tilde{\mathcal{D}}$ is also an invariant subspace of $\hat{K}$. Analogously, for the remaining $\{m_r\}$ operators of F_e we can consider the same one trotter slice propagator with only one variables flipped to -1:

$$\sigma_r=-1,\ for\ r=r'$$

$$\sigma_r=1\ otherwise \tag{A3.1}$$

Since $\tilde{\mathcal{D}}$ is an invariant subspace under F_σ it should be in particular also an invariant subspace of the described operator:

$$e^{-\frac{\Delta\tau}{2}K}e^{-2m'_r}e^{-\frac{\Delta\tau}{2}K}e^{M} \tag{A3.2}$$

Now since $e^{-\frac{\Delta\tau}{2}K}$ is a non singular operator ($\det e^{-\frac{\Delta\tau}{2}K}=e^{-\mathrm{tr}\,\frac{\Delta\tau}{2}K}>0$) which has $\tilde{\mathcal{D}}$ as an invariant subspace, $e^{-2m_{r'}}$ for any r' has also to leave invariant the subspace $\tilde{\mathcal{D}}$. Of course, since m'_r is hermitian $\tilde{\mathcal{D}}$ is also invariant subspace of $m_{r'}$ for any r'. $\tilde{\mathcal{D}}$ is therefore invariant for all the family of operators F_e and this is also impossible.

APPENDIX IV

(a)

We consider $Q^*_M(\beta)$ (2.3.4) defined in terms of a basis $\{\Phi_i\}$ of a given irreducible subspace $\mathcal{D}$ and *we show in this part that*:

$$Q^*_M(\beta_k) \;=\; h^*(\beta_k)\exp -E^*(\beta_0)\beta_k \tag{A4.1}$$

where $h^*_M(\beta)$ *satisfies:*

$$\frac{1}{d} \;\leq\; h^*_M(\beta_k) \;\leq\; 1 \quad \forall k \tag{A4.2}$$

and d is the dimension of the irreducible subspace.

We consider $(Q^*_M(\beta))^2$:

$$(Q^*_M(\beta))^2 \;=\; (\max_{\{ij\}} Q^M_{ij}(\beta))^2 \tag{A4.3}$$

Since as shown in app.2 $(Q^M_{ij}(\beta))^2 \;\leq\; Q^M_{ii}(2\beta)$ we can get for $Q^*_M(\beta)$ an inequality similar to the one satisfied by Q^β_M (A2.3). In fact:

$$Q^*_M(\beta)^2 \;\leq\; \left[\max_{ij} Q^M_{ij}(\beta)\right]^2 \;\leq\; \max_{\{i\}} Q^M_{ii}(2\beta) \;\leq\; Q^*_M(2\beta) \tag{A4.4}$$

Moreover by inserting in the integrand of $Q^*_M(2\beta)$ a complete set $\{\Phi_i\}$ in $\mathcal{D}$, one can also easily show a further inequality satisfied by $Q^*(2\beta)$:

$$Q^*_M(2\beta) = \max_{\{ij\}} \int d\mu_\sigma \left| \sum_k < \Phi_i U_\sigma(2\beta,\beta)\Phi_k > < \Phi_k U_\sigma(\beta,0)\Phi_j > \right|$$
$$\leq \max_{ij} \sum_k Q^M_{i,k}(\beta) Q^M_{k,j}(\beta) \leq d\, Q^{2^*}(\beta) \qquad \text{(A4.5)}$$

Collecting the two previous inequalities $Q^*_M(2\beta)$ satisfies:

$$(Q^*_M(\beta))^2 \leq Q^*_M(2\beta) \leq d(Q^*(\beta))^2 \qquad \text{(A4.6)}$$

Based on the two sided inequality (A4.6) the limit:

$$E^*(\beta_0) = \lim_{k\to\infty} -\frac{1}{\beta_k} \ln Q^*(\beta_k) \qquad \text{(A4.7)}$$

converges to a well defined quantity– $E^*(\beta_0)$– that can in principle depend on β_0. Actually it will be shown later that this is not the case.

So far we write $Q^*_M(\beta)$ as a function $h^*_M(\beta)$ times the exponential asymptotic factor $e^{-\beta_k E^*(\beta_0)}$:

$$Q^*(\beta_k) = h^*(\beta_k) \exp -E^*(\beta_0)\beta_k. \qquad \text{(A4.8.)}$$

Then after substitution of (A4.8) in inequality (A4.6) the exponential factors cancel and:

$$h^*_M(\beta)^2 \leq h^*_M(2\beta) \leq d\, h^*_M(\beta)^2 \qquad \text{(A4.9)}$$

Now from (A4.9) $h^*_M(\beta)$ has to be a bounded function (A4.2) in order to be consistent with the definition of the limit (A4.7). In fact supposing that h^*_M violates the bounds (A4.2), by iterating the inequalities (A4.9) as is done in the text for $h_M(\beta)$ (see 2.1.10-12) one gets that h^*_M vanishes or diverges exponentially and this would contradict the limit (A4.7).

(b)

We show in the following that

$E^*(\beta_0)$ defined in (A4.7) does not depend on β_0 the initial inverse temperature considered in the sequence $\beta_k = 2^k\beta_0$.

Suppose without loss of generality that for two different initial β_0: β_0^1, β_0^2

$$E^*(\beta_0^1) \geq E^*(\beta_0^2) \tag{A4.10}$$

then for arbitrary large values of k we can decompose N^*, defined as the integer closest to $\frac{2^k\beta_0^2}{\beta_0^1}$, in its binary representation containing c significant digits:

$$N^* = \sum_{i=1}^{c} 2^{k_i} \tag{A4.11}$$

with $c \leq log_2(N^*)$. So far we can write $2^k\beta_0^2$ as:

$$2^k\beta_0^2 = N^*\beta_0^1 + \tau = \sum_{i=1}^{c} \beta_0^1 2^{k_i} + \tau \tag{A4.12}$$

with $|\tau| < \beta_0^1$. Consider now Q_{ij}^M in the definition (A2.2), according to the binary decomposition (A4.11) in the integrand of $Q_{ij}^M(2^k\beta_0^2)$ we can split up the propagator into the product of many different ones that –apart the last one– propagates the trial wavefunction for imaginary time intervals as large as a power of two the initial inverse temperature β_0^1 of the first sequence:

$$U_\sigma(2^k\beta_0^2, 0) = U_\sigma(2^k\beta_0^2, 2^k\beta_0^2 - \tau)\prod_{i=1}^{c} U_\sigma(\beta_i, \beta_{i-1}) \tag{A4.13}$$

with $\beta_0 = 0$, $\beta_1 = 2^{k_1}\beta_0^1$, $\beta_2 = \beta_1 + 2^{k_2}\beta_0^1, \ldots, \beta_c = N^*\beta_0^1$

In this way, in the RHS of expression (A4.13), at each given imaginary time β_i, we can insert a complete set of states in $\mathcal{D}$ and then we find the following inequality

$$\begin{aligned} Q_{ij}^M(2^k\beta_0^2) &= \int d\mu_\sigma \sum_{i_1,\ldots,i_c} |< \Phi_i U_\sigma(2^k\beta_0^2,\beta_c)\Phi_{i_c} > < \Phi_{i_c} U_\sigma(\beta_c,\beta_{c-1})\Phi_{i_{c-1}} > \\ &\quad \ldots < \Phi_{i_1} U_\sigma(\beta_1,0)\Phi_j >| \\ &\leq \sum_{i_1,\ldots,i_c} \int d\mu_\sigma \, |< \Phi_i U_\sigma(2^k\beta_0^2,\beta_c)\Phi_{i_c} >| \; |< \Phi_{i_c} U_\sigma(\beta_c,\beta_{c-1})\Phi_{i_{c-1}} >| \\ &\quad \ldots |< \Phi_{i_1} U_\sigma(\beta_1,0)\Phi_j >| \end{aligned} \tag{A4.14}$$

In the last inequality we can easily rewrite all the terms in the sum as suitable products of different "pseudo" partition function $Q_{i,j}^M$ because, from the definition of $d\mu_\sigma$ (see 1.1.21) all the variables appearing in each propagator $U_\sigma(\beta_{i+1},\beta_i)$ are decoupled each other. Then using the definition of Q_M^* (2.3.4) we find

$$Q_{ij}^M(2^k\beta_0^2) \leq d^c \prod_{i=1}^{c} Q^*(2^{k_i}\beta_0^1) Q^*(\tau) \tag{A4.15}$$

In the previous inequality (A4.15) we separately find a bound for each factor:

$$Q_M^*(\tau) \leq e^{-E_{\min}\tau} \leq e^{-E_{\min}\beta_0^1} \tag{a}$$

where $E_{\min} < 0$ is defined in (1.1.24)

$$Q^*(2^{k_i}\beta_0^1) \leq e^{-E^*(\beta_0^1)2^i\beta_0^1} \tag{b}$$

from (A4.1) and (A4.2) and finally:

$$d^c \leq d^{k\log_2\left\{\frac{\beta_0^2}{\beta_0^1}\right\}} \tag{c}$$

from the definition (A4.11).

Hence we conclude that for any k

$$Q^*_M(2^k\beta_0^2) \leq d^{k\ln\left\{\frac{\beta_0^2}{\beta_0^1}\right\}} e^{-E^*(\beta_0^1)2^k\beta_0^2} \exp -2E_{\min}\beta_0^1 \tag{A4.16}$$

In other words the asymptotic $k \to \infty$ limit of $Q^*_M(2^k\beta_0^2)$ is essentially dominated by the exponential $e^{-E^*(\beta_0^1)2^k\beta_0^2}$ apart for less relevant term in this limit. In fact using the definition (A4.7):

$$E^*(\beta_0^2) = \lim_{k\to\infty} -\frac{1}{2^k\beta_0} \ln Q^*(2^k\beta_0^2) \geq E^*(\beta_0^1) \tag{A4.17}$$

Since we have considered the case (A4.10) $E^*(\beta_0^2) \leq E^*(\beta_1)$ and we have obtained $E^*(\beta_0^2) \geq E^*(\beta_1)$ it follows that

$$E^*(\beta_0^1) = E_)(\beta_0^2) \quad \forall\ \beta_0^1\ \beta_0^2 \tag{A4.18}$$

and therefore the limit (A34.7) does not depend on the initial inverse temperature β_0 as asserted in this appendix.

(c)

In this part we are going to show that E^* defined in (2.3.10) does not depend on the particular choice of the basis $\{\Phi_i\}$ in $\mathcal{D}$.

To this purpose we introduce an analogous "pseudo" partition function as in (2.3.4)

$$Q^*_N(\beta) = \max_{\{i\}} Q^\beta_N(\Phi_i) \tag{A4.19}$$

For any field configuration of $\sigma_{r,l}$ and any couples of states Φ_i, Φ_j of the chosen basis one has

$$|< \Phi_i U_\sigma \Phi_j >| \leq \|U_\sigma |\Phi_j >\| \leq \sum_i |< \Phi_i U_\sigma \Phi_j >| \qquad \text{(A4.20)}$$

Hence by using the definition of Q_N^* and Q_M^* it follows that:

$$Q_M^*(\beta) \leq Q_N^*(\beta) \leq d Q_M^*(\beta) \qquad \text{(A4.21)}$$

From the previous one the infinite limit

$$E_N^* = \lim_{\beta \to \infty} -\frac{1}{\beta} \ln Q_N^*(\beta) \qquad \text{(A4.22)}$$

converges to the same value E^* defined in (2.3.10).

In order to prove the assertion (c) it is enough to show that $E_N^* = E^*$ does not depend on the particular choice of the basis set in the irreducible subspace $\mathcal{D}$.

We consider two complete set in $\mathcal{D}$, $\{\Phi_i^1\}$ and $\{\Phi_i^2\}$ (that can be eventually non orthonormal basis) and the corresponding asymptotic energy

$$E^{*i} = \lim_{\beta \to \infty} -\frac{1}{\beta} \ln Q_N^{*i} \qquad \text{(A4.23)}$$

where now the index i labels in (A4.23) the two different basis $i = 1, 2$. Without loss of generality we can analyze the case with $E^{*1} \geq E^{*2}$. We will show that also $E^{*2} \geq E^{*1}$ holds and therefore $E^{*1} = E^{*2}$.

In fact due to the completeness of the two basis any vector of the second basis can be expressed as a linear combination of the first one

$$|\Phi_i^2 > = \sum a_j^i |\Phi_j^1 > \qquad \text{(A4.24)}$$

The coefficient a_j^i are finite because the subspace $\mathcal{D}$ has finite dimension and we can define the constant:

$$c_{\max} = \max |a_j^i| \tag{A4.25}$$

For any vector of the second basis Φ_i^2 we consider $Q_N(\Phi_i^2)$, Their integrand according to the change of basis (A4.23) can be easily bounded by use of the triangular inequality:

$$\left\| U_\sigma \Phi_i^2 \right\| \leq \sum_j |a_j^i| \left\| U_\sigma \Phi_j^1 \right\|. \tag{A4.26}$$

By integrating both sides of the previous inequality and using the definition of Q_N^* (A4.19) and $c_{\max}$ (A4.25) we find:

$$Q_N(\Phi_i^2) \leq \sum_i |a_j^i| Q_N(\Phi_i^1) \leq d\, c_{\max} Q_N^{*1}(\beta). \tag{A4.27}$$

Therefore, since the last inequality is valid for arbitrary i it is also in particular valid for the state Φ_k^2 such that $Q_N(\Phi_k^2) = Q_N^*$ and we find that:

$$Q^{*2}(\beta) \leq d c_{\max} Q^{*1}(\beta \tag{A4.28}$$

From which $E_2^* \geq E_1^*$ holds and the statement (c̃) is proven.

APPENDIX V

In this appendix we show that if

ψ_T belongs to an irreducible subspace $\mathcal{D}_i$ as defined in the test (see 2.3.2) the actual value of

$$E_M(\psi_T) = \lim_{\beta\to\infty} -\frac{1}{\beta}\ln Q_M^{\beta}(\psi_T) = \lim_{\beta\to\infty} -\frac{1}{\beta}\ln Q_N^{\beta}(\psi_T) \qquad \text{(A5.1)}$$

exists and is independent of ψ_T in the irreducible subspace $\mathcal{D}_i$.

PRELIMINARY STATEMENTS

Let us consider the subspace $\mathcal{D}_{\psi_T}^L \subset \mathcal{H}$ spanned by all the possible vectors $U_\sigma(\beta,0)|\psi_T>$ obtained by propagating ψ_T trough U_σ for any $\beta \leq L\Delta\tau$ (we assume in the following a discretized imaginary time). By the definition $\mathcal{D}_{\psi_T}^{L+1} \supset \mathcal{D}_{\psi_T}^L$ and the dimension of these subspaces is bounded for any L :

$$\dim\{\mathcal{D}_{\psi_T}^L\} \leq D \qquad \text{(A5.2)}$$

because of the finite dimension D of the Hilbert space. From the previous two properties it follows that exists a finite L_0 such that for any $L \geq L_0$

$$\mathcal{D}_{\psi_T}^L = \mathcal{D}_{\psi_T}^{L_0} \qquad \text{(A5.3)}$$

or formally

$$\mathcal{D}^*_{\psi_T} = \lim_{L\to\infty} \mathcal{D}^L_{\psi_T}. \tag{A5.4}$$

(a)

$\mathcal{D}^*_{\psi_T}$ is an invariant subspace for all the family of propagators U_σ

In fact suppose $\psi \in \mathcal{D}^*_{\psi_T}$ we have to prove that

$$U_\sigma(\beta,0)|\psi> \in \mathcal{D}^*_{\psi_T} \quad \forall\sigma \text{ and } \beta, \text{ and } \psi \in \mathcal{D}^*_{\psi_T} \tag{A5.5}$$

A complete basis of vectors $\{\psi_i\}$ in $\mathcal{D}_\psi$ is by hypothesis a set of vectors generated by propagating ψ_T for some configuration $\{\sigma\}_i$ and inverse temperature $\beta_i \leq L_0\Delta\tau$

$$\psi_i = U_{\{\sigma\}_i}(\beta_i,0)|\psi_T> \tag{A5.6}$$

The "completeness" of this set of functions allows to write ψ as:

$$\psi = \sum a_i|\psi_i> \tag{A5.7}$$

for suitable a_i. Hence $\forall\{\sigma\}$ configuration and $\forall\beta$ by the linearity of the propagator:

$$U_{\{\sigma\}}(\beta,0)|\psi> = \sum a_i U_{\{\sigma\}}(\beta,0)|\psi_i> \tag{A5.8}$$

Using the definition of ψ_i (A5.6) the propagation of $|\psi_i>$ through $U_\sigma(\beta,0)$ can be thought as a composite propagation acting on $|\psi_T>$ by :

$$U_{\{\sigma\}}(\beta,0)U_{\{\sigma\}_i}(\beta_i,0)|\psi_T> \tag{A5.9}$$

under a suitable $\{\tilde{\sigma}\}_i = \{\sigma\} \cup \{\sigma_i\}$ configuration of fields for a time interval $\beta + \beta_i$. Therefore from (A5.9)

$$U_\sigma(\beta, 0)|\psi> = \sum a_i U_{\{\tilde{\sigma}\}_i}(\beta + \beta_i, 0)|\psi_T> \qquad \text{(A5.10)}$$

is again expressed in terms of a linear combination of vectors obtained by simply propagating ψ_T. This is again by definition belonging to $\mathcal{D}_{\psi_T}$, and this conclude our proof.

As mentioned in Sect.4 the total Hilbert space can be decomposed in terms of irreducible subspace $\mathcal{D}_i$ under all the propagators $U_\sigma(\beta, 0)$ (see 2.3.2).

(b)

If ψ_T belongs to one of these irreducible subspace $\mathcal{D}_i$ the subspace $D^*_{\psi_T}$ (A5.4) (generated by propagating the trial wavefunction ψ_T for sufficiently large imaginary time) must coincide with $\mathcal{D}_i$.

In fact, suppose that $D^*_{\psi_T}$ does not coincide with $\mathcal{D}_i$, then $\mathcal{D}_i$ contains a subspace $D^*_{\psi_T}$ which is invariant from the previous statement (a) and different from $\{0\}$ because $D^*_{\psi_T}$ contains at least ψ_T. Hence $\mathcal{D}_i$ would not be irreducible and this contradicts its definition.

It is now possible to prove using (b) the main statement of this appendix. We consider any function $\psi_T \in \mathcal{D}_i$, arbitrary β and $\tau = L\Delta\tau \leq L_0\Delta\tau$ (see A5.3) and we restrict for simplicity to the discrete HST described by (1.1.18). From the

simple identity

$$\|U_\sigma(\beta,0)|\psi_T>\| = \left\|U_\sigma(\beta,\tau)\frac{\psi_\tau}{\|\psi_\tau\|}\right\| \|\psi_\tau\| \qquad \text{(A5.11)}$$

with $\psi_\tau = U_\sigma(\tau,0)|\psi_T>$ we have that $\forall\tau \leq L_0\Delta\tau$

$$Q_N^{\beta+\tau}(\psi_T) = \sum_{\{i\}} Q_N^\beta\left(\frac{\psi_\tau^i}{\|\psi_\tau^i\|}\right)\|\psi_\tau^i\|2^{-LN_a} \qquad \text{(A5.12)}$$

where the index $\{i\}$ labels all the possible 2^{LN_a} wavefunctions ψ_τ^i generated by U_σ for a fixed propagation time $\tau = L\Delta\tau$. In the RHS of the previous expression there is a sum of positive definite term, for large β and fixed τ only the ones with the faster exponential behaviour will be dominant in the sum. From this property we notice that, at variance of the "pseudo" partition function Q where different contributions can have opposite sign and cancel out each other, this positive definite "pseudo" partition function may have —as we are going to show— a quite different dependence on the trial wavefunction.

Since as shown in (1.2.12) $\|\psi_\tau^i\| \geq \exp -\tau E_{\max}$ one can write:

$$Q_N^{\beta+\tau}(\psi_T) \geq e^{-\tau E_{\max}}2^{-LN_a}Q_N^\beta\left(\frac{\psi_\tau^i}{\|\psi_\tau^i\|}\right) \qquad \text{(A5.13)}$$

On the other hand:

$$\|U_\sigma(\beta+\tau,0)|\psi_T>\| =$$

$$\|U_\sigma(\beta+\tau,\beta)U_\sigma(\beta,0)|\psi_T>\| \leq \exp -E_{\min}\tau\,\|U_\sigma(\beta,0)|\psi_T>\| \qquad \text{(A5.14)}$$

$\forall\tau \leq L_0\Delta\tau$ and correspondingly by integrating in $d\mu_\sigma$ both sides of (A5.14):

$$Q_N^{\beta+\tau}(\psi_T) \leq e^{-E_{\min}\tau}Q_N^\beta(\psi_T) \qquad \text{(A5.15)}$$

From (A5.13) and (A5.15) it follows that for all ψ_τ^i with any $\tau \leq L_0 \Delta\tau$

$$Q_N^\beta(\psi_T) \geq \exp -\tau(E_{\max} - E_{\min}) 2^{-pN_a} Q_N^\beta \left(\frac{\psi_\tau^i}{\|\psi_\tau^i\|} \right)$$
$$\geq \exp -L_0 \Delta\tau (E_{\max} - E_{\min}) 2^{-L_0 \Delta\tau} Q_N^\beta \left(\frac{\psi_\tau^i}{\|\psi_\tau^i\|} \right) \qquad \text{(A5.16)}$$

The subspace generated by all the vectors $\{\psi_k^\tau\}$ for all $\tau \leq L_0 D\tau$ named $\mathcal{D}_{\psi_T}^*$ coincides, as shown in (b), with the given irreducible subspace $\mathcal{D}_i$, hence among all the possible vectors generated by $U_\sigma(\tau, 0)$ for $\tau \leq L_0 \Delta\tau$ it is possible to select a complete set of independent vectors in the given irreducible subspace $\mathcal{D}_i$.

$$\Phi_i = \{\psi_\tau^k\} \qquad \text{(A5.17)}$$

for some $\tau \leq L_0 \Delta\tau$ and i. In particular we choose among the overcomplete set of vectors ψ_τ^i a complete set $\{\Phi_i\}$ such that contains the trial wavefunction $|\psi_T>$. Using the previous inequality (A5.16) and the definition of Q_N^* (A4.19) with the chosen basis $\{\Phi_i\}$ we finally have that:

$$c_{L_0} Q_N^*(\beta) \leq Q_N^\beta(\psi_T) \leq Q_N^*(\beta) \qquad \text{(A5.18)}$$

with

$$c_{L_0} = e^{-(E_{\max} - E_{\min}) L_0 \Delta\tau} \cdot 2^{-L_0 \Delta\tau} \qquad \text{(A5.19)}$$

Now having in mind the definition of E_N^* in (A4.22) and its independence of the chosen basis app.4c the previous inequality finally gives that

$$E_N = \lim_{\beta \to \infty} -\frac{1}{\beta} \ln Q_N^\beta(\psi_T) = E_N^* = E^* \qquad \text{(A5.10)}$$

Thus E^* does not depend on ψ_T in any irreducible subspace $\mathcal{D}_i$ and we finally have proved the statement of this appendix.

Appendix VI

Given the definitions (2.4.13,16) in the text we are going to show

(a) *Negative U*

$$Q_M(\psi^\uparrow \otimes \psi^\downarrow) \leq \sqrt{Q(\psi^\uparrow \otimes \psi^\uparrow)Q(\psi^\downarrow \otimes \psi^\downarrow)} \tag{A6.1}$$

(b) *Positive U*

$$Q_M(\psi^\uparrow \otimes \psi^\downarrow) \leq \sqrt{Q(\psi^\uparrow \otimes c\psi^\uparrow)Q(c\psi^\downarrow \otimes \psi^\downarrow)} \tag{A6.2}$$

(a)

$U < 0$

By definition

$$Q_M(\psi^\uparrow \otimes \psi^\downarrow) = \int d\mu_\sigma \, |< \psi_\uparrow U_\sigma \psi_\uparrow > < \psi_\downarrow U_\sigma \psi_\downarrow >| \tag{A6.3}$$

Then by the Schwartz inequality:

$$\begin{aligned} Q_M(\psi^\uparrow \otimes \psi^\downarrow) &\leq \sqrt{\int d\mu_\sigma < \psi_\uparrow U_\sigma \psi_\uparrow >^2 \int d\mu_\sigma < \psi_\downarrow U_\sigma \psi_\downarrow >^2} \\ &= \sqrt{Q(\psi^\uparrow \otimes \psi^\uparrow)Q(\psi^\downarrow \otimes \psi^\downarrow)} \end{aligned} \tag{A6.4}$$

(b) $U > 0$

$$Q_M(\psi^\uparrow \otimes \psi^\downarrow) = \int d\mu_\sigma \, |< \psi_\uparrow U_\sigma \psi_\uparrow >< \psi_\downarrow U_\sigma \psi_\downarrow >| \tag{A6.5}$$
$$= \int d\mu_\sigma \left| \exp -\frac{\sum \sigma_{r,i}}{2} < \psi_\uparrow U_\sigma \psi_\uparrow > \right| \left| \exp \frac{\sum \sigma_{r,i}}{2} < \psi_\downarrow U_\sigma \psi_\downarrow > \right|$$

Then applying the same Schwartz inequality as before, we have that

$$Q_M(\psi^\uparrow \otimes \psi^\downarrow) \leq \sqrt{\int d\mu_\sigma \left(\exp -\frac{\sum \sigma_{r,i}}{2} < \psi^\uparrow U_\sigma \psi^\uparrow > \right)^2} \sqrt{\int d\mu_\sigma \left(\exp \frac{\sum \sigma_{r,i}}{2} < \psi^\downarrow U_\sigma \psi^\downarrow > \right)^2} \tag{A6.6}$$

We note that each factor in the RHS of the previous expression correspond to $Q^{1/2}(c\psi^\uparrow \otimes \psi^\uparrow)$ and $Q^{1/2}(\psi^\downarrow \otimes c\psi^\downarrow)$ respectively (see eqs.(2.4.16,17) in the text) and the statement (b) of the Appendix is proven.

APPENDIX VII

In this appendix we prove the basic assertion (2.4.29,30) used in Sect.5 i.e.:

$$\|\psi_{2i+1} - \psi_K\| < \alpha \|\psi_{2i} - \psi_K\| \tag{A7.1a}$$

with $\alpha < e^{-\frac{\Delta}{2}\Delta\tau}$ *if:*

$$\|\psi_{2i} - \psi_K\| < \sqrt{2 - \sqrt{2}} \tag{A7.1b}$$

PRELIMINARY STATEMENT

First of all we show that during the systematic evolution (2.4.27) the propagated wavefunction is attracted to the ground state of $\hat{K}$ at least as:

$$\frac{< \psi_{2i+1} | \psi_K >^2}{1 - < \psi_{2i+1} | \psi_K >^2} \geq \frac{\psi_{2i} | \psi_K >^2}{1 - < \psi_{2i} | \psi_K >^2} \exp 2\Delta_K \Delta\tau \tag{A7.2}$$

In fact we rewrite the LHS of the previous inequality using eq.(2.4.27) for ψ_{2i+1}:

$$\frac{< \psi_{2i+1} | \psi_K >^2}{1 - < \psi_{2i+1} | \psi_K >^2} = \frac{< \psi_{2i} e^{-\Delta\tau \hat{K}} \psi_K >^2}{< \psi_{2i} e^{-2\Delta\tau \hat{K}} \psi_{2i} > - < \psi_{2i} e^{-\Delta\tau \hat{K}} \psi_K >^2} \tag{A7.3}$$

We now express ψ_{2i} in terms of the basis of eigenstates of the kinetic term ψ_K^j, $j = 1, \ldots, D-1$ with $\psi_K^0 = \psi_K$ the ground state:

$$\frac{<\psi_{2i+1}|\psi_K>^2}{1-<\psi_{2i+1}|\psi_K>^2} = \frac{e^{-E_0\Delta\tau}<\psi_{2i}|\psi_K>^2}{\sum_{j\neq 0} e^{-2E_j\Delta\tau}<\psi_{2i}|\psi_K^j>^2} \tag{A7.4}$$

We notice that the denominator in the RHS of the previous expression is easily bounded:

$$\begin{aligned}\sum_{j\neq 0} e^{-2E_j\Delta\tau}<\psi_{2i}|\psi_K^j>^2 &\leq e^{-2(E_0+\Delta_K)\Delta\tau}\sum_{j\neq 0}<\psi_{2i}|\psi_K^j>^2 \\ &= e^{-2(E_0+\Delta_K)\Delta\tau}\left\{1-<\psi_{2i}|\psi_K>^2\right\}\end{aligned} \tag{A7.5}$$

where as mentioned Δ_K is the gap of the kinetic term.

Therefore one easily get the basic result (A7.2).

It is now possible to prove the basic assertion (A7.1), that is to show that the propagated wavefunction ψ_{2i} and the ground state of $\hat{K}$ ψ_K became closer in an exponential way after the systematic evolution (2.4.27), provided ψ_{2i} is sufficiently close to ψ_K.

We notice that since $\|\psi_{2i}-\psi_K\|^2 = 2-2<\psi_{2i}|\psi_K>$ and $\|\psi_{2i}-\psi_K\| < \sqrt{2}$ by assumption, the overlap of ψ_{2i} with ψ_K is positive and such that

$$<\psi_{2i}|\psi_K>^2 > \frac{1}{2} \tag{A7.6}$$

On the other hand $<\psi_{2i}|\psi_K>$ has the same sign of $<\psi_{2i}|\psi_K>$ because from the definition

$$<\psi_{2i+1}|\psi_K> = \frac{<\psi_{2i}\psi_K> e^{-E_0\Delta\tau}}{\|e^{-k\Delta\tau}\psi_{2i}\|} \tag{A7.7}$$

So we have that $< \psi_{2i}|\psi_K >$ and $< \psi_{2i+1}|\psi_K >$ are both positive. Moreover from (A7.2) it follows that

$$< \psi_{2i+1}|\psi_K > \geq < \psi_{2i}|\psi_K > \tag{A7.8}$$

On the other hand the same inequality (A7.2) can be written in the following way:

$$1 - < \psi_{2i+1}|\psi_K >^2 \leq \frac{1 - < \psi_{2i}|\psi_K >^2}{1 + (e^{2\Delta\,\Delta\tau} - 1) < \psi_{2i}|\psi_K >^2} \tag{A7.9}$$

From the bound $< \psi_{2i}|\psi_K > \geq \frac{1}{2}$ coming from the condition (A7.1) the denominator in the left hand side of the previous eqs. is larger then $\frac{\exp 2\Delta\,\Delta\tau + 1}{2}$ and (A7.9) becomes:

$$1 - < \psi_{2i}|\psi_K >^2 \leq \left[1 - < \psi_{2i}|\psi_K >^2\right] \frac{2}{\exp 2\Delta\,\Delta\tau + 1} \tag{A7.10}$$

Noting that $1 - < \psi_{2i}|\psi_K >^2 = (1 - < \psi_{2i}|\psi_K >)\,(1 + < \psi_{2i}|\psi_K >)$ we can rewrite the previous relation as:

$$\begin{aligned} 1 - < \psi_{2i+1}|\psi_K > &\leq \frac{2}{1 + \exp 2\Delta\,\Delta\tau}\,(1 - < \psi_{2i}|\psi_K >)\left(\frac{1 + < \psi_{2i}|\psi_K >}{1 + < \psi_{2i+1}|\psi_K >}\right) \\ &\leq \frac{2}{1 + \exp 2\Delta\,\Delta\tau}\,(1 - < \psi_{2i}|\psi_K >) \end{aligned} \tag{A7.11}$$

where the last inequality holds from (A7.8). Finally we use that, in the previous inequality, $\frac{2}{1+\exp 2\Delta\,\Delta\tau} < \exp -\Delta\,\Delta\tau$ and that the distance between two unit vectors is simply related to their overlap $\left(\|\psi_{2i+1} - \psi_K\| = \sqrt{2 - 2 < \psi_{2i+1}|\psi_K >}\right)$. Then (A7.1) holds from (A7.11).

BIBLIOGRAPHY

[1] Parola A., Sorella S., Parrinello M. and Tosatti E., submitted for publication in Phys. Rev. Lett.

[2] Oitmaa J. and Betts D.D., Can. J. Phys. **56** (1978) 897

[3] Dagotto E. and Moreo A., Phys. Rev. B **38** (1988) 5087

[4] Soos Z.G. and Ramasesha S., Phys. Rev. B **29** (1984) 5410

[5] Kohn W. and Sham L.J., Phys. Rev. A **140** 1133.

[6] Gutzwiller M.C., Phys. Rev. Lett. **10** (1963) 159, Phys. Rev. **134** (1964) A923, Phys. Rev. **137**, A1726.

[7] Trivedi N. and Ceperley D., preprint

[8] Bickers N.E., Scalapino D.J. and White S.R., Phys. Rev. Lett. **62** 961 (1989)

[9] Schrieffer J.R., Wen X.G. and Zhang S.C., Phys. Rev. B **39** 11663 (1989)

[10] Fetter A.L. and Walecka J.D. 1971, Quantum Theory of Many Particles Systems (McGraw-Hill)

[11] Linqvist S. and March N.H. (eds.) 1983, Theory of the Inhomogeneous Electron Gas (New York: Plenum).

[12] Car R. and Parrinello M., Phys. Rev. Lett. **55** (1985) 2471

[13] Hubbard J., Proc. Roy. Soc. (London) Ser. A 276 (1963) 238 and **277** (1964) 237

[14] Ceperley D.M., "Recent Progress in Many-Body Theories" Springer Verlag, Berlin (1981) 262

[15] Kalos M.H., "Monte Carlo Method in Quantum Physics", NATO ASI Series, D. Reidel Publ. Co.–Dordrecth (1984) 19

[16] Ceperley D. M. and Alder B.J., J. Chem. Phys. **81** (1984) 5833

[17] Hirsch J.E., Scalapino D.J., Sugar R.L and Blankenbecker R., Phys. Rev. B **26** (1982) 5033

[18] Hirsch J.E., Sugar R.L, Scalapino D.J. and Blankenbecker R., Phys. Rev. B **26** (1982) 5033

[19] Morgenstern I. and Wortz D.Z., Phys. B **61**, 219 (1985)

[20] Reger J.D. and Young P.A., Phys. Rev. B **37** (1988) 5978

[21] Koonin S.E., Sugiyama G. and Friedriech H., *Proceedings of the International Symposium Bad Honnef*, edited by K. Goeke and P.G. Greinhard (Springer Verlag, Berlin, 1982), p. 214

[22] Sugiyama G. and Koonin S.E., Annals of Physics **168** (1986) 1-26

[23] Hirsch J.E., Phys. Rev. B **31**,4403 (1985)

[24] Loh E.Y. Jr., Gubernatis J.E., Scalettar R.T, White S.R., Scalapino D.J. and Sugar R.L., Phys. Rev. B to appear

[25] Moreo A., Scalapino D.J., Sugar R.L., and White S.R., Phys. REV. B to appear

[26] Hirsch J. E. and Lin H.Q., Phys. Rev. B **37**,5070 (1988)

[27] Blankenbecker R., Scalapino D.J. and Sugar R.L., Phys. Rev. D **24** (1981) 2278

[28] Hirsh J.E., Phys. Rev. B **28** (1983) 4059

[29] Hirsh J.E. and Tang S., Phys. Rev. Lett. **62** (1989) 591

[30] Hirsh J.E. and Scalapino D.J., Phys. Rev. Lett. **56** (1986) 273.

[31] Sorella S., Car R., Baroni S. and Parrinello M., Europhys. Lett. **8** (1989) 663

[32] Sorella S., Tosatti E., Baroni S., Car R. and Parrinello M., Int. J. Mod. Phys. B **1** (1988) 993

[33] Satoh K. and Takada S., (1989) **58** 783

[34] Imada M., J. Phys. Soc. Jpn. **57** (1987) 42,2689,3128

[35] Scalettar R.T., Scalapino D.J., Sugar R.L. and Toussant D., Phys. Rev. B **34** (1986) 7911, Phys Rev. B **36** (1987) 8632

[36] Helgason S., "Differential Geometry, Lie Group, and Symmetric Spaces" Orlando, Academic Press, New York (1978)

[37] Lieb E.H. and Wu F.Y., Phys. Rev. Lett. **20** (1968) 1445

[38] Parisi G. and Yougshi W., Scientia Sinica **24** (1981) 483

[39] Press W.H., Flannery B.P., Teukolsky S.A. and Vetterling W.T. 1986, Numerical Recipes Cambridge University Press (Cambridge)

[40] Gunsteren W.F. and Berendsen H.J., Mol. Phys. **45**, 637 (1982).

[41] Batrouni G.G., Katz G.R., Kronfeld A.S., Lepage G.P., Svetitsky B. and Wilson K.G., Phys. Rev. D **32** (1985) 2736.

[42] White S.R., Wilkins J. and Wilson K., Phys. Rev. Lett. **56** (1986) 4.

[43] Fest M.D., Fleck J.A. and Steiger A., J. Comp. Phys. **47** (1982) 412

[44] Young C.N. and Young C.P., Phys. Rev. **150** (1966) 321,327

[45] Lieb E.H. and Mattis D.C., Phys. Rev. **125** (1962) 164

[46] Brinkmann W.F. and Rice T.M., Phys. Rev. B **2** (1970) 4302.

[47] Vollhard D., Rev. Mod. Phys. **56** (1984) 99

[48] Metzner W. and Vollhardt D., Phys. Rev. Lett. **62** (1989), 324

[49] Shiba H., J. Phys. Soc. of Jap. **50** (1987) 3582

[50] Anderson P.W., Science **235**, 1196 (1987); Varenna Lectures (1987) and references therein.

[51] "Proceedings of the Adriatico Research Conference on High Temperature Superconductivity" Edited by E. Linqvist, E. Tosatti, M.P. Tosi and Yu Lu World Scientific–Singapore (1988)

[52] Pines D. and Noziers P., "The Theory of Quantum Liquids", W.A. Benjamin inc. – New York (1966)

[53] Devreux F., Phys. Rev. B, 4651 (1978)

[54] Comes R., Shapiro S.M., Shirane G., Garito A.F. and Heeger A.J., Phys. Rev. Lett. **35** 1519 (1975)

[55] Villain J., Phys. Rev. Lett. **36**, 173 (1975).

[56] Shiba H. and Pincus P., Phys. Rev. B **5** (1972) 1982

[57] Shiba H., Phys. Rev. B **6**, 930 (1972) and references therein

[58] Takahashi M., Prog. Theor. Phys. **43** (1970); **42** (1969) 1098

[59] Takahashi M., J. Phys. C **10** (1977) 1289

[60] Carmelo J. and Baeriswyl D., Phys. Rev. B **37**, 7541 (1988) and references therein

[61] Yokoyama H. and Shiba H., J. Phys. Soc. of Japan 56 (1987) 1490

[62] Fazekas P. and Penc K., Int. Jour. Mod. Phys. B1, 1021.

[63] Lin H.Q. and Hirsch J.E., Phys. Rev. B **33** 8155 (1986)

[64] Hirsch J.E. and Scalapino D.J., Phys. Rev. B **29** 5554 (1984), **27** 7169 (1983)

[65] Bourbonnais C., Nelisse H., Reld A., Tremblay A.-M.S. Phys. Rev. B **40** (1989) 2297

[66] von der Linden W., Morgenstern I. and de Raedt H. preprint

[67] Ogata M. and Shiba H., preprint

[68] Solyom J., Adv. in Phys. **28**, 201 (1979)

[69] Dzyaloshinsky I.E. and Larkin A.I., Zh. Eksp. Teor. Fiz. **65** (1973) 411 (Sov. Phys. JEPT, **38** (1974) 202)

[70] Mattis C.D. and Lieb E.H., Jour. Math. Phys. **6** 375 (1965)

[71] Fye R.M. and Hirsch J.E., Phys. Rev. Lett. **56** (1986) 2521

[72] Gubernatis J.E., in *Quantum Monte Carlo Methods*, ed. M. Suzuki, (Springer Verlag, New York, 1987) p.216